Lawrence Berkeley Laboratory
UNIVERSITY OF CALIFORNIA

ENERGY & ENVIRONMENT
DIVISION

SENSIBLE HEAT STORAGE FOR A SOLAR THERMAL POWER PLANT

Thomas F. Baldwin, Scott Lynn, and Alan S. Foss
(Filed as M. S. thesis)

July 1979

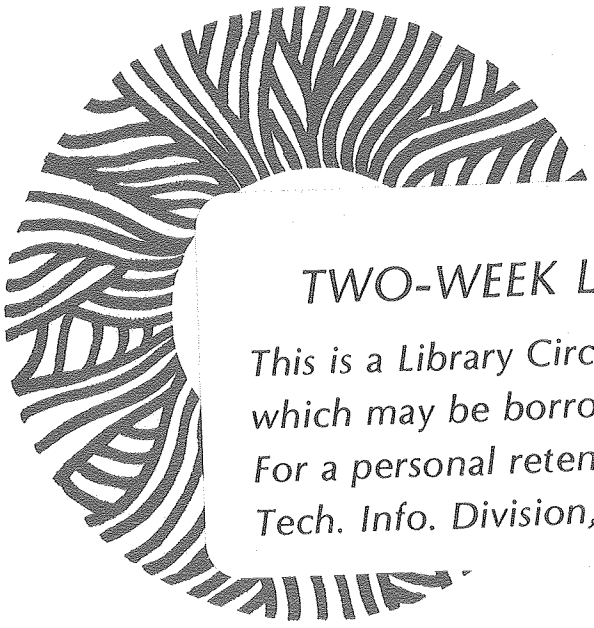

Prepared for the U.S. Department of Energy under Contract W-7405-ENG-48

DISCLAIMER

SENSIBLE HEAT STORAGE FOR A SOLAR THERMAL POWER PLANT

Thomas F. Baldwin, Scott Lynn, and Alan S. Foss

University of California
Lawrence Berkeley Laboratory
Berkeley, California

This work was prepared with the support of the U. S. Department of Energy under Contract W-7405-ENG-48.

TABLE OF CONTENTS

Chapter		Page
1.	INTRODUCTION	1
	1.1 Available Energy Storage Methods	2
	1.2 Scope of the Thesis	6
2.	SOLAR POWER PLANT DESIGN	7
	2.1 Study Guidelines	7
	a. Heat Transfer Gas	9
	b. Sensible-Heat Storage Medium	10
	c. Thermal Insulation	13
	d. Selection of Reasonable Pipe Diameters and Reasonable Insulation Thicknesses	13
	e. Reference Solar Power Plant Design	15
	2.2 Power Plant Flowsheet	15
	a. Daytime Power Plant Operation	19
	b. Nighttime Power Plant Operation	19
3.	ANALYSIS AND COMPUTER DESIGN OF THE STORAGE UNIT	21
	3.1 Storage Operation	21
	3.2 A Mathematical Model for Storage Analysis and Design	27
	3.3 Computer Design of the Sensible-Heat Storage Unit	34
	3.4 Details on Computer Design Calculations	37
4.	DESIGN OF THE POWER PLANT SUBSYSTEMS	40
	4.1 The Heat-Collection Subsystem	41
	4.2 The Sensible-Heat Storage Subsystem	49
	a. Design of the Brick Checkerwork	49

Chapter Page

b. Design of the Steel Tanks 51

c. Layout of the Storage Tanks 56

d. Estimated Costs of the Storage Unit 56

4.3 The Heat-Exchange Subsystem 59

4.4 The Gas-Circulation Subsystem 63

4.5 The Power-Generation Subsystem 74

4.6 An Overview of the Solar Power Plant 78

5. THE EFFECTS OF SEVERAL MAJOR DESIGN PARAMETERS ON COST AND OPERATION OF THE SOLAR POWER PLANT 85

5.1 Storage-Vessel Design 85

5.2 Cross-sectional Area For Gas Flow in the Storage Checkerwork 87

5.3 Operating Pressure of the Heat-Transfer Fluid 89

5.4 Elimination of Nighttime Electric Generation 92

5.5 Duration of the Storage Discharge 92

5.6 Choice of the Gas Used as Heat-Transfer Medium . . . 95

5.7 Choice of Method of Heat Dissipation 98

6. ALTERNATIVE FLOWSHEETS FOR A SOLAR POWER PLANT WITH SENSIBLE-HEAT STORAGE 102

6.1 Division of the Storage Unit Into Several Storage Tank Sets 102

6.2 Brayton-Cycle Topping of the Steam-Cycle Power Plant 106

7. A COMPARISON OF SENSIBLE-HEAT STORAGE WITH CHEMICAL-HEAT STORAGE FOR A STEAM SOLAR ELECTRIC PLANT 111

8. CONCLUSIONS AND RECOMMENDATIONS . . . . . 1[illegible]

NOTATION . . . . . 1[illegible]

Page

REFERENCES 123

APPENDIX

I. COST ESTIMATION METHODS 128

1. Storage Subsystem Costs 128

a. Storage Tanks: Welded Carbon-Steel Pressure Vessel Cost 128

b. Storage Tanks: Prestressed Cast Iron Vessel Cost 129

c. Magnesia Brickwork Cost 130

d. Kaowool Insulation Cost 130

2. Gas-Circulation Subsystem Costs 130

a. Gas Piping Cost 130

b. Flow Control Valve Costs 131

c. Gas Compressor Cost 131

3. Heat-Collection Subsystem Costs 132

4. Heat-Exchange Subsystem Costs 132

5. Power-Generation Subsystem Costs 133

a. Steam Turbine-Generator Cost 133

b. Dry-Cooling Tower Costs 133

c. Wet-Cooling Tower Costs 133

II. STORAGE UNIT MODELING PROGRAM-HREGEN 135

1. Subroutine Directory for Program HREGEN 135

2. Definitions of the Physical Variables Used in Program HREGEN 136

3. HREGEN Program Listing 148

Appendix Page

4. HREGEN Sample Output for the Reference Storage Design 161

a. Input Data for this Case 161

b. Output Generated During Program Iteration to a Satisfactory Design 161

c. Output Data for the Reference Storage Design . . 162

III. RECEIVER MODELING PROGRAM-TUBE2. 177

1. Definitions of the Physical Variables used in Program TUBE2 177

2. TUBE2 Program Listing 180

3. TUBE2 Sample Output for the Reference Central Receiver Design 182

ILLUSTRATIONS

Figure		Page
1-1.	The daytime flow arrangements for three solar power plants.	4
2-1.	The proposed flowsheet for a solar power plant with sensible-heat storage	18
3-1.	A cross-sectional detail of the checkerwork of magnesia bricks	22
3-2.	Predicted gas and brick temperatures during charging of the sensible-heat storage unit	23
3-3.	Predicted gas and brick temperatures during discharging of the sensible-heat storage unit	24
3-4.	Predicted gas temperatures during charging of the sensible-heat storage unit	25
3-5.	Predicted gas mass flow rates during charging of the sensible-heat storage unit	26
3-6.	A three-dimensional detail of the brick checkerwork control volume	28
3-7.	Cross-sectional views of the proposed model for heat transfer between the bricks and the gas	31
4-1.	Conceptual design of the Boeing central receiver	42
4-2.	Conceptual design of the welded carbon-steel storage tanks.	53
4-3.	Determination of the range of acceptable storage tank insulation thicknesses	55
4-4.	Conceptual layout of the storage tanks	57
4-5.	Flow arrangement for the heat-exchange subsystem	60
4-6.	The proposed piping arrangement for the gas-circulation subsystem	66
4-7.	Determination of the range of reasonable piping insulation thicknesses for the storage-to-heat-collection piping run	69
4-8.	Determination of the range of reasonable piping flow diameters for the storage-to-heat-collection piping run	70

Figure		Page
4-9.	Layout of the power-generation subsystem	75
5-1.	A parametric study on the effects of the cross-sectional area for gas flow through storage on the amount of electric energy generated and its cost	90
5-2.	A parametric study on the effects of the heat-transfer fluid operating pressure on the amount of electric energy generated and its cost	91
6-1.	An alternative flowsheet for a solar power plant with the sensible-heat storage unit broken into two storage tank sets	103
6-2.	Charging gas mass flow rates for an alternate solar power plant with the storage unit divided into two storage tank sets	105
6-3.	An alternative flowsheet for a solar power plant with Brayton-cycle gas turbine topping	108

TABLES

Table		Page
2-1.	Important Heat-Transfer Properties of Helium	11
2-2.	Properties of Refractory Bricks	12
2-3.	Properties of Kaowool Insulation	14
2-4.	Reference Solar Power Plant Design	16
3-1.	The Effects of Varying the Number of Time and Length Increments on Storage Size	39
4-1.	Model Predictions for the Effects of Proposed Modifications on Central Receiver Operation	46
4-2.	Heat-Collection Subsystem Summary	48
4-3.	Computer-Assisted, Sensible-Heat Storage Unit Design	50
4-4.	Sensible-Heat Storage Subsystem Summary	58
4-5.	Proposed Basic Exchanger Designs	62
4-6.	Sizing Calculations for the Heat Exchanger Network	64
4-7.	Heat-Exchange Subsystem Summary	65
4-8.	Gas-Circulation Piping Design Details	72
4-9.	Gas-Circulation Subsystem Summary	73
4-10.	Approximate Size of the Natural-Draft Dry-Cooling Tower	77
4-11.	Power-Generation Subsystem Summary	79
4-12.	An Overall Summary of the Proposed Solar Power Plant Design	81
4-13.	The Impact of Sensible-Heat Storage on the Cost of Electricity Generated by this Solar Power Plant	83
5-1.	The Impact of Storage Vessel Design on the Sensible-Heat Storage Subsystem	86
5-2.	The Impact of Storage Vessel Design on the Solar Power Plant	88

Table		Page
5-3.	The Effect of Eliminating Nighttime Electric Generation on the Solar Power Plant	93
5-4.	The Effect of Varying Storage Discharge Time on the Solar Power Plant	94
5-5.	Heat-Transfer Gas Properties	96
5-6.	Model Predictions for the Effect of Changing the Heat-Transfer Fluid on Central Receiver Operation	97
5-7.	The Effect of the Heat-Transfer Fluid on the Solar Power Plant	99
5-8.	A Comparison of Wet-Cooled and Dry-Cooled Solar Power Plant Designs	100
6-1.	The Effects on Performance of Dividing the Storage Unit into Several Storage Tank Sets	107
6-2.	The Effect of Brayton Cycle, Gas Turbine Topping on the Gross Thermal Efficiency of a Solar Power Plant	110
7-1.	A Comparison of the Proposed Sensible-Heat Storage Subsystem with a Sulfur Oxide Chemical-Heat Storage Process	112
7-2.	A Comparison of Two Energy Storage Processes for a Solar Power Plant	114
I-1.	Important Sources of Cost Estimation Data	134

DEDICATION

This report is dedicated to all of the people who encouraged and supported me. I especially wish to thank Dr. Scott Lynn, Dr. Alan S. Foss and Dr. Joshua Dayan for the technical insights they provided during this work. I also want to thank my parents and all of my friends who supported me through out the course of this work. Finally, I want to thank Mr. Mark Orazem who was always there to encourage me onward.

SENSIBLE HEAT STORAGE FOR A SOLAR THERMAL POWER PLANT

Thomas F. Baldwin, Scott Lynn, and Alan S. Foss

Energy and Environment Division, Lawrence Berkeley Laboratory and
Department of Chemical Engineering, University of California,
Berkeley, California 94720

ABSTRACT

The energy input to a solar power plant is dependent on the amount of insolation reaching the collection field. Maintenance of a constant level of power generation through the early evening hours or through a period when the cloud cover is varying requires integration of the heat collection unit and the power generation unit with some type of energy storage unit.

This report examines one possible configuration for a solar power plant with a sensible-heat storage unit. The proposed flowsheet allows thermal energy storage between the heat collection unit and the power generation unit without a reduction in the thermodynamic availability of the energy supplied to the power turbines. Energy is stored by heating a checkerwork of magnesia bricks. A gas that is circulated from the solar collector through the storage unit and the power plant boiler serves as the heat-transfer medium. Nitrogen was found to be preferable to helium for this purpose.

A computer model was used to predict the behavior of the sensible-heat storage unit and to aid in sizing the storage unit. Procedures were developed to estimate the cost of electricity generated by the solar power plant. These procedures illustrate the effects of changes

in the energy storage unit on the cost of electricity. The effects on the storage unit and on the total plant design of changing several process and design parameters were then evaluated. This study has led to the design of two alternative process configurations for solar power plants with sensible-heat storage. The sensible-heat storage process was also compared to the sulfur oxide chemical-heat storage process described by Dayan, Lynn and Foss [9].

The proposed configuration for a solar power plant with sensible-heat storage for nighttime electricity generation produces electricity at the cost of \$87 per MW_e-hr. An alternate configuration for a solar power plant without energy storage for nighttime generation produces electricity for \$76 per MW_e-hr. Both of these power plants convert 32% of the energy absorbed by their solar collectors into usable electric energy. It is concluded that sensible-heat storage can provide energy storage for a solar power plant at a reasonable price using technology that is presently available.

1. INTRODUCTION

Interest in alternate energy resources to augment fossil fuel and nuclear energy supplies has grown rapidly in recent years. This interest has been sparked by a recognition that environmental concerns and depletion of fossil fuel reserves will act to limit the growth of conventional energy sources, resulting in higher energy prices and energy shortages.

The earth is continually receiving a large amount of solar radiation, and a wide variety of concepts are under development to more effectively harness its potential. Heat derived from solar radiation is being used for building and water heating. Research is also under way to develop photovoltaic cells that will economically convert solar energy directly into electric energy. Other researchers are studying the possibility of running a conventional turbine-generator to produce electricity by concentrating solar energy and collecting the resulting thermal energy in a high-temperature working fluid.

Present designs for concentrating solar-thermal energy use a large number of heliostacs directed by computer to reflect solar radiation toward an elevated central receiver. Solar radiation reaching the central receiver is absorbed as thermal energy by a heat-transfer fluid and used directly or indirectly to run a conventional turbine. Alternate design proposals are being examined which propose use of either Brayton-cycle gas turbines or Rankine-cycle steam turbines in the solar power plant.

Energy collection by such a power plant is limited to periods when appreciable direct solar radiation is available. Maintaining power generation overnight or throughout an intermittently-cloudy day requires energy storage for those times when insufficient energy is collected in the central receiver.

This thesis examines the feasibility of a sensible-heat storage unit used in conjunction with a high-temperature, gas-cooled central receiver and a steam-cycle power plant. To transport heat, a gas stream is circulated from the receiver to the power plant and back. The process configuration proposed here maximizes the efficiency of converting thermal energy to electric energy during storage unit discharge by maintaining the flow of inlet steam to the turbine at design conditions. The sensible-heat storage unit proposed by Boeing Engineering and Construction[2,4] has been modified for use with this new system.

The storage device is a checkerwork of magnesia bricks placed in the gas-circulation loop between the central receiver and the power plant. At night and during other periods when the central receiver is not supplying enough energy to the heat-transfer gas, energy is withdrawn from storage by reversing the direction of flow through the checkerwork, thereby heating the gas before it is sent to the power plant boilers.

1.1 AVAILABLE ENERGY STORAGE METHODS

Solar power plants can store energy either before or after the heat has been converted to electricity. Pumped-hydroelectric storage

and battery storage are typical of the grid-integrated storage systems that have been proposed to meet peak electric demands with electricity initially generated during off-peak hours. Such systems could be modified to insure constant output from a solar power plant. However, a problem is still posed by the thermal strains on the high-pressure steam turbine caused by rapid insolation fluctuations. Storage of thermal energy ahead of the turbine has been proposed as a solution for this problem for solar power plants, since it will allow thermal buffering between the receiver and the turbine as well as providing for energy storage. Sensible-heat storage, latent-heat storage, and chemical-heat storage have all been suggested as possible methods for energy storage which could be integrated with the receiver.

Boeing Engineering and Construction has compared systems of sensible-, latent-, and chemical-heat storage units for a Brayton-cycle solar power plant.[2,4] More extensive work on chemical-heat storage for a Rankine-cycle solar power plant has recently been completed by Hill.[14] This work has been revised and condensed by Dayan, Lynn, and Foss.[9] Martin-Marrietta has also investigated sensible-heat storage, choosing to integrate the storage unit into a Rankine-cycle solar power plant.[17,18] These references serve to illustrate the point that costs and energy losses associated with thermal energy storage depend upon the details of storage design and upon how the storage unit is integrated into the power plant.

This thesis investigates the use of a sensible-heat storage unit integrated into a Rankine-cycle solar power plant. Figure 1-1 compares

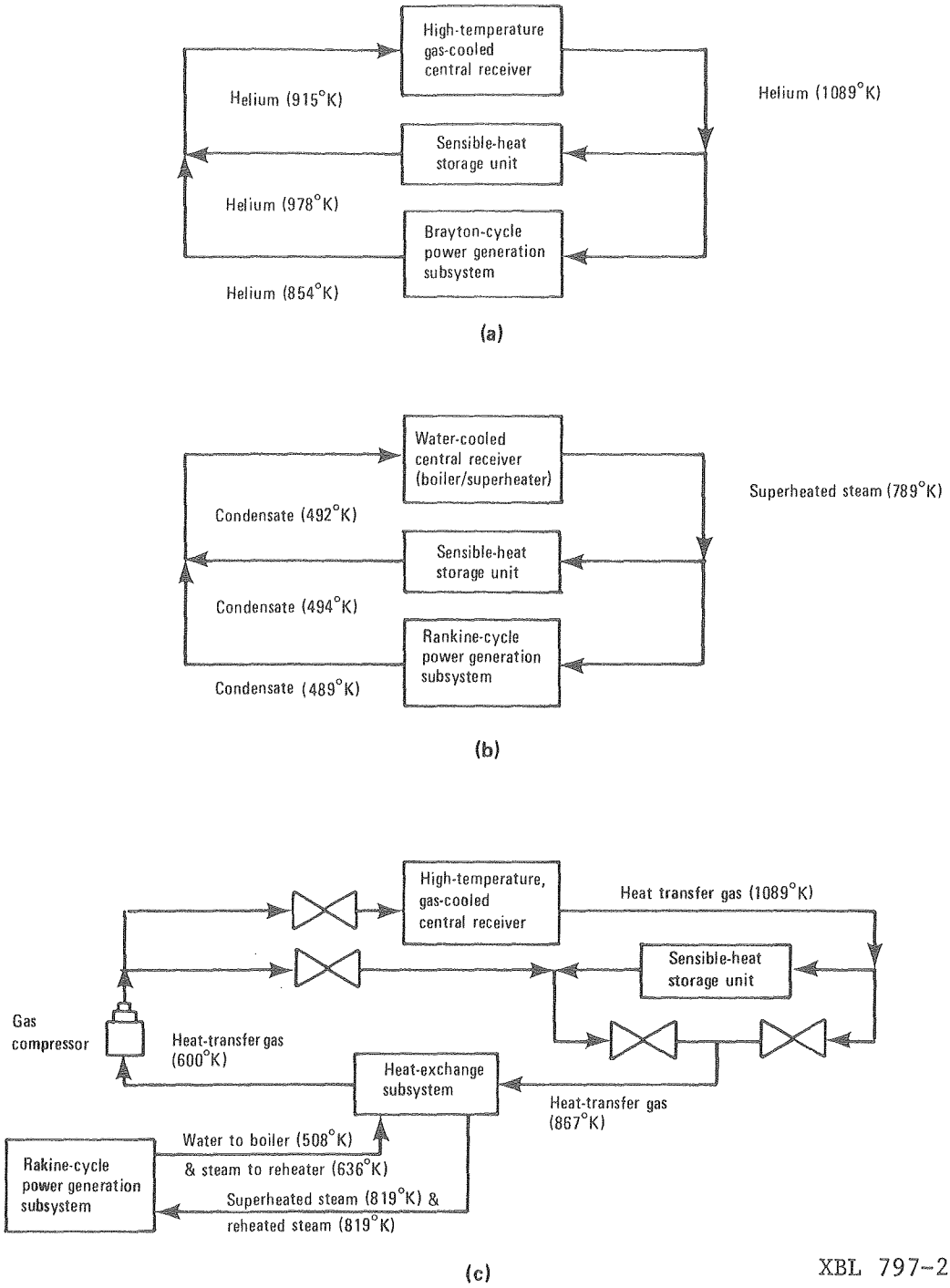

Fig. 1-1. The daytime flow arrangements for three solar power plants; (a) is the flow arrangement for Boeing's Brayton-cycle solar power plant (see references 2 and 4), (b) is the flow arrangement for Martin-Marrieta's Rankine-cycle solar power plant (see references 17 and 18), and (c) is the flow arrangement for the Rankine-cycle solar power plant proposed in this report.

the proposed flowsheet for a solar power plant with two earlier flowsheets. The flowsheet investigated in this report modifies the high-temperature, gas-cooled central receiver concept and the sensible-heat storage concept proposed by Boeing Engineering and Construction[2,3,4] for use with a Rankine-cycle steam turbine.

Boeing's solar power plant generates electricity by passing helium through a Brayton-cycle gas turbine. The inlet gas temperature to the turbine and the thermal efficiency of power generation have been increased by use of a high-temperature central receiver. The storage unit is charged in parallel with power generation. Martin-Marrietta has suggested using the central receiver to boil water and superheat steam for use in running a Rankine-cycle steam turbine or for use in charging the heat storage unit. Both of these solar power plant designs call for inlet temperatures to the turbines that are limited by the temperature levels available from their receivers. Heat-transfer limitations within storage will therefore cause a drop in the inlet temperatures to both turbines during discharge, decreasing the thermal efficiencies of power generation for both solar power plant designs.

In this study, the use of a high-temperature, gas-cooled central receiver is combined with use of a Rankine-cycle steam turbine. Gas from the central receiver first flows through the heat-storage unit and then through the heat exchangers where steam is generated to run the turbines. This solar power plant can supply steam to the turbines at design conditions in both the charge and discharge operational modes, since the central receiver heats gas to a much higher temperature than

steam generation requires. Steam quality during discharge does not drop, because of the high temperature of operation of the storage unit.

1.2 SCOPE OF THE THESIS

This project was started by developing a flowsheet for a solar power plant capable of providing steam to a Rankine-cycle turbine at design conditions in both charge and discharge modes of operation. The plant studied has been designed to charge storage in eight hours, assuming constant heat input to the receiver. Enough thermal energy is stored for a discharge period with a nominal length of six hours. The length of the discharge period will actually be shortened by heat losses from storage and by alternate requirements for thermal energy to maintain the turbines at "hot standby" overnight.

A detailed computer model was then developed to simulate the behavior of a sensible-heat storage module in response to flow through the brick checkerwork of a gaseous heat-transfer medium with arbitrary physical properties, a time-dependent inlet temperature, and a time-dependent flow rate. This computer model has been used to size the storage unit and to evaluate the effects of changing process and design parameters on the storage unit and on the total plant design.

Cost estimation was then undertaken for the proposed solar power plant. Special care has been taken to estimate the costs associated with thermal energy storage in an attempt to illustrate the effects of the proposed storage unit on the cost of electricity generated by a solar power plant.

2. SOLAR POWER PLANT DESIGN

This chapter presents the guidelines and flowsheet developed for design of a solar power plant that converts thermal energy into electric energy. The section on study guidelines discusses important considerations used to develop the power plant flowsheet. The proposed flowsheet is then presented with a description of power plant operation during charge and discharge modes.

2.1 STUDY GUIDELINES

This work was undertaken to provide a basis for economic and operational comparisons between the sulfur oxide chemical-heat storage process described by Dayan, Lynn, and Foss[9] and a sensible-heat storage system. Both solar power plants absorb thermal energy in high-temperature, gas-cooled central receivers similar in design to the central receiver design proposed by Boeing Engineering and Construction[3] and use Rankine-cycle steam turbines for power generation. The decision to use a central receiver capable of supplying high-temperature gas (~1100°K) while generating power with a steam turbine requiring inlet steam at 820°K was made in order to allow for the possibility of substantial thermal degradation of the stored heat without decreasing the thermal efficiency of power generation. Both solar power plant process configurations have been arranged to provide superheated and reheated steam to the turbines at design conditions in either the charge or discharge mode of operation.

The outlet gas from Boeing's central receiver is heated to 1089°K, close to the maximum allowable working temperature for the heat

exchanger tubes. It is expected that lowering the central receiver outlet temperature will decrease the cost of the receiver which could be constructed of less expensive materials. The costs of most of the remaining power plant components would be increased due to the increase in gas flow rates associated with a lower maximum gas temperature. Decreasing the outlet temperature from the central receiver would increase the required size of a sensible-heat storage system by limiting the maximum storage temperature.

Seasonal and daily variations in insolation were ignored in designing and evaluating both solar power plants. This study used a simplified solar model which assumed constant heat input to the central receiver 8 hours per day, 256 days of operation per year. Reduced insolation due to cloud cover and plant shutdowns for maintenance and repair were accounted for by assuming the central receiver will be out of operation 30% of the days each year.

Both solar power plants were designed to operate 12.4 MPa (1800 psia) 811°K/811°K (1000°F/1000°F) high-backpressure turbine-generators. Turbine performance was estimated by scaling down the 330 megawatt Black Hills turbine-generator designed for back pressures between 20 kPa, absolute and 50 kPa, absolute.[12] The use of a high-backpressure turbine was mandated by the desire to reduce plant water demand through use of a dry-cooling system for heat rejection from the power plant. Chapter 5 discusses a solar power plant design which could be used in an area with sufficient water supplies to allow wet cooling.

During the daytime, heat-transfer gas passing through the central receiver in the solar power plant absorbs 440 MW_t. Fifty-seven percent of the heat absorbed (250 MW_t) is sent to the turbines to generate 100 MW_e, gross electric power. Storage has been sized to store all of the remaining thermal energy absorbed over an eight hour charging period, or 1500 MW_t-hr. If all of the thermal energy not sent immediately to power generation could be stored for later release, 600 MW_e-hr of gross electric power could be generated during the discharging period. Heat losses from the storage unit, gas piping, and power-generation heat exchangers reduce the amount of thermal energy available from storage and part of the thermal energy stored is used to maintain the turbines at "hot standby" overnight. These effects significantly reduce nighttime electric generation.

The high-efficiency turbines chosen for this solar power plant are not well adapted to thermal cycling, and bringing even a small turbine-generator to full load from a cold start can take four hours [18, p. II-11]. Therefore, the turbines are to be kept at "hot standby" condition overnight. Steam requirements for turbines maintained at "hot standby" are estimated to be 5% of the full-load steam requirements.[11]

2.1a Heat-Transfer Gas

Boeing Engineering and Construction developed their gas-cooled central receiver to heat pressurized helium gas kept at a working pressure of 3.45 MPa (500 psia). The reference design examined in this study adopts those choices for the heat-transfer fluid and operating

pressure. Important properties of helium gas are reviewed in Table 2-1. A study in Chapter 5 of the effect of operating pressure on the solar power plant supports the decision to operate at a system pressure of 3.45 MPa. Chapter 5 also evaluates the use of nitrogen and water vapor as alternative heat-transfer fluids. Problems associated with the use of water vapor as a heat-transfer fluid, including the possibility of brick deterioration due to formation of magnesium hydroxide and the condensation problems, resulted in the water vapor concept being dropped early in the study. A solar power plant using nitrogen as the heat-transfer fluid has been designed in detail and looks quite promising.

2.1b Sensible-Heat Storage Medium

Boeing Engineering and Construction examined the possibilities for high-temperature sensible-heat storage and concluded that refractory materials, particularly magnesia brick, laid in a checkerwork within pressure vessels offered a reasonable type of sensible-heat storage device for solar power plant applications.[4] Mr. Mikami of Kaiser Aluminum and Chemical Corporation was contacted for information about commercially available refractory materials which would be suitable for the sensible-heat storage application. His information on properties and costs of refractory materials is summarized in Table 2-2. Various refractory materials differ only slightly in their densities and specific heats. Low cost and relatively high thermal conductivity make magnesia brick the favored storage medium.

Table 2-1. Important Heat-Transfer Properties of Helium

Working Pressure:	3.45 MPa
Density $\Big\vert_{\text{working pressure}}^{600°K}$:	2.77 kg/m^3
Density $\Big\vert_{\text{working pressure}}^{1089°K}$:	1.52 kg/m^3
Thermal Conductivity $\Big\vert^{1089°K}$:	0.377 W/m°K (22, p. 3-215)
Heat Capacity $\Big\vert^{1089°K}$:	5200 J/kg·°K (22, p.3-215)
Gas Viscosity $\Big\vert^{1089°K}$:	4.8×10^{-5} N·s/m^2 (22, pp.3-210&3-211)
Prandtl Number:	0.64

Table 2-2. Properties of Refractory Bricks

Type of Brick	Magnesia	Alumina	Alumina-Chrome
Kaiser Brand*	K-98B	Kricor	Kritab
Standard Size, mm.	229×114×76	229×114×76	229×114×76
Density, kg/m^3	2930	3000	3200
Specific Heat $\Big\vert^{1000°F}$, J/kg°K	1067	1167	1000
Thermal Conductivity $\Big\vert^{1000°F}$, W/m°K	5.48	3.59	2.58
Price per Standard Size Brick, f.o.b. Plant, $	2.92	5.29	8.15

*Brick properties were obtained through contact with Kaiser Aluminum and Chemical Corporation.[26]

2.1c Thermal Insulation

Kaowool, in two different forms, has been chosen for insulating plant piping, power-generation heat exchangers, and storage vessels. Kaowool block capable of supporting the brick checkerworks is used for insulation inside the storage tanks. Elsewhere, kaowool-blanket insulation is used because its lower density results in decreased insulating costs. The properties of kaowool insulation are shown in Table 2-3. Literature data on the thermal conductivity of kaowool filled with air [3, p. 43] is used to estimate the thermal conductivity of nitrogen-filled kaowool. The thermal conductivity of kaowool filled with nitrogen is greater than the thermal conductivity of nitrogen but substantially less than the thermal conductivity of helium. Both forms of kaowool have very high porosity values, so the thermal conductivity of helium-filled kaowool is estimated to equal the thermal conductivity of helium. The error in this estimate should be no greater than the difference in thermal conductivity between nitrogen-filled kaowool and nitrogen gas (±25% at 1800°K, ±10% at 600°K).

2.1d Selection of Reasonable Pipe Diameters and Reasonable Insulation Thicknesses

Selection of reasonable pipe diameters, piping insulation thicknesses, and storage insulation thicknesses requires a series of economic assumptions relating energy losses and plant capital costs to energy values and annual operating costs. Power plant capitalization is assumed to require 14% of the total capital investment annually. An additional 4% of the total capital investment is allowed annually to cover plant operating and maintenance expenses. Increased capital

Table 2-3. Properties of Kaowool Insulation

	Kaowool Block	Kaowool Blanket	Heat Transfer Gas
Insulation Density, kg/m^3	240[1]	130[1]	
Estimated Insulation Porosity	~90%[2]	~95%[2]	
Thermal Conductivity When Filled With With $N_2\|^{1089°K}$, W/m°K	0.137[1]	0.167[1]	0.070[3]
Thermal Conductivity When Filled With $N_2\|^{600°K}$, W/m°K	0.069[1]	0.064[1]	0.045[3]
Estimated Thermal Conductivity When Filled With $He\|^{600°K}$, W/m°K	0.25[4]	0.25[4]	0.25[3]
Kaowool Installed Cost as of June, 1978, $/kg	12.8[5]	12.8[5]	

Estimation Procedures and References:

[1] Reference 3, p.43

[2] Kaowool porosity was estimated assuming the crystalline density was 2500 kg/m^3. (2500 kg/m^3 is the density for calcium metasilicate (β), a common insulating material).

[3] Reference 22, p. 3-215

[4] The thermal conductivity of helium-filled Kaowool is estimated to equal the thermal conductivity of helium. The error in this estimate should be no greater than the difference between the thermal conductivity of N_2 and the thermal conductivity at N_2 filled Kaowool [±25% at 1089°K, ±10% at 600°K].

[5] Reference 2, p. 2-23

investment can be justified only if the annual reduction in the value of energy losses is greater than 18% of the increased investment. Values of \$100 per MW_e-hr for electric energy and \$40 per MW_t-hr for thermal energy are used in the optimization studies.

2.1e Reference Solar Power Plant Design

Table 2-4 summarizes the reference design for this solar power plant and elaborates on the design of the sensible-heat storage unit. Optimization studies which were important in choosing the storage insulation thickness and the total cross-sectional area of gas-flow channels through storage are explained in Chapter 5. The choices of 1510 MW_t-hr energy capacity for storage, and use of helium for the heat-transfer fluid were both arbitrary. Welded carbon-steel tanks were chosen for the reference design because of their proven reliability. Preliminary investigation on the use of prestressed cast-iron storage vessels indicates that this new storage vessel concept may improve performance while cutting the total cost of the sensible-heat storage unit in half.

2.2 POWER PLANT FLOWSHEET

The proposed flowsheet for a solar power plant that converts thermal energy into electric energy is shown in Fig. 2-1. Daytime and nighttime power plant operations are described below with a detailed explanation of how a constant output from the steam turbines is maintained. Equipment design for the proposed solar power plant is explained in Chapter 4.

Table 2-4. Reference Solar Power Plant Design

Heliostats and Central Receiver:	Modification of Boeing's High-Temperature, Gas-Cooled Central Receiver Design
Energy Storage:	Sensible-Heat Storage Unit (described below)
Heat Exchangers:	Conventional Designs with heat-transfer gas shell side.
Power Generation:	811°K/811°K, 124 bars, High-Back pressure Turbine-Generator
Cooling Tower:	Dry-Cooling Tower
Heat-Transfer Fluid:	Helium at an operating pressure of 34.5 bars.
Piping:	Welded, Carbon-Steel piping with internal Kaowool-Blanket Insulation
Gas Compression:	Single-stage, Axial Compressor

Approximate Heat and Energy Balances (Ignoring Losses and Compressive Heating)

Heat Absorbed in the Receiver, Charge:	441 MW_t for 8 hours
Heat Stored in the Storage Unit, Charge:	189 MW_t for 8 hours
Heat Released from the Storage Unit, Discharge:	252 MW_t for 6 hours
Heat Transferred to Power Generation:	252 MW_t for 14 hours
Gross Power Generation:	100 MW_e for 14 hours
Storage Capacity:	1500 MW_e-hr per cycle
Simplified Solar Model:	Constant Heat input to the receiver 8 hours per day, 256 days per year

Table 2-4 (Cont'd.)

Design Heat Transfer Gas Temperatures	
Entering the heat exchanger network -	867°K
Leaving the heat exchanger network -	600°K
Leaving the receiver, charge -	1089°K
Leaving the storage unit, charge -	600°K-867°K
Leaving the storage unit, discharge -	1089°K-867°K
Input Parameters for the Sensible-Heat Storage Unit Design	
Storage Capacity -	1500 MW_t-hr per cycle
Time Required for Charging at a Constant Rate -	8 hours
Time Required for Discharging at a Constant Rate -	6 hours
Inlet Gas Temperature, Charging -	1089°K
Maximum Outlet Gas Temperature, Charging -	867°K
Inlet Gas Temperature, Discharging -	600°K
Minimum Outlet Gas Temperature, Discharging -	867°K
Sensible-Heat Storage Media -	Magnesia Bricks
Storage Unit Insulation -	Kaowool Block
Cross Section of each Brick -	76 mm × 114 mm
Cross Section of each Gas-Flow Channel -	20.5 mm × 114 mm
Total Cross-Sectional Area of the Brick Checkerwork -	56.5 m^2
Total Cross-Sectional Area for Gas Flow Through Storage -	12.0 m^2
Total Channel Perimeter Through Storage -	1380 m
Channel Perimeter Assumed Effective for Heat Transfer -	1170 m

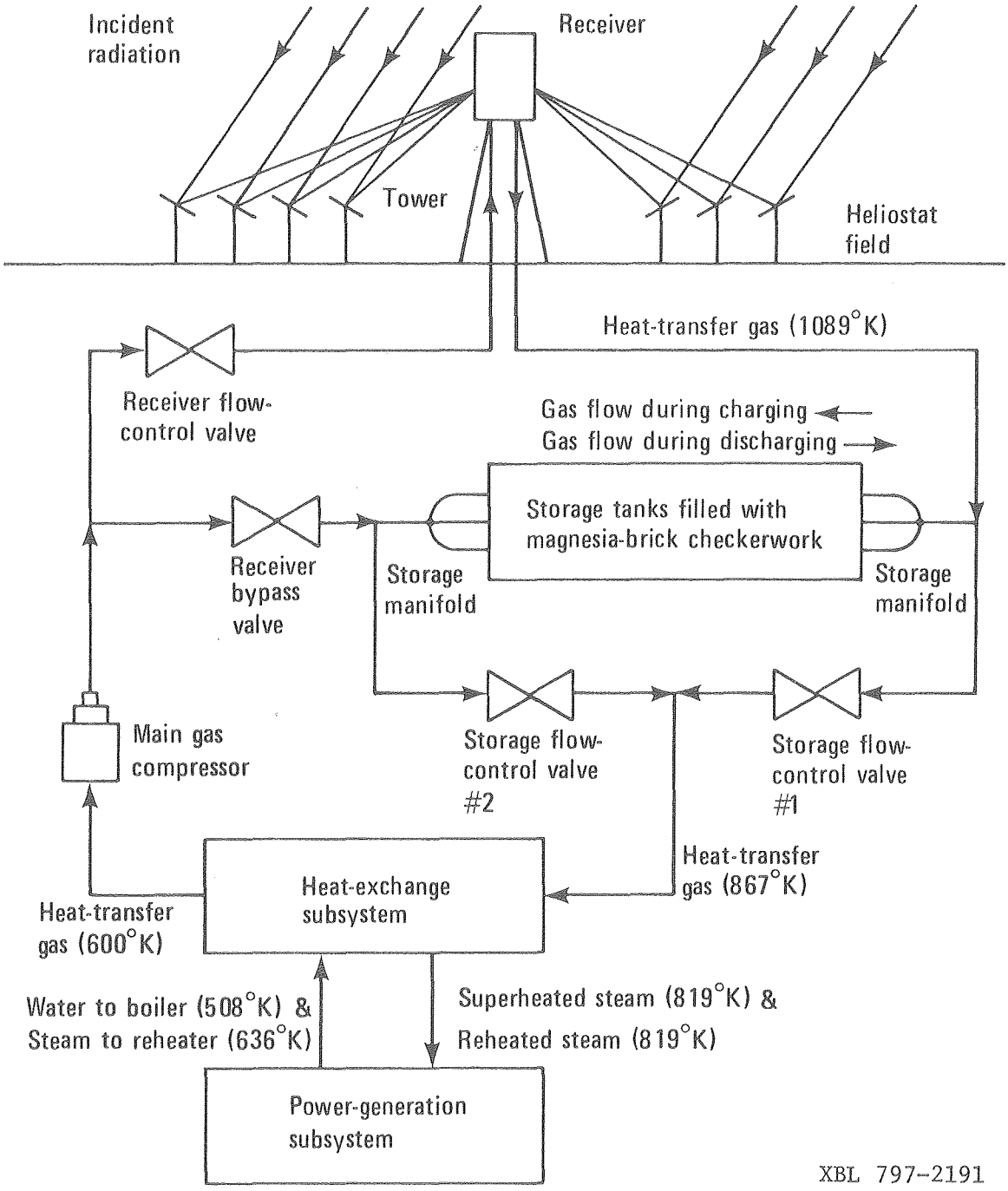

Fig. 2-1. The proposed flowsheet for a solar power plant with sensible-heat storage. The heat-transfer gas temperatures shown are for the reference design for a solar power plant summarized in Table 2-4.

2.2a Daytime Power Plant Operation

During the daytime, thermal energy is absorbed in the central receiver, then transferred to the storage or power-generation units. Heat-transfer gas, leaving the heat-exchange network at a temperature of 600°K, is compressed and heated by the main gas compressor. Most of this gas is sent to the central receiver to absorb thermal energy, although a portion bypasses both the central receiver and the storage unit to temper the inlet-gas temperature to the power-generation heat exchangers. Gas leaves the receiver at an outlet temperature of 1089°K and flows to the storage unit. There the gas flow is split, with part of it transferring energy to the storage unit. The gas temperature leaving storage rises from 600°K early in the morning to 880°K at the end of the charge cycle. The temperature of the gas stream entering the heat exchangers is maintained constant at 867°K by continually adjusting the proportion of gas which bypasses storage. The heat exchangers use energy obtained from cooling the heat-transfer gas to produce the steam required to operate the turbine-generator.

2.2b Nighttime Power Plant Operation

Nighttime power generation is provided by releasing thermal energy from the sensible-heat storage unit. Cool heat-transfer gas leaving the heat-exchange network at 600°K is recompressed by the main gas compressor and sent to storage. The flow is then split into a stream that bypasses storage and a stream that goes through the storage unit. These two streams are mixed and returned to the heat exchangers. The direction of gas flow through storage is reversed during discharge,

in order to reduce the storage unit size. The storage unit outlet-gas temperature drops from 1089°K to 867°K during discharge. A constant inlet-gas temperature of 867°K to the heat exchangers is maintained by adjusting the proportion of the gas bypassing storage.

3. ANALYSIS AND COMPUTER DESIGN OF THE STORAGE UNIT

This chapter describes the principles underlying storage operation and presents a mathematical model which has been used as the basis for computer design and simulation of the sensible-heat storage unit. Details of the implementation of this computational model, including flow diagrams, a program source listing, and sample output, are given in Appendix II. Chapter 4 includes vessel and piping designs for the storage unit.

3.1 STORAGE OPERATION

The sensible-heat storage unit consists of a group of pressure vessels insulated on the inside and filled with magnesia bricks. The bricks are laid in a checkerwork with thin vertical channels between adjacent bricks as shown in Figure 3-1. These channels allow gas flow through the brickwork and provide heat-transfer area between the bricks and the gas. Thermal energy is transferred from the gas to the bricks during the day, then released to allow nighttime power generation.

Cyclic operation is anticipated for the sensible-heat storage unit. Figures 3-2 and 3-3 show the dependence of brick and gas temperatures on axial position in the brick bed at several times during the charge and discharge cycles. These temperature profiles were obtained using the storage analysis developed below, and are mentioned here to show the wave nature characteristic of the charging and the discharging of the storage unit. Further information on solar power plant operation during charging of the storage unit is contained in Figs. 3-4 and 3-5. Figure 3-4 shows that the temperature of gas leaving the storage unit

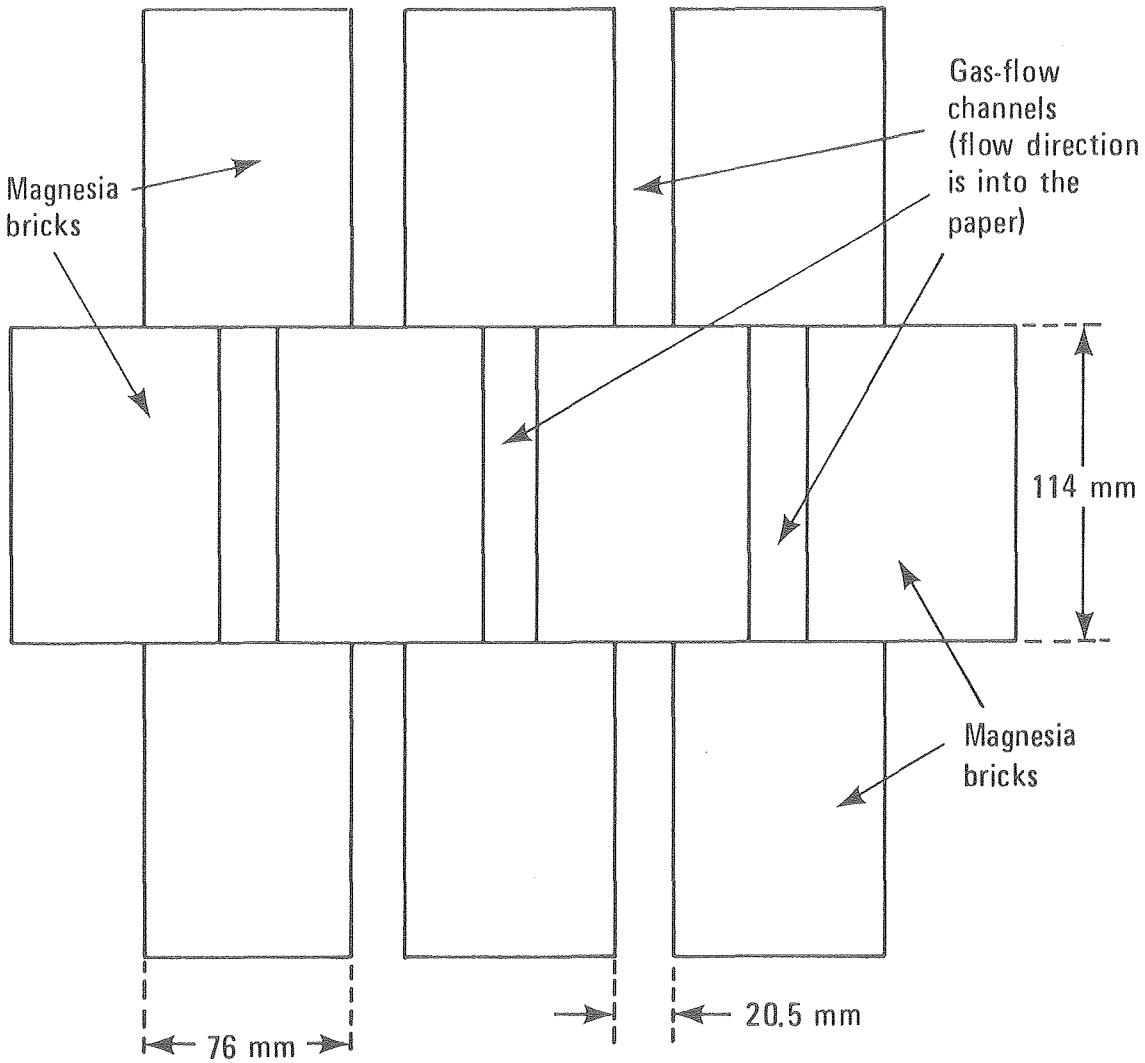

XBL 797-2188A

Fig. 3-1. A cross-sectional detail of the checkerwork of magnesia bricks. The bricks and channels for gas flow both extend lengthwise into the paper.

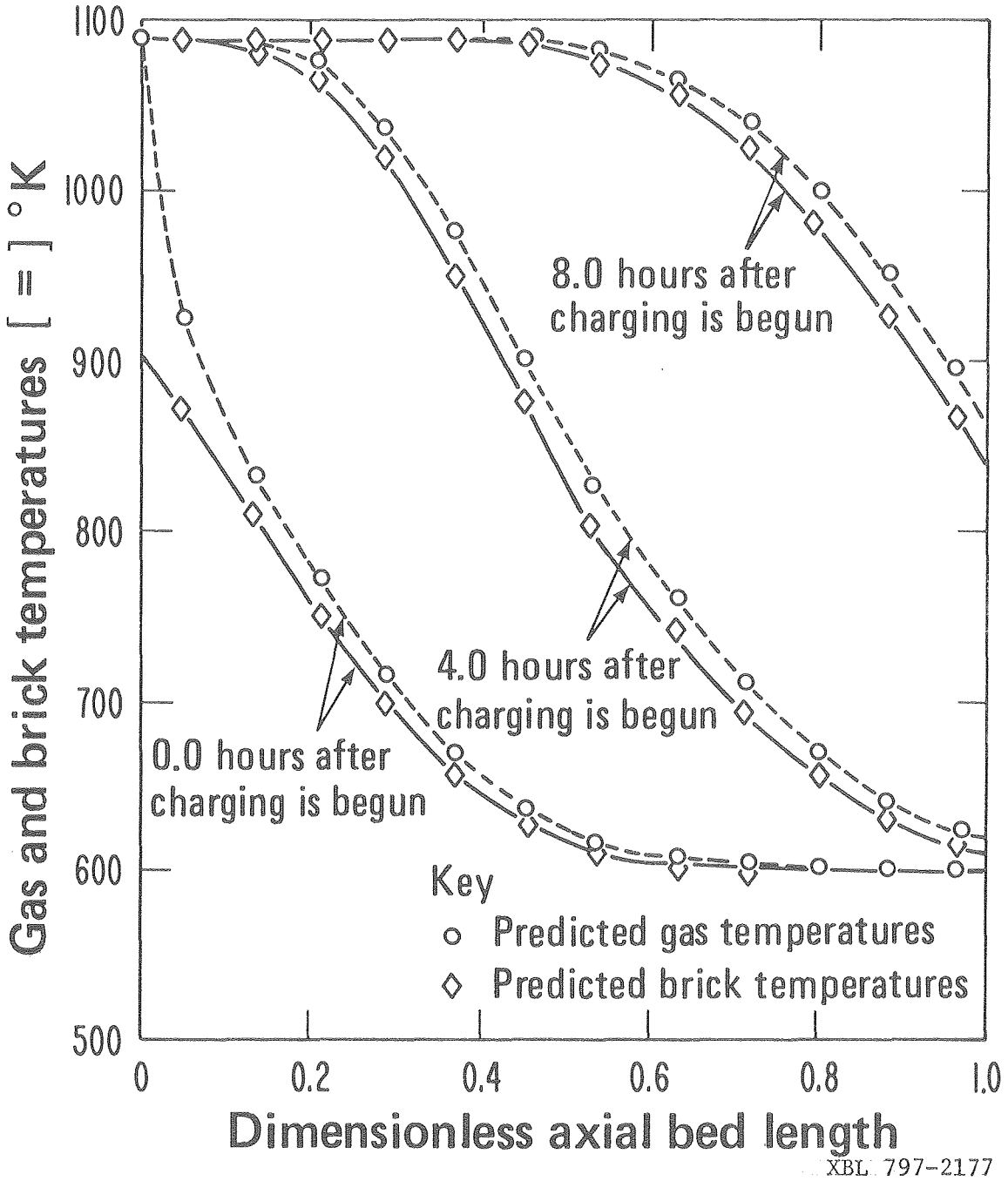

Fig. 3-2. Predicted gas and brick temperatures during charging of the sensible-heat storage unit. Gas flows through the storage unit during charging in the direction of increasing dimensionless axial bed length. Three sets of curves show the predicted gas and brick temperature profile at different time intervals after charging is begun. These temperature profiles were predicted based on the solar power plant design described in Table 2-4.

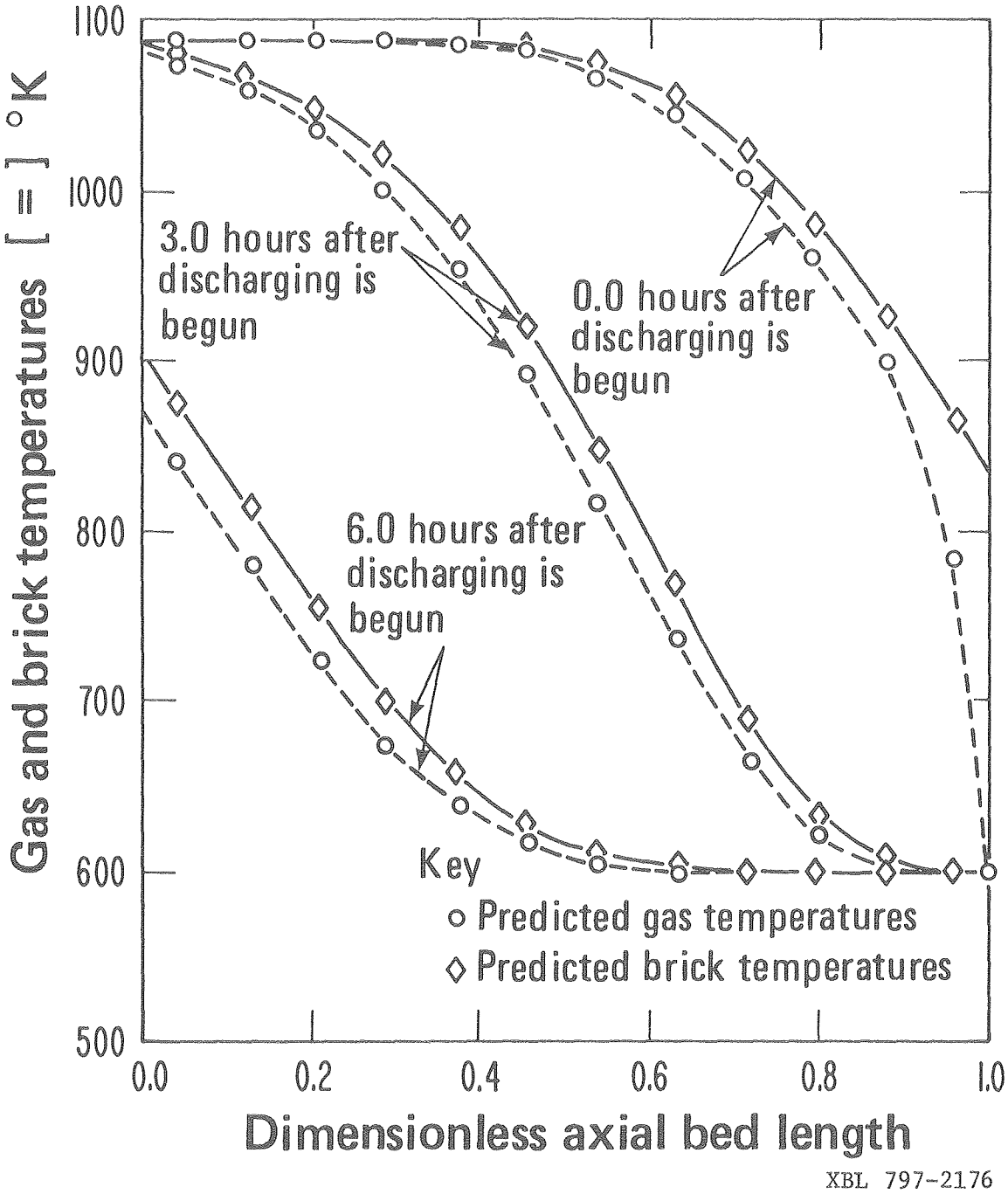

Fig. 3-3. Predicted gas and brick temperatures during discharging of the sensible-heat storage unit. Gas flows through the storage unit during discharging in the direction of decreasing dimensionless axial bed length. Three sets of curves show the predicted gas and brick temperature profiles at different time intervals after discharging is begun. These temperature profiles were predicted based on the solar power plant design described in Table 2-4.

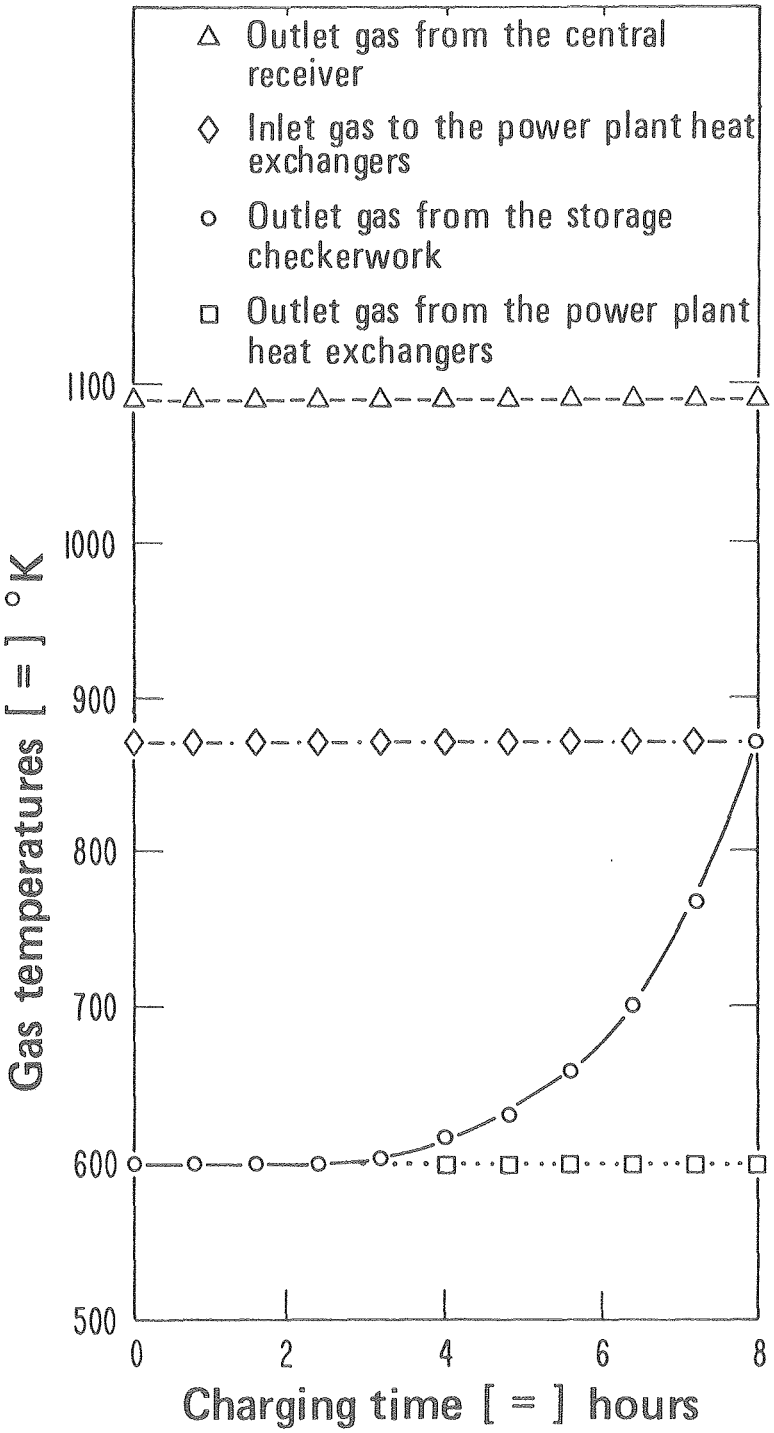

XBL 797-2179

Fig. 3-4. Predicted gas temperatures during charging of the storage unit. These gas temperatures were predicted based on the proposed design for a solar power plant shown in Table 2-4.

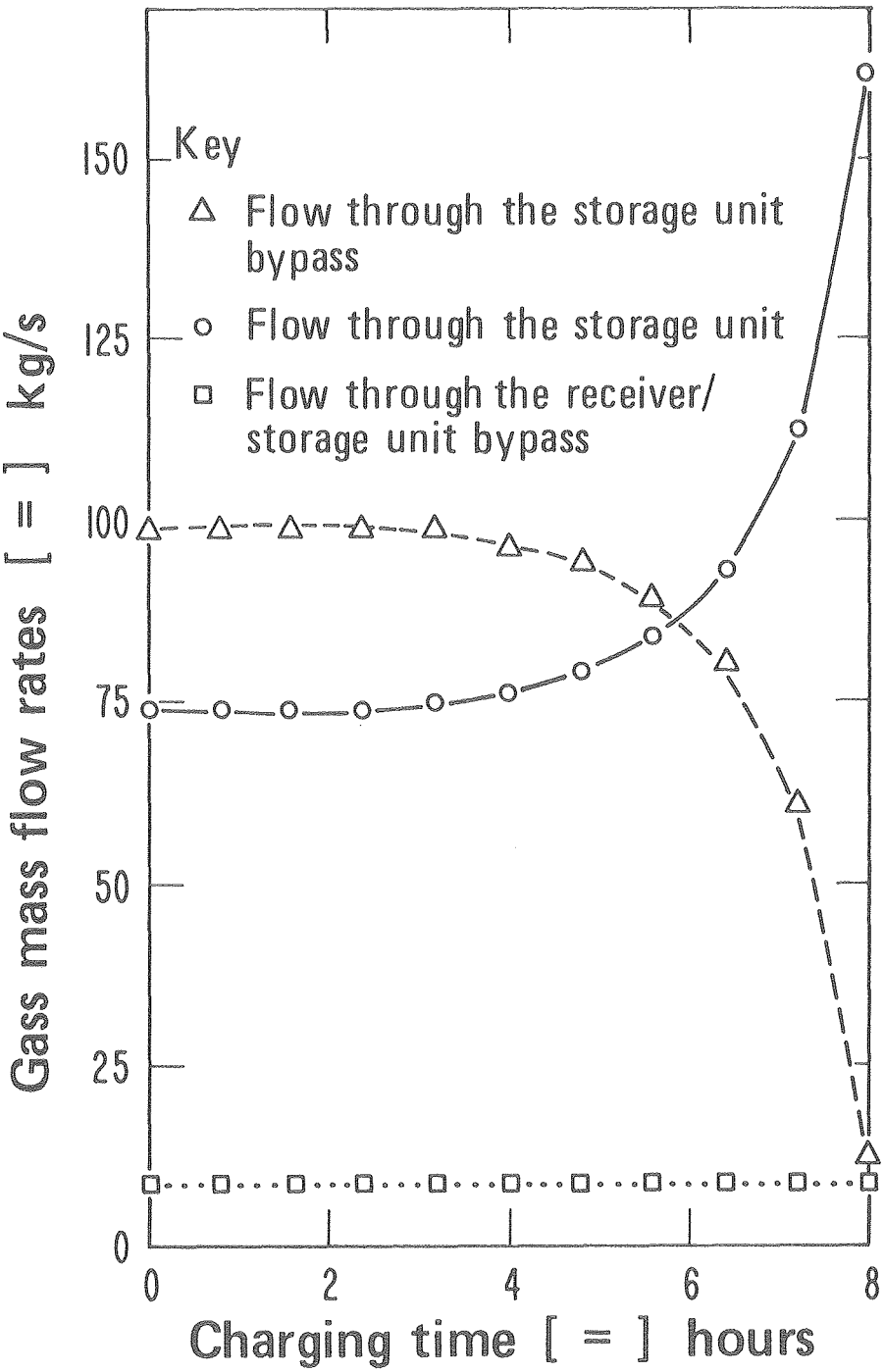

Fig. 3-5. Predicted gas mass flow rates during charging of the storage unit. These gas mass flow rates were predicted based on the proposed design for a solar power plant shown in Table 2-4.

slowly rises from 600°K to 880°K in the second half of the charging cycle. The temperature of gas being sent to the heat exchangers is kept constant at 867°K by adjusting the gas mass flow rates through and bypassing the storage unit. The necessary flow rate adjustments to be made during charging of the sensible-heat storage unit are displayed in Fig. 3-5. Gas leaves the storage unit at a constant temperature of 880°K and is then mixed with a small gas stream that bypasses both the receiver and the storage unit.

3.2 A MATHEMATICAL MODEL FOR STORAGE ANALYSIS AND DESIGN

Storage operation has been analyzed by simultaneous solution of two coupled differential equations. The first differential equation arises from an energy balance over a control volume consisting of an incremental length of the storage unit. The second differential equation has been obtained by noting that the rate of energy accumulation within the brick portion of the control volume will be determined by the effective local heat flux from the gas to the bricks and by the amount of interfacial area that is effective for heat transfer. A simplified model has been developed to estimate the effective local heat flux and effective interfacial heat-transfer area.

Consider the control volume shown in Fig. 3-6, $(A_{brick} + A_{channel})\Delta Z$, consisting of incremental volumes of storage bricks, $A_{brick}\Delta Z$, and of gas flow channels, $A_{channel}\ \Delta Z$. Equation 1 expresses the rate of thermal energy accumulation within the control volume.

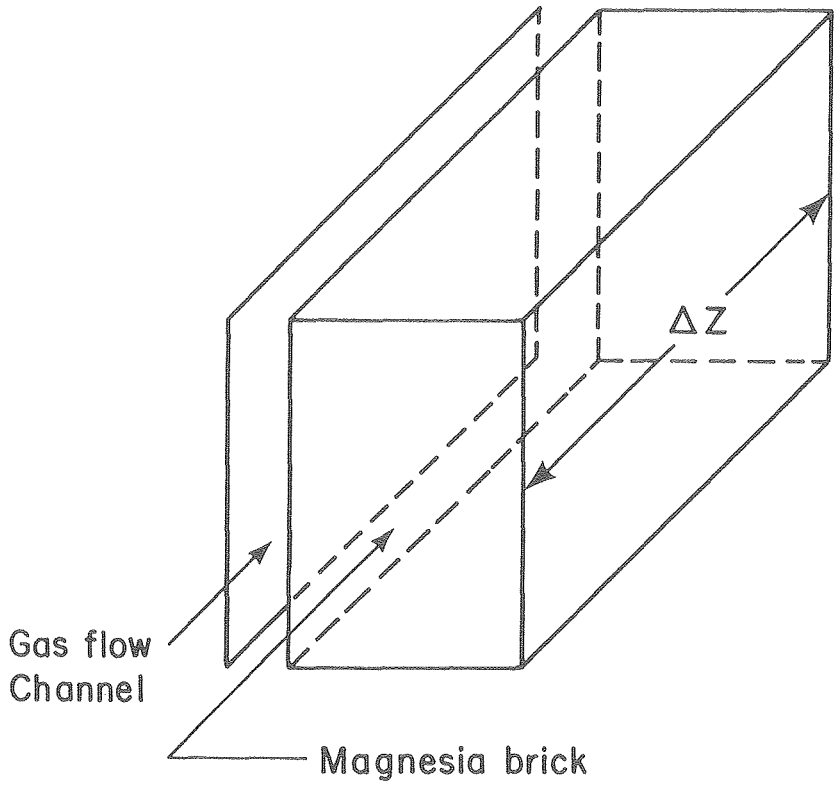

XBL 797-2185

Fig. 3-6. A three-dimensional detail of the brick checkerwork control volume. The total cross-sectional area for gas flow through storage, $A_{channel}$, and the total brick cross-sectional area through storage, A_{brick}, are determined by multiplying the cross-sectional areas shown by the number of flow channels through storage.

$$\text{Rate of thermal energy accumulation in the control volume} = \frac{\partial(C_{brick} \cdot (A_{brick} \cdot \Delta Z \cdot \rho_{brick}) \cdot T_{avg,brick}(\theta,Z))}{\partial\theta} + \frac{\partial(C_{V,gas} \cdot (A_{channel} \cdot \Delta Z \cdot \rho_{gas}(\theta,z)) \cdot T_{gas}(\theta,Z))}{\partial\theta} \quad (1)$$

This equation can be simplified, since thermal energy accumulation in the gas is a negligible fraction of the total accumulation in the control volume.

$$\text{Rate of thermal energy accumulation in the control volume} = \frac{\partial(C_{brick} \cdot (A_{brick} \cdot \Delta Z \cdot \rho_{brick}) \cdot T_{avg,brick}(\theta,Z))}{\partial\theta} \quad (2)$$

Neglecting diffusion, the net rate of heat transport into the control volume is:

$$\text{Net rate of energy transport into the control volume} = -\dot{M}_{gas}(\theta,Z) \cdot C_{p,gas} \cdot T_{gas}(\theta,Z)\Big|_{Z}^{Z+\Delta Z} \quad (3)$$

For small incremental lengths Eq. (3) can be rearranged in differential form.

$$\text{Net rate of energy transport into the control volume} = -\frac{\partial \dot{M}_{gas}(\theta,Z) \cdot C_{p,gas} \cdot T_{gas}(\theta,Z)}{\partial Z} \cdot \Delta Z \quad (4)$$

An energy balance for the control volume demands that the rate of thermal energy accumulation within the control volume equal the net rate of energy transport into the control volume.

$$\frac{\partial(C_{brick} \cdot (A_{brick} \cdot \Delta Z \cdot \rho_{brick}) \cdot T_{avg,brick}(\theta,Z))}{\partial\theta} = -\frac{\partial \dot{M}_{gas}(\theta,Z) \cdot C_{p,gas}(\theta,Z) \cdot T_{gas}(\theta,Z)}{\partial Z} \cdot \Delta Z \quad (5)$$

The brick and gas heat capacities, cross-sectional area of the brick checkerwork and brick density are all constant for the anticipated operating conditions. The gas mass flow rate is strongly dependent on time, but has only a negligible dependence on position. This dependence of the gas mass flow rate on position is caused by a slow change in the mass of gas contained within the checkerwork as the storage unit changes temperature. The first design equation, Eq. A, is a rearrangement of Eq. (5) based on these observations.

$$\frac{\partial T_{gas}(\theta,Z)}{\partial Z} = - \frac{C_{brick} \cdot A_{brick} \cdot \rho_{brick}}{\dot{M}_{gas}(\theta) \cdot C_{p,gas}} \cdot \frac{\partial T_{avg,brick}(\theta,Z)}{\partial \theta} \qquad (A)$$

Development of the second design equation is begun by noting that the net rate of energy accumulation within control volume bricks can be related to the effective local heat flux density from the gas to the bricks and to the effective interfacial heat-transfer area.

$$C_{brick} \cdot (A_{brick} \cdot \Delta Z \cdot \rho_{brick}) \frac{\partial T_{avg,brick}(\theta,Z)}{\partial \theta} = q_{eff}(\theta,Z) \cdot P_{eff} \cdot \Delta Z \qquad (6)$$

Figure 3-7 illustrates the model chosen to represent heat transfer between the gas and the bricks. Figure 3-7(a) shows that heat transfer in the vertical direction is ignored. Only the sides of the magnesia bricks are assumed to provide heat-transfer surfaces which can be included in determining the effective heat-transfer perimeter. Using this assumption, about 85% of the total interfacial area provides

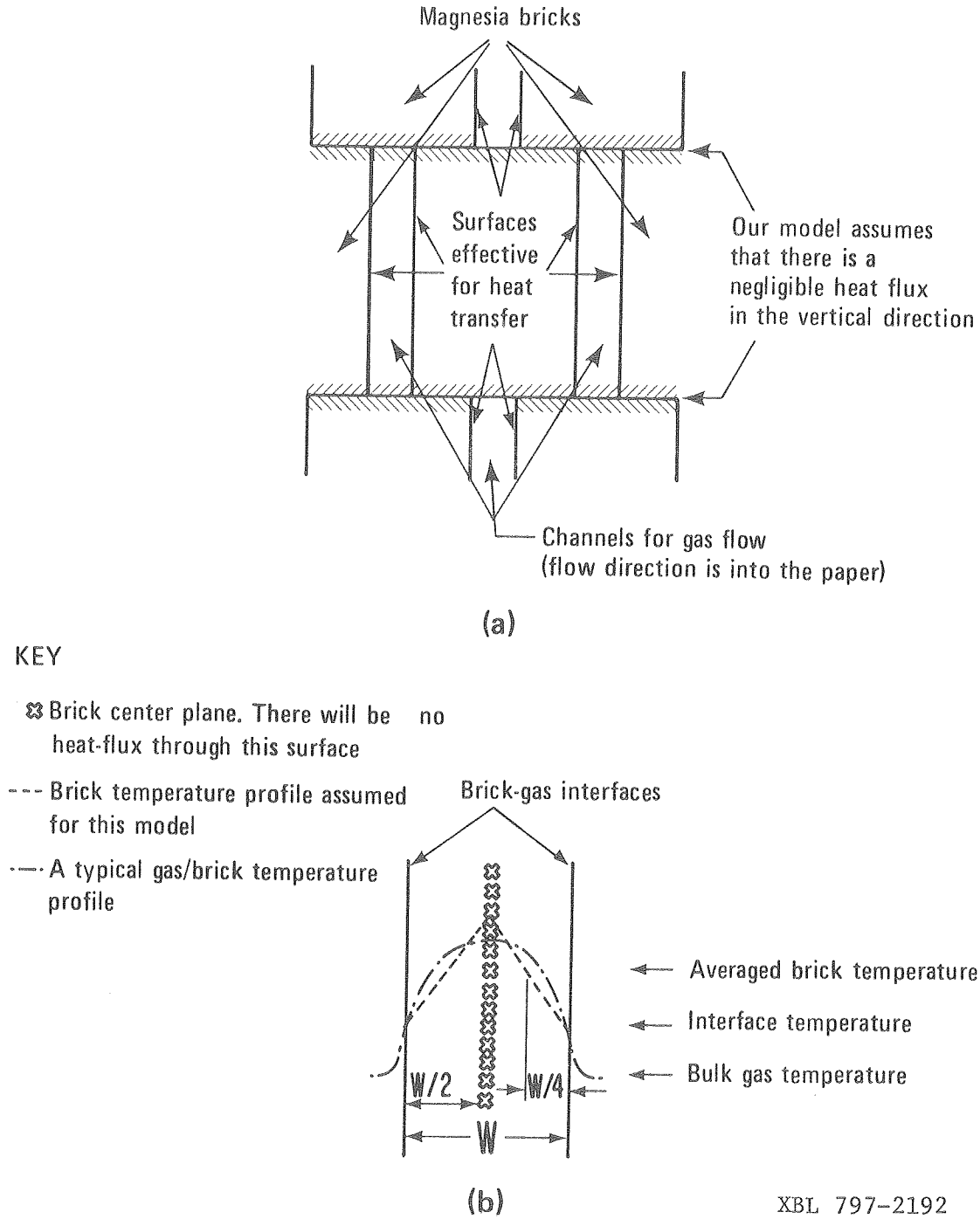

Fig. 3-7. Cross-sectional views of the proposed model for heat transfer between the bricks and the gas; (a) is the model used to determine the interfacial area which provides effective heat transfer between the bricks and the gas and (b) is the model used to estimate the change in brick temperature with distance from the interface, based on an assumed brick temperature profile.

effective heat-transfer area. Determination of the effective local heat flux density is more complicated. First, the effective local heat flux density is related to the gas film heat-transfer coefficient and an unknown interface temperature.

$$q_{eff}(\theta,Z) = h_{gas}(\theta,Z)\cdot(T_{gas}(\theta,Z) - T_{interface}(\theta,Z)) \qquad (7)$$

Gas Reynolds numbers in the proposed storage unit range from 4,500 to 16,000. The gas film heat-transfer coefficient is estimated using an empirical correlation presented by Sieder and Tate for fully turbulent fluid flow in pipes [23, p. 542]. This correlation overestimates heat transfer for the low Reynolds number conditions by about 20%.

$$h_{gas}(\theta,Z) = 0.023\cdot K_{gas}(\theta,Z)\cdot Re(\theta,Z)^{0.8}\cdot Pr^{0.333}/D \qquad (8)$$

The effective local heat flux density is then related to the thermal conductivity of the brick and temperature gradient in the brick at the interface.

$$q_{eff}(\theta,Z) = K_{brick} \cdot \left.\frac{\partial T_{brick}(\theta,Z,X)}{\partial X}\right|_{interface} \qquad (9)$$

An approximation method is used to determine the temperature gradient in the brick at the interface which assumes that the temperature gradient is constant in either half width of the brick. This model underestimates the expected temperature gradient at the interface as shown in Fig. 3-7(b) since it corresponds to all of the available heat being transferred to the center plane of the brick.

$$\left.\frac{\partial T_{brick}(\theta,Z,X)}{\partial X}\right|_{interface} = \frac{T_{interface}(\theta,Z)-T_{avg,brick}(\theta,Z)}{(W/4)} \qquad (10)$$

$$q_{eff}(\theta,Z) = K_{brick} \cdot \frac{T_{interface}(\theta,Z) - T_{avg,brick}(\theta,Z)}{(W/4)} \qquad (11)$$

Simultaneous solution of Eqs. (7) and (11) is used to eliminate the unknown interface temperature.

$$q_{eff}(\theta,Z) = U_o(\theta,Z)\cdot(T_{gas}(\theta,Z) - T_{avg,brick}(\theta,Z)) \qquad (12a)$$

where

$$U_o(\theta,Z) = 1/(1/h_{gas} + (W/4)/K_{brick}) \qquad (12b)$$

The small dependence of the overall heat-transfer coefficient on position (±5%) due to changes in gas temperature is ignored in modeling the storage unit. The second design equation is now derived by substituting Eqs. (12a) and (12b) into Eq. (6).

$$\frac{\partial T_{avg,brick}(\theta,Z)}{\partial \theta} = \frac{U_o(\theta)\cdot\rho_{eff}}{C_{brick}\cdot A_{brick}\cdot\rho_{brick}} \cdot (T_{gas}(\theta,Z) - T_{avg,brick}(\theta,Z)) \qquad (B)$$

The proposed model was derived under a series of assumptions which could lead to significant errors in the estimation of the heat flux at any given position and time. The error that these assumptions make in final sizing of the storage unit, however is expected to be minimal.

One parameter study presented in Chapter 5-2 investigated the effects of varying the cross-sectional area for gas flow through the storage checkerwork. Even when the length of the storage unit is increased by a factor of six and the overall heat-transfer coefficient is approximately doubled the size of the storage unit changes by only 10%.

3.3 COMPUTER DESIGN OF THE SENSIBLE-HEAT STORAGE UNIT

A computer program, HREGEN, was developed to estimate the size of the energy-storage unit required for the proposed solar power plant. HREGEN flow diagrams, a source listing, and a sample output are included in Appendix II. This section explains the design approach selected for computer modeling of the storage unit. Pertinent information relating to computer design calculations is reviewed in Chapter 3.4.

The key to modeling the energy storage unit lies in the ability to rearrange and interatively solve finite-difference forms of Eqs. A and B. Rearranging these equations allows determination of the bulk gas temperature at time θ and position $Z+\Delta Z$ and allows determination of the mass-averaged brick temperature for an incremental volume of bricks at time $\theta+\Delta\theta$ and position Z, from knowledge of the average brick and bulk gas temperatures at time θ and position Z.

$$T_{gas}(\theta,Z+\Delta Z) = T_{gas}(\theta,Z) - \frac{U_o \cdot P_{eff} \cdot \Delta Z}{\dot{M}_{gas}(\theta) \cdot C_{p,gas}} \cdot (T_{gas}(\theta,Z) - T_{avg,brick}(\theta,Z)) \qquad (I)$$

$$T_{avg,brick}(\theta+\Delta\theta,Z) = T_{avg,brick}(\theta,Z) - \frac{U_o \cdot P_{eff} \cdot \Delta\theta}{C_{brick} \cdot A_{brick} \cdot \rho_{brick}} \cdot$$

$$(T_{gas}(\theta,Z) - T_{avg,brick}(\theta,Z)) \qquad \text{(II)}$$

Use of Eqs. (I) and (II) to model the storage unit requires estimation of the initial average brick temperatures at all length increments, and knowledge of gas inlet temperatures at all time increments.

Design of a storage unit is begun by guessing what the mass-averaged brick temperatures for the entire bed will be before and after charging. These guesses are used to estimate storage unit size and the initial mass-averaged brick temperatures for incremental lengths of the storage unit. A subroutine, HRGCRG, then models the storage charging cycle. Hot gas is passed through the storage unit, with the gas mass flow rate being adjusted to store thermal energy at a specified rate. This is continued until all the available energy has been stored. The mass-averaged brick temperature for the entire bed after charging should match the guess made earlier. Storage discharge is then modeled by another subroutine, HRGDIS. The gas flow direction is reversed and cool gas is passed through the unit. The rate of thermal-energy discharge is controlled by continually adjusting the gas mass flow rate through storage. Discharge is stopped when the gas temperature exiting from storage drops to the specified minimum value. This method of determining when to stop storage discharge is expected to improve the estimated mass-averaged brick temperature profile before charging after

each modeling of a complete charge/discharge cycle. A new estimate for the entire bed mass-averaged brick temperature before charging will also be obtained, unless the energy discharged from storage exactly equals the energy charged to storage.

The proposed sensible-heat storage unit is designed for cyclic operation. This means that identical mass-averaged brick temperature profiles are expected before and after each complete charge/discharge cycle. Our model relaxes this requirement and only demands that the mass-averaged brick temperature for the entire bed before charging should be almost equal before and after the charge/discharge cycle. This criterion is checked by comparing the amount of energy stored during charge to the amount of energy released during discharge. The second design criterion used for determining if an adequate storage design has been found is that the gas temperature exiting from storage at the end of the charge cycle should almost equal the desired value.

Design of the storage unit proceeds as follows. Pertinent design data on the storage unit and proposed operating conditions are established. Inlet gas temperatures to storage, and thermal energy transfer rates between the gas and the storage unit are specified for both the charge and the discharge cycles. The desired gas temperatures exiting from storage at the end of the charge and discharge cycles are also chosen. Finally, storage-unit, heat-transfer-gas, and magnesia-brick physical properties are specified. Control of the storage unit design is next assumed by program subroutine DESIGN. DESIGN makes initial estimates for the entire bed mass-averaged brick temperatures

before and after charging. The storage unit is sized and initial mass-averaged brick temperatures for incremental storage lengths are estimated. DESIGN then calls the storage charging model, subroutine HRGCRG, and the storage discharging model, subroutine HRGDIS. HRGDIS stops storage discharging when the exiting gas temperature falls to the minimum acceptable level. This model feature automatically adjusts the entire bed mass-averaged brick temperature before charging upon completion of each charge/discharge cycle. The storage design criteria are now checked. If both criteria are met, storage design is considered to be complete. Otherwise, the entire bed mass-averaged brick temperature after charging is reestimated based on the deviation of the gas temperature exiting storage at the end of charging from the desired value. The storage unit is then resized, and storage charging and discharging models are called again to be used with these new data.

3.4 DETAILS ON COMPUTER DESIGN CALCULATIONS

The computer program, discussed above and in Appendix II, was run on a CDC 7600 computer. When time was discretized into 300 increments and length was discretized into 300 increments, 2.7 seconds of computing time was required for modeling a complete charge/discharge cycle. The two design criteria used for determining when storage was accurately modeled were that the gas temperature exiting from storage at the end of the charge cycle should approach a desired value and that the energy stored during charging should almost equal the energy released during discharging. These criteria were normalized by dividing by the range of gas temperatures and by the energy stored during charging,

respectively. The computer design model reduced the error in both normalized criteria to less than 0.4% within 4 charge/discharge cycles and subsequent parameter readjustments.

The error in computer modeling caused by use of a finite number of time and length increments is expected to result in less than 2% error in estimation of the storage unit size. This error estimate is based on the data shown in Table 3-1. The actual change in estimated storage unit size when the number of time and length increments were cut in half was 1.2%.

Table 3-1. The Effects of Varying the Number of Time and Length Increments on Storage Size

	Reference Design	Vary the number of time increments		Vary the number of length increments		Vary length and time increments	
Number of time increments	300	200	150	300	300	200	150
Number of length increments	300	300	300	204	156	204	156
Fraction of total time per increment	0.0033	0.0050	0.0067	0.0033	0.0033	0.0050	0.0067
Fraction of total length per increment	0.0033	0.0033	0.0033	0.0050	0.0067	0.0050	0.0067
Storage Weight (10^6 kg, brick)	13.81	13.77	13.74	13.76	13.72	13.73	13.64
Change in storage size relative to reference design	---	-0.3%	-0.5%	-0.35%	-0.65%	-0.6%	-1.2%

4. DESIGN OF THE POWER PLANT SUBSYSTEMS

The flowsheet to be studied and the guidelines for power plant eration have been presented in Chapter 2. For conceptual purposes, e flowsheet (see Fig. 2-1) has been broken down into five subsystems. ie heat-exchange and power-generation subsystems are shown on Fig. 2-1 s boxes, and are described more fully in this chapter. The heat- ollection subsystem uses heliostats and a central receiver mounted n top of a tower to concentrate sunlight for warming heat-transfer luid to a high temperature. The sensible-heat storage subsystem alternately stores or releases thermal energy. This subsystem consists of two storage flow-control valves, two gas-distribution storage manifolds and a number of storage tanks filled with magnesia-brick checkerwork. The final subsystem is the gas-circulation subsystem, which includes the main gas compressor, the receiver flow-control valve, the receiver bypass valve, and gas piping for the heat-collection, sensible-heat storage, and heat-exchange subsystems.

This chapter presents design considerations, proposed designs, and cost estimates for each of the subsystems mentioned above. Expected energy losses are also discussed. The discussion in this chapter is centered on a system that meets the specifications laid out in Table 2-4. Chapter 5 summarizes a series of parametric studies of the ways that plant costs and energy losses are affected by the heat-transfer gas chosen, by the pressure of the heat-transfer gas, by the cross-sectional area for gas flow through the storage medium, and by the rate at which storage is discharged.

4.1 THE HEAT-COLLECTION SUBSYSTEM

Concentration of sunlight and collection of the concentrated energy at a high temperature is the basis of operation for a central solar thermal power plant. A variety of heliostat and central receiver designs have been proposed for study.[3,17] The proposed solar power plant uses a modified scale-up of the closed-cycle, high-temperature central receiver design proposed by Boeing Engineering and Construction.[3] This section reviews the central receiver design that Boeing has proposed, and discusses the effects of operational modifications on the performance of the heat-collection subsystem.

Conceptual design of the Boeing high-temperature central receiver is shown in Fig. 4-1. A cavity-type receiver design is employed to reduce reradiation from the receiver to the surroundings. Computer-directed heliostats reflect solar radiation through the aperture to the lower walls of the cavity. This energy then reflects or reradiates within the cavity until it is absorbed as heat by gas flowing through the heat-exchange tubes or it is lost to the surroundings. Estimated heat losses total 15% of the solar energy input to the receiver.[3] These losses are caused by reflection and reradiation out of the aperture, convective losses to the air from the receiver aperture, and conductive losses through the walls of the receiver cavity.

An accurate determination of heat transfer within the receiver cavity is difficult to obtain due to the complexities of energy reflection and reradiation between the inner cavity walls and the heat-exchange tubes. Boeing analyzed their central receiver design with

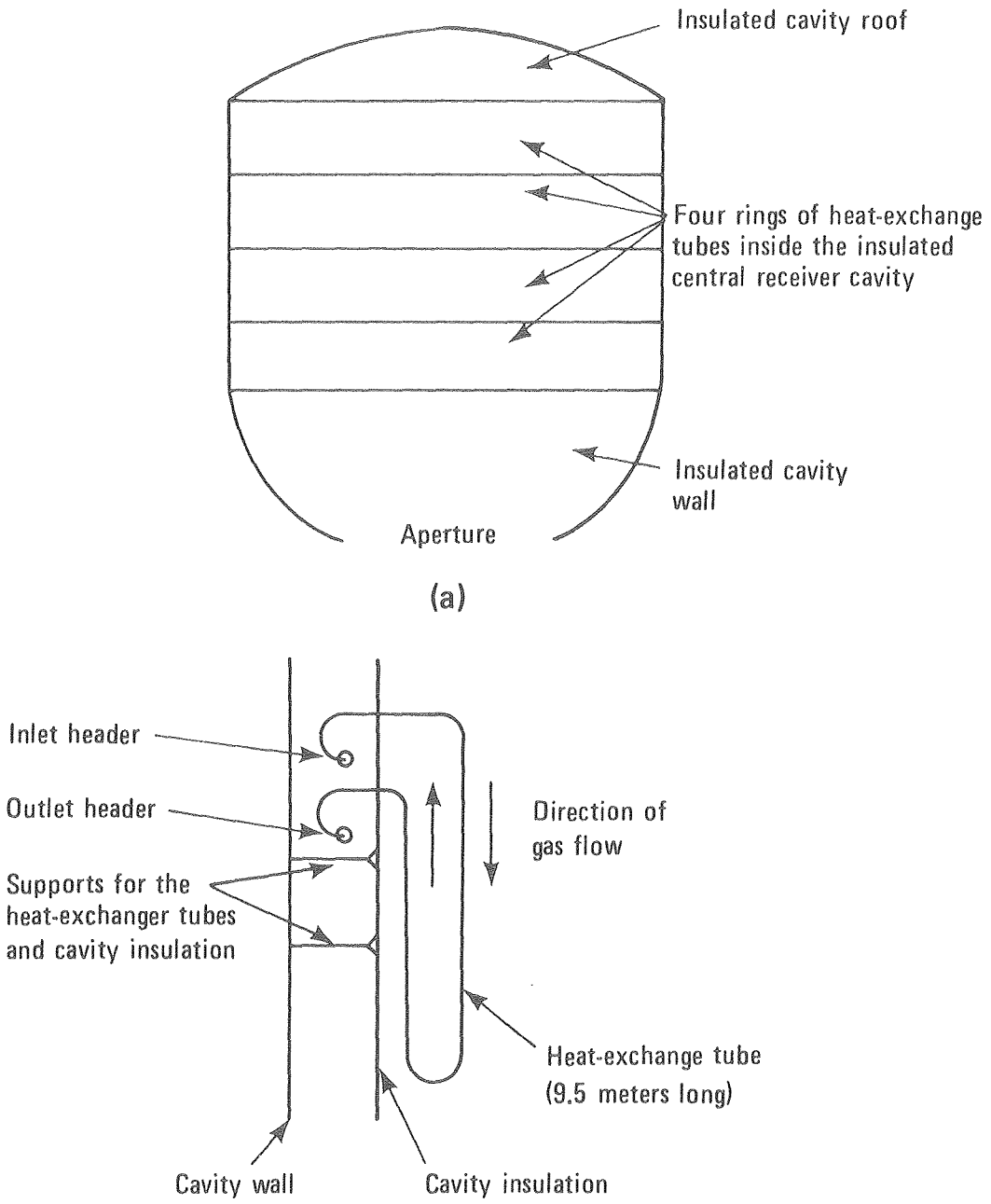

XBL 797-2190

Fig. 4-1. Conceptual design of the Boeing central receiver; (a) shows the structural arrangement of the central receiver and (b) gives a heat-exchange tubing detail.

a ray-tracing computer model.[3] A much simplier heat-transfer model of the receiver was used in this study to approximate the effects of a variety of central receiver operational modifications. The proposed central receiver absorbs the same thermal energy per tube and heats gas to the same outlet temperature as Boeing's central receiver, but introduces gas to the receiver at a lower inlet temperature. This operational modification is expected to decrease the gas flow per receiver tube, change the overall heat-transfer coefficient between the outer walls of the exchanger tubes and the bulk gas, change wall temperatures of the heat-exchange tubes, and result in temperature changes throughout the cavity.

The heat-transfer model analyzes radiative heat transfer to a single heat-exchange tube within the receiver, assuming that the oxidized outer tube wall is a gray body that exchanges energy with black surroundings at a single effective temperature, $T_{eff,cavity}$. The local heat flux density from the cavity to the tube wall is given by the expression

$$q_{\text{cavity to tube wall}}(Z) = [\varepsilon_1 \cdot \sigma \cdot T^4_{eff,cavity} - \alpha_{12} \cdot \sigma \cdot T_{\text{tube wall}}(Z)^4] \quad (1)$$

The heat flux density from the tube wall to the gas is represented by

$$q_{\text{tube wall to gas}}(Z) = U_o \cdot [T_{\text{tube wall}}(Z) - T_{gas}(Z)] \cdot (D_i/D_o)$$

where

$$U_o = 1/[1/h_{gas} + t_{wall}/K_{wall}] \quad (2)$$

and

$$h_{gas} = 0.023\ K_{gas} \cdot Re^{0.8} \cdot Pr^{0.333} / D_i$$

Heat accumulation in the tube walls is a negligible portion of the local heat fluxes; thus the heat flux from the cavity to the tube wall should equal the heat flux from the tube wall to the gas

$$q_{\text{cavity to tube wall}}(Z) = q_{\text{tube wall to gas}}(Z) = q(Z) \qquad (3)$$

Finally, an energy balance relates the change in gas temperature to position.

$$dT_{gas}(Z) = \frac{q(Z) \cdot (\pi \cdot D_o)}{\dot{M}_{\text{gas per tube}} \cdot C_{p,gas}} \cdot dZ \qquad (4)$$

These are the pertinent equations used to model receiver heat transfer. The assumption that the oxidized outer surface of the heat-exchange tube is a gray body matches Boeing's modeling procedures. Boeing assumed a value of 0.88 for both tube emittance (ε_1) and tube absorptance (α_{12}) (3,p.43). The assumption that all surfaces of the receiver cavity act as black bodies at a single effective temperature, $T_{eff,cavity}$, greatly simplifies the receiver model but introduces most of the discrepancy between this model and Boeing's more thorough analysis. The heat-transfer properties assumed for helium gas are given in Table 2-1. The thermal conductivity of the tube wall is estimated to be 15 W/m°K, based upon typical thermal conductivities of metals

(22, p. 3-220).

Computer solution for this model can now be obtained using finite difference methods. The inlet-gas temperature is known, and the desired total heat flux per tube is specified to be equal to Boeing's heat-flux values. Choice of the desired outlet-gas temperature allows calculation of the mass flow rate of gas in each tube.

$$\dot{M}_{\text{gas per tube}} = Q_{\text{tube}}/[C_{p,\text{gas}} \cdot (T_{\text{gas,out}} - T_{\text{gas,in}})] \qquad (5)$$

An initial value is assumed for the effective cavity temperature. Starting from the inlet of the heat-exchange tube, Eqs. (1), (2), and (3) are simultaneously solved for the tube-wall temperature and for the local heat flux to an incremental length of the tube. Equation (4) is then used to estimate the gas temperature at the start of the next length increment. This procedure is repeated until the outlet of the heat-exchange tube is reached. If the proper effective cavity temperature has been chosen the total heat flux to the tube and the value of the gas temperature at the outlet of the tube will approximate their desired values. Otherwise, a new value is assumed for the effective cavity temperature, and a new solution is obtained for Eqs. (1), (2), (3), and (4).

A comparison of the predictions made by this central receiver model for the effects of proposed modifications on central receiver operation is shown in Table 4-1. The proposed central receiver design has a lower gas flow rate per tube and a lower gas inlet temperature, although the

Table 4-1. Model Predictions for the Effects of Proposed Modifications on Central Receiver Operation*

	Boeing's Design	The Proposed Design
Gas Flow Rate Per Tube, kg/s	0.0436	0.0248
Heat Flux to Gas Per Tube, W	63,000	63,000
Inlet Gas Temperature, °K	811	600
Outlet Gas Temperature, °K	1089	1089
Central Receiver Operating Pressure, MPa	3.45	3.45
Overall Heat Transfer Coefficient, Tube Wall to Gas, W/m^2 °K	1420	1010
Model Prediction for the Effective Cavity Temperature, °K	1276	1254
Model Prediction for the Maximum Tube Wall Temperature, °K	1133	1137
Model Prediction for Pressure Drop Through the Heat Exchanger Tubing, MPa	0.046	0.015

*This table lists conditions found for the lowest row of heat exchanger tubes in each design. These tubes have the highest heat flux per tube.

heat transferred to the gas in each tube is identical with Boeing's design. The receiver model predicts that these changes will result in a sharp decrease in the tube-wall-to-gas heat-transfer coefficient accompanied by a decrease in the effective cavity temperature. These changes compensate and result in little change in the maximum predicted tube-wall temperature. Based on this analysis, the proposed operational modification is expected to have only a minor effect on receiver design.

Expected performance and costs of the heat-collection subsystem are outlined in Table 4-2. Cost estimates are based on Boeing's costs per unit of heat absorbed for the heliostats and for the central receiver. The proposed solar power plant requires almost twice as much thermal-energy input as the Boeing receiver is designed to provide. If receiver scale up proves to be infeasible the size of the solar power plant will have to be reduced.

Capital costs associated with the heliostats dominate the cost of the heat-collection subsystem making heliostat design, which was not considered in this study, paramount in determining the feasibility of the solar power plant. Uncertainty in heliostat cost estimation does not greatly influence evaluation of the sensible-heat storage subsystem. Doubling the cost of the heliostats would increase the value of energy losses from the proposed storage unit by $1,000,000 per year or about $4 per MW_e-hr of net electric generation. This is the only way that the cost of heliostats affects the storage subsystem. Receiver heat losses are fairly high, totaling 15% of the energy which is reflected into the central receiver. About 1% of the total

Table 4-2. Heat-Collection Subsystem Summary

Heat Input to the Receiver -	513 MW_t
Heat Losses from the Receiver -	77 MW_t
Heat Absorbed by the Heat Transfer Gas -	436 MW_t
Annual Thermal Energy Absorbed by the Heat Transfer Gas -	893,000 MW_t-hr
Gas Flow Rate, Charging -	173 kg/s
Inlet Gas Velocity Range, Charging -	11.6 m/s - 23.5 m/s
Inlet Reynolds Number Range, Charging -	23,000-47,000
Receiver Pressure Drop, Charging -	0.021 MPa
Receiver Parasitic Pumping Power, Charging -	1.8 MW_e
Annual Receiver Parasitic Pumping Energy -	3,600 MW_e-hr
Installed Cost of the Heliostats* -	$59,300,000
Installed Cost of the Central Receiver, Tower and Heat-Exchange Tubes* -	$20,900,000
Total Installed Cost of the Heat-Collection Subsystem* -	$80,200,000

*Costs are as of June, 1978.

electricity generated is required for parasitic pumping of gas through the receiver.

4.2 THE SENSIBLE-HEAT STORAGE SUBSYSTEM

The concept of storing thermal energy in a magnesia-brick checkerwork was described briefly in Chapter 3. Each brick is exposed to a continuous flow of pressurized heat-transfer gas, and the entire brick checkerwork is contained within welded, carbon-steel tanks that act as pressure-containment vessels. The vessels are internally lined with insulating kaowool blocks to reduce thermal losses and to keep the metal shells close to ambient temperature. These insulated tanks filled with magnesia bricks are the heart of the sensible-heat storage subsystem. Remaining parts of the storage subsystem include inter-tank piping, inlet and outlet gas-distribution manifolds, and storage flow-control valves.

The subsystem design for sensible-heat storage developed for this chapter is based upon the characteristics of the reference solar power plant described in Table 2-4. Chapter 5 compares a series of alternative solar power plant designs with this reference design.

4.2a Design of the Brick Checkerwork

Design of the sensible-heat storage unit was carried out using the proposed storage model and is outlined in Table 4-3. The input parameters required for storage unit design are contained in Table 2-4. The computer model for sizing the storage unit predicts that for this design the mass-averaged brick temperature for the entire bed will be 1039°K after charging and 669°K after discharging. From these

Table 4-3. Computer-Assisted, Sensible-Heat Storage Unit Design.

Input Parameters	
Storage Capacity -	1510 MW_t-hr per cycle
Constant Charging Rate and Time Required for Charging -	189 MW_t for 8 hours
Constant Discharging Rate and Time Required for Discharging -	252 MW_t for 6 hours
Inlet Gas Temperature, Charging -	1089°K
Maximum Outlet Gas Temperature, Charging -	867°K
Inlet Gas Temperature, Discharging -	600°K
Minimum Outlet Gas Temperature, Discharging -	867°K
Sensible-Heat Storage Medium -	Magnesia Bricks
Storage Unit Insulation -	Kaowool Block
Cross Section of each Brick -	76 mm × 114 mm
Cross Section of each Gas Flow Channel -	20.5 mm × 114 mm
Total Gross-Sectional Area of the Brick Checkerwork -	56.5 m^2
Total Cross-Sectional Area for Gas Flow Through Storage -	12.0 m^2
Total Channel Perimeter Through Storage -	1380 m
Channel Perimeter Assumed Effective for Heat Transfer -	1170 m
Storage Unit Design Parameters Obtained by Use of the Computer Model	
Predicted Average Brick Temperature at the End of Charging -	1039°K
Predicted Average Brick Temperature at the End of Discharging -	669°K
Brick Mass Required for Sensible Heat Storage -	13.8×10^6 kg
Total Required Brick Checkerwork Length -	106 m

predictions it is estimated that 13.8×10^6 kg of magnesia brick is required for sensible-heat storage. The bricks are arranged to form a checkerwork 106 m long, with a total cross-sectional area of 56.5 m^2. Sufficient checkerwork length can be obtained by connecting several storage tanks in series. Similarly, sufficient total cross-sectional area can be obtained by distributing the heat-transfer gas among several series of storage tanks.

The brick-checkerwork diameter within each storage tank is 3.0 m, in consideration of storage tank size limitations. The brick checkerwork has 20.5 mm gaps between adjacent bricks. This gas flow-channel size allows easy checkerwork fabrication. About 21% of the total cross-sectional area of the checkerwork is composed of the channels for gas flow, providing 1.50 m^2 of gas-flow area through a 3.00 m diameter checkerwork. This channel size provides 170 m of channel perimeter at any cross section in a tank. The heat-transfer model assumes that 145 m of this perimeter is effective in heat transfer.

4.2b Design of the Steel Tanks

The use of welded, carbon-steel vessels for pressure containment and brick storage is backed up by years of experience. No problems are ancicipated in adapting these vessels to meet our storage requirements. Storage vessel wall and head thicknesses were chosen based on the recommendations given in the ASME Boiler and Pressure Vessel Code: Section VIII, Division I.[1] Specifications made in sizing the welded, carbon-steel pressure vessels were as follows. Vessel design assumed an internal pressure of 3.8 MPa, 10% above the expected working pressure.

Storage vessel joints were assumed to be fully radiographed butt joints, as attained by double-welding, allowing use of a joint efficiency of 1.00 in calculating vessel thicknesses. SA-516, Grade 70 carbon steel was the preferred material of construction because of its high tensile strength and relatively low cost.

Welded, carbon-steel tanks can be shop fabricated and shipped to location or fabricated on location. Rail shipping of shop-fabricated vessels limits vessel dimensions to lengths less than 27.4 m, outside diameters less than 3.86 m, and weights under 90,000 kg.[6] Fabrication on location allows construction of much larger vessels. Increasing the vessel diameter decreases the ratio of surface area to volume, decreasing the heat loss, and decreasing the fraction of storage volume devoted to insulation. These benefits are offset by a substantial cost increase if vessels are fabricated on location.[6] Shop-fabricated vessels were chosen for use in this solar power plant design in an attempt to minimize storage vessel costs.

Shop-fabricated vessels are restricted in size by the necessity of shipping them by railroad. The conceptual design for a welded, carbon-steel storage tank is shown in Fig. 4-2. The 17.6 m long cylindrical portion of each storage tank is filled with magnesia bricks and kaowool-block insulation. Both ends of the tank are closed by tank heads, which allow for gas distribution into flow channels through the checkerwork. Large pipes (1.0 m flow diameter) are used between storage tanks to keep expansion and contraction pressure losses small. This allows fairly even gas flow-distribution among all the flow channels.

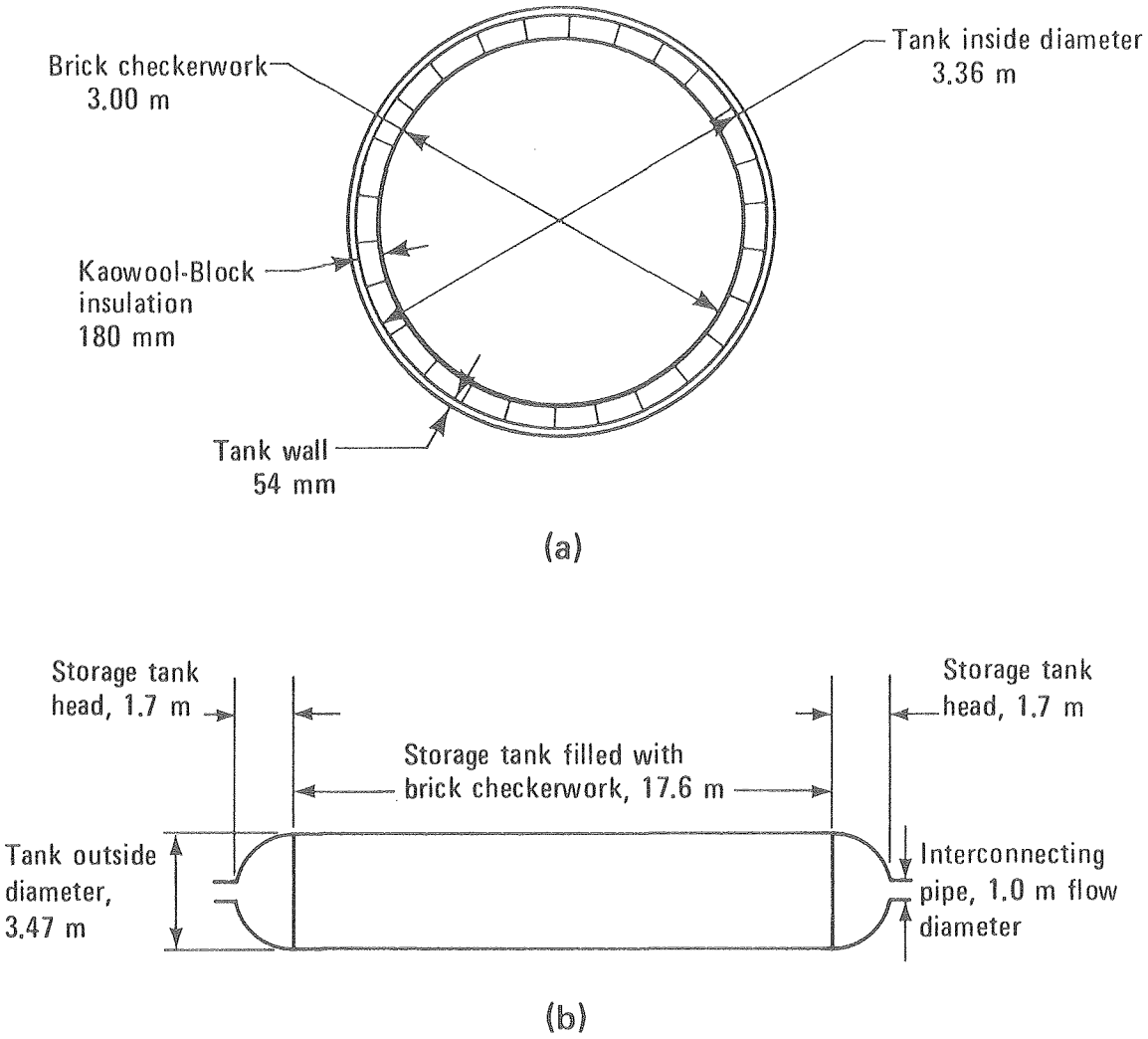

XBL 797-2189

Fig. 4-2. Conceptual design of the welded carbon-steel storage tanks; (a) is a cross-sectional view of the storage tank filled with brick checkerwork and (b) is a longitudinal view of the storage tank design.

The choice of 180-mm thick insulation inside the storage tanks was made on the basis of a trade-off between the annual fixed costs for capitalization, operating, and maintenance, and the annual value of thermal losses. This trade-off is displayed graphically in Fig. 4-3. In this study, the diameter of the brick checkerwork was specified to be 3.0 m. Increasing insulation thickness required use of a larger storage tank and also increased the amount kaowool-block insulation required. Determination of the total installed cost of an incremental length of storage tank was made following the methods outlines in Appendix I and was related to the annual fixed costs by assuming that annual capitalization, operating, and maintenance charges amounted to 18% of total installed cost. Estimations of the heat flux to the surroundings from the storage unit were based on a series of assumptions discussed below. These estimations were combined with the expected operating cnnditions outlined in Table 2-4 to estimate the annual thermal losses. The value of these losses was estimated by assuming thermal energy to be worth \$40 per MW_t-hr. This insulation-thickness analysis showed that 180 mm was a reasonable thickness for the kaowool-block insulation inside each storage tank.

Heat-flux estimation requires that assumptions be made concerning the brick and storage tank temperatures and the thermal conductivity of porous kaowool block filled with helium. The thermal conductivity of kaowool block in a helium atmosphere is assumed to equal the thermal conductivity of the helium that fills its pores. This assumption is examined in greater detail in Chapter 2.1c. The storage tank wall

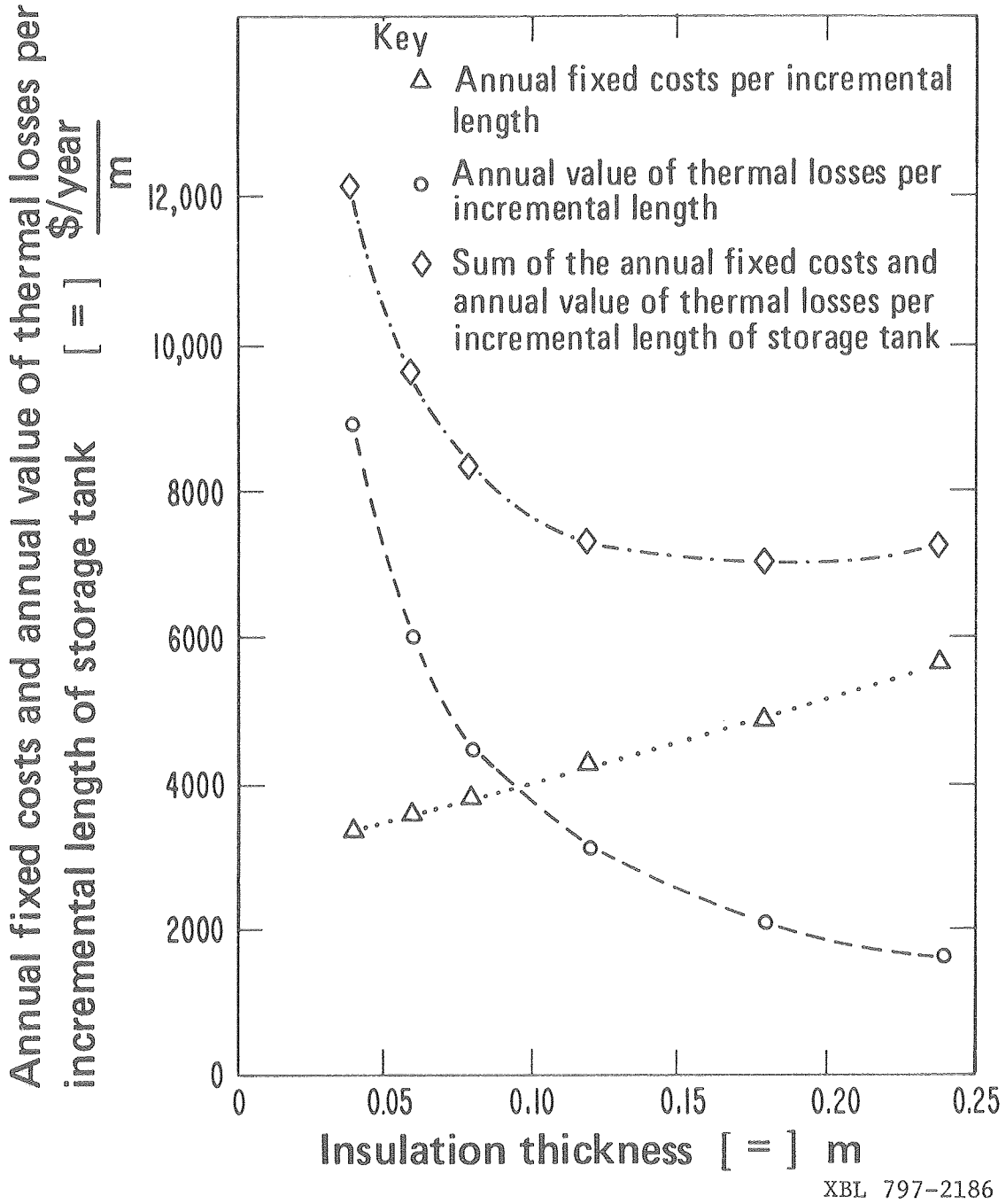

Fig. 4-3. Determination of the range of acceptable storage tank insulation thicknesses. This figure was prepared for a storage tank containing a 3.0-m-diameter checkerwork. Helium is the heat-transfer gas. The estimation of heat flux through the insulation is discussed in Chapter 4.2b. Thermal energy is assumed to have a value of \$40 per MW_t-hr. The annual fixed costs per incremental length of storage tank for capitalization, operating, and maintenance are estimated to total 18% of the incremental installed costs.

temperature is assumed to be close to ambient temperature (300°K), since there will be minimal heat-transfer resistance between the tank and the atmosphere. Brick temperatures vary with both bed position and time. The appropriate brick temperature for use in estimating the heat flux from the discharged storage unit is the mass-averaged brick temperature over the entire bed at the end of discharging (669°K). The average heat flux during each charging/discharging cycle is estimated assuming the bricks are at the entire bed mass-averaged brick temperature after charging (1039°K) half the time and at the entire bed mass-averaged brick temperature after discharging (669°K) the other half.

4.2c Layout of the Storage Tanks

The conceptual layout of the field of storage tanks is shown in Fig. 4-4. Six tanks are required in series to provide the required 106-m length of brick checkerwork. Tanks are stacked two high, eight across, and three in a row. The three tanks in each row are joined in series by short (3m) pipes. Gas turnaround piping joins the top and bottom rows at one end connecting six tanks in series. Two gas-distribution manifolds connect eight of these tank series together in parallel to provide a storage unit with a total of 12.0 m^2 of cross-sectional area for gas flow and a total of 56.5 m^2 of brick-checkerwork cross-sectional area. Two control valves regulate gas flow through and around the storage tanks.

4.2d Estimated Costs of the Storage Unit

A summary of sensible-heat storage subsystem costs and energy losses is presented in Table 4-4. The storage design chosen is

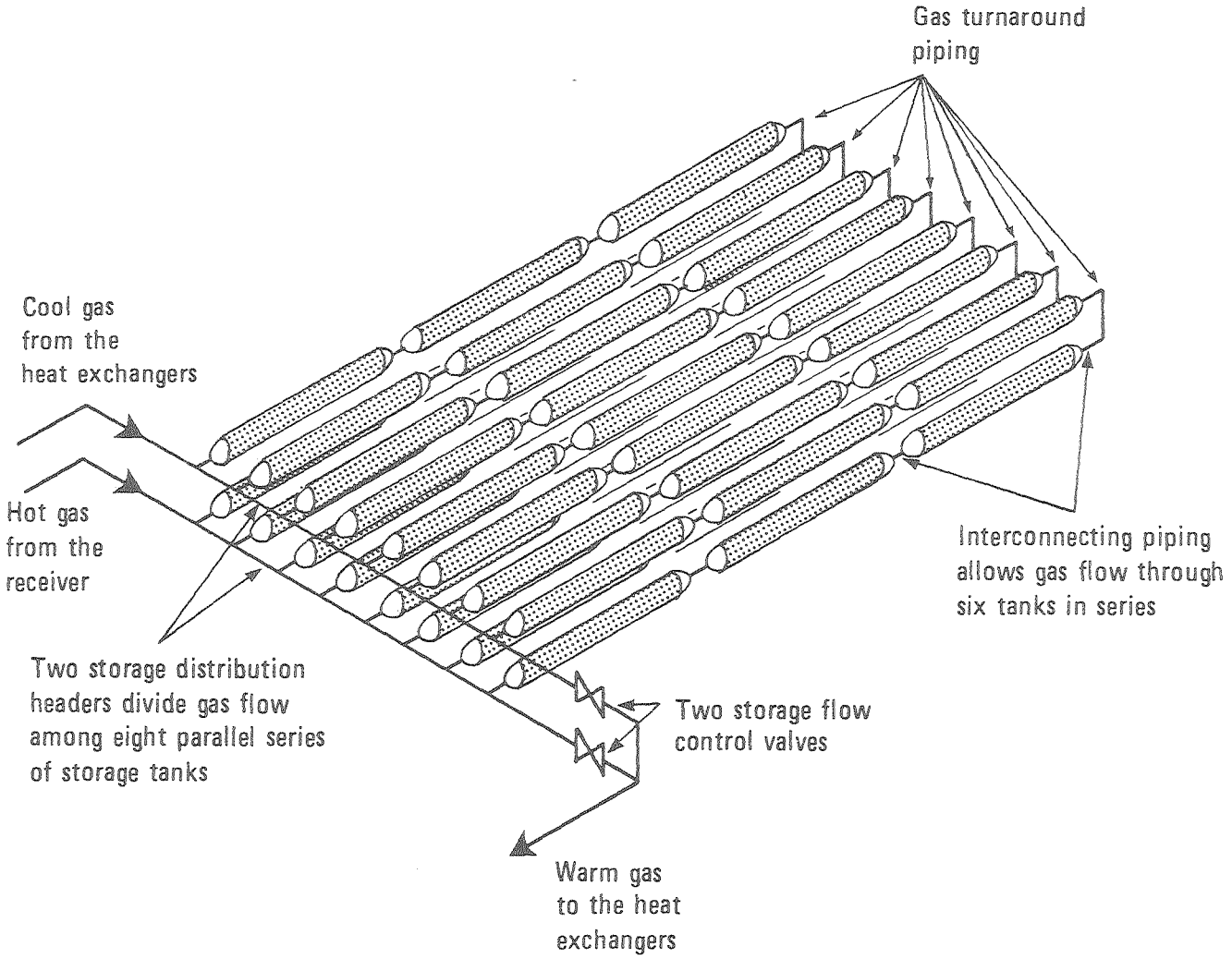

XBL 797-2194

Fig. 4-4. Conceptual layout of the storage tanks.

Table 4-4. Sensible-Heat Storage Subsystem Summary

Thermal Energy Stored per Cycle -	1,510 MW_t-hr
Average Storage Heat Loss per Cycle -	230 MW_t-hr
Thermal Energy Returned per Cycle -	1,280 MW_t-hr
Annual Thermal Energy Input to Storage -	387,000 MW_t-hr
Annual Heat Losses from Storage -	60,000 MW_t-hr
Mass of Magnesia Bricks for the Storage Unit -	13.8×10^6 kg
Number of Storage Tanks -	48
Inside Diameter of Storage Tanks -	3.36 m
Length of Storage Tanks -	21.0 m
Volume of Storage Tanks -	180 m^3
Total Volume of the Storage Unit -	9000 m^3
Gas Flow Rate Range, Charging -	74 kg/s-162 kg/s
Inlet Gas Velocity Range, Charging -	4.1 m/s-8.9 m/s
Inlet Reynolds Number Range, Charging -	4,500 - 9,900
Pressure Drop Range, Charging -	3 kPa - 25 kPa
Gas Flow Rate Range, Discharging -	99 kg/s-182 kg/s
Inlet Gas Velocity Range, Discharging -	3.0 m/s - 5.5 m/s
Inlet Reynolds Number Range, Discharging -	9,500 - 17,000
Pressure Drop Range, Discharging -	8 kPa - 20 kPa
Average Pressure Drop, Charging -	9 kPa
Average Parasitic Pumping Power, Charging -	0.7 MW_e
Average Pressure Drop, Discharging -	11 kPa
Average Parasitic Pumping Power, Discharging -	0.9 MW_e
Annual Parasitic Pumping Energy	2,500 MW_e-hr
Installed Storage Tank Cost* -	$19,500,000
Installed Magnesia Brick Cost* -	$9,200,000
Installed Storage Tank Insulation Cost* -	$5,800,000
Installed Storage Piping, Headers, and Valves Cost* -	$1,700,000
Total Installed Cost of the Sensible-Heat Storage Unit* -	$36,200,000

*Costs are as of June, 1978.

successful in keeping parasitic pumping losses low. The annual parasitic pumping energy through storage (2,500 MW_e-hr) is less than 1% of the gross electric generation. Thermal losses from storage are more critical, however, amounting to over 15% of the thermal energy placed in storage each year. The primary reasons for these high thermal losses are the large ratio of surface area to volume for the small-diameter storage tanks and the high thermal conductivity of kaowool-block insulation in a helium atmosphere. The costs of various subsystem components were estimated following the procedures described in Appendix I. The total installed cost of the sensible-heat storage subsystem is $36,200,000 based on prices in June of 1978. The storage subsystem cost is particularly sensitive to the price of storage tanks, which for this design represented 54% of the total subsystem cost.

4.3 THE HEAT-EXCHANGE SUBSYSTEM

The heat-exchange subsystem effects energy transfer from the heat-collection subsystem or the heat-storage subsystem to the power-generation subsystem. Power is generated by running a Rankine-cycle turbine-generator. The heat-exchange subsystem provides separate sets of exchangers for heating feedwater, boiling the saturated liquid, superheating this steam, and reheating this steam after it is partially expanded. Figure 4-5 shows the flow arrangement for the heat-exchange subsystem. The heat-transfer gas and water/steam pass in opposite directions through a series of single pass, countercurrent heat exchangers. This flow arrangement has been chosen to minimize the total size of the heat-exchange subsystem by providing the largest possible

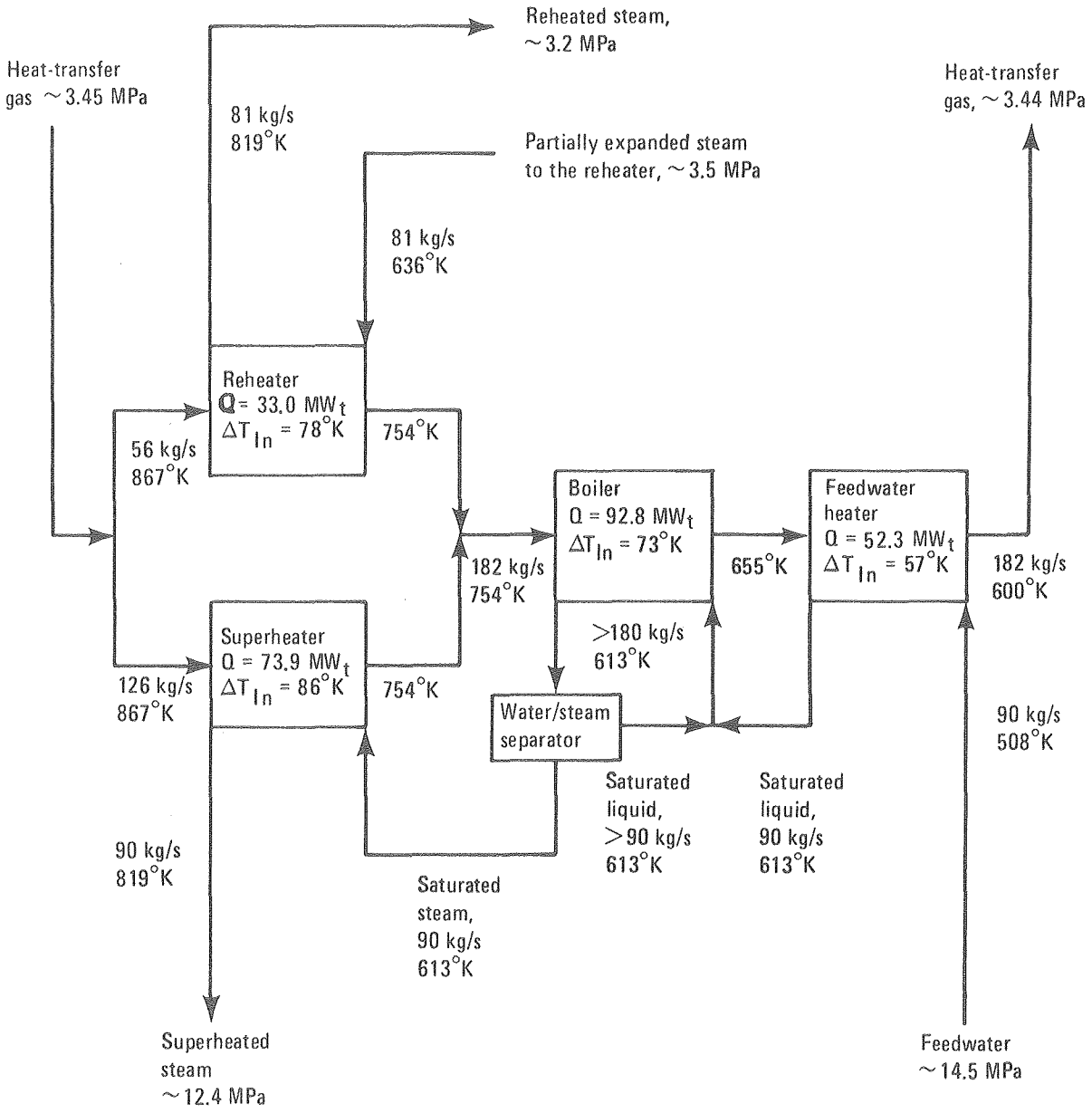

XBL 797-2175

Fig. 4-5. Flow arrangement for the heat-exchange subsystem.

log-mean temperature differences in the superheater and in the reheater. Hot heat-transfer gas flow is first split between the superheaters and the reheaters. These flows are then recombined and passed first through the boilers and then through the feedwater heaters.

The proposed designs for the superheaters, boilers, and feedwater heaters are presented in Table 4-5. The heat-transfer gas, at a moderate pressure (3.45 MPa), flows through the shell side of each exchanger. Each exchanger shell is fabricated from carbon steel with an inside diameter of 1.72 m. The exchangers are insulated internally with 100 mm of kaowool-blanket insulation to reduce thermal losses. The proposed exchanger design uses 19-mm (3/4-inch) OD exchanger tubes laid in a 40-mm (1 9/16-inch) square-pitch pattern. This large tube separation is effective in reducing the shellside parasitic pumping power losses, although it limits heat-transfer area per exchanger. The power required to push the heat-transfer gas into and out of the exchangers accounts for most of the pumping-power requirement for the heat-exchange subsystem. Large-diameter (1.44 m ID), insulated inlet and outlet pipes are used to allow gas flow across a longer length of the exchanger tubes, in an attempt to reduce these important exchanger entering and exiting losses. Table 4-5 also summarizes exchanger tubing details. The superheating and reheating exchangers require 316 stainless steel tubes because of high operating temperatures. Carbon-steel tubes are adequate for the operating conditions found in the boilers and feedwater heaters.

The numbers and sizes of the various power-generation heat

Table 4-5. Proposed Basic Exchanger Designs

Basic Exchanger Description

Shell Construction -	Carbon Steel
Shell Inside diameter -	1.72 m
Kanwool-blanket insulation thickness -	100 mm
Insulation Inside diameter -	1.52 m
Tube outside diameter -	19.0 mm (3/4")
Tube Layout -	Tubes laid out in a 1 9/16" sq. pitch
Number of tubes per exchanger -	1036
Tube outside perimeter per exchanger -	62 m
Effective diameter, shell side -	92 mm
Shell side cross-sectional flow area per exchanger -	1.53 m^2
Heat-transfer gas flow -	Shell side
Water/Steam flow -	Tube side

Exchanger Tubing Details

	Superheaters and Reheaters	Boilers and Feedwater Heaters
Tube Construction	316 stainless steel	carbon steel
Tube Outside diameter, mm	19.0	19.0
Tube Inside diameter, mm	14.8	13.5
Tube B.W.G. gage	14	12
Tube side cross-sectional flow area per exchanger, m^2	0.179	0.148

Heat Transfer Gas Piping Details

Piping Construction -	Carbon Steel
Piping Inside Diameter -	1.44 m
Kaowool-Blanket Insulation Thickness -	120 mm
Insulation Inside Diameter -	1.20 m
Piping Positioning -	Inlet and outlet pipes are on opposite ends and opposite sides of each exchanger
Exchanger Positioning -	Exchangers are laid side by side to minimize the lengths of inter-exchanger pipes.

exchangers are shown in Table 4-6. Table 4-6 also shows the required numbers and lengths of heat-transfer gas piping within the heat-exchange network.

Table 4-7 summarizes the operation of the heat-exchange subsystem and the estimated cost. The proposed exchanger design reduces both the thermal losses and the required parasitic pumping power to acceptable levels (~2% of the energy transferred). The estimated total installed subsystem cost is $7,000,000 based on June, 1978 price levels.

4.4 THE GAS-CIRCULATION SUBSYSTEM

Thermal energy is transferred within the heat-collection, storage, and heat-exchange subsystems by a heat-transfer gas. Figure 4-6 shows the conceptual piping arrangement of the gas-circulation subsystem. Daytime operation involves pumping the gas from storage through the heat exchangers to the main gas compressor, splitting the flow so that most of the gas flows through the central receiver while part is bypassed, and finally returning all of the gas to the storage subsystem. At nighttime, gas is pumped between the heat exchangers and the storage unit. Two flow-control valves regulate the gas flow. The placement of the main gas compressor, so that the heat-transfer gas is recompressed at its lowest temperature, minimizes the compressor work required. Piping runs between the heat-exchange network and the storage unit are short to reduce their cost. Longer piping runs are required between the storage unit and the central receiver, which is mounted on top of a 300-m tall tower.

A single-stage axial compressor is used for gas circulation. This

Table 4-6. Sizing Calculations for the Heat Exchanger Network

	Superheater	Boiler	Feedwater Heater	Reheater
Total required heat duty, MW_t	73.9	92.8	52.3	33.0
Number of exchanger series in parallel	4	6	6	2
Total outside tube perimeters for parallel exchangers, m	248	372	372	124
Total shell side gas flow, kg/s	126	182	182	56
Shell side gas film heat-transfer coefficient, W/m^2 °K	370	360	360	340
Total tube side water/steam flow, kg/s	90	>180	90	81
Tube side gas film heat-transfer coefficient, W/m^2 °K	900	>3300	2000	1200
Overall heat-transfer coefficient based on the outside tube area, W/m^2 °K	240	310	290	250
Log-Mean average temperature difference, °K	86	73	57	78
Minimum area needed to meet the heat duty, m^2	3600	4100	3200	1700
Practical exchanger length, m	4.88(16ft)	6.10(20ft)	4.88(16ft)	4.88(16ft)
Available surface area per exchanger, m^2	300	380	300	300
Number of exchangers required in series	3	2	2	3
Total number of exchangers required	12	12	12	6

Heat Transfer Gas Piping

Connectors Between Piping from Storage and Superheaters or Reheaters -	6 - 10m pipes
Interconnectors Between 6 sets of 7 exchangers in series -	6 × 6 - 2m pipes
Connectors Between Feedwater Heaters and Piping to Storage -	6 - 10m pipes

Table 4-7. Heat-Exchange Subsystem Summary

Exchanger Network Heat Duty -	252 MW_t
Annual Thermal Energy Exchanged -	824,000 MW_t-hr
Annual Heat Losses from the Heat-Exchange Network* -	12,000 MW_t-hr
Gas Flow Rate -	182 kg/s
Inlet Gas Velocity Range -	9.6 kg/s-10.7 kg/s
Inlet Reynolds Number Range -	42,000-47,000
Average Pressure Drop -	0.009 MPa
Parasitic Pumping Power -	0.7 MW_e
Annual Parasitic Pumping Energy -	2400 MW_e-hr
Total Installed Heat-Exchange Subsystem Cost** -	$7,000,000

*Annual heat losses from the exchanger network have been estimated assuming that the exchangers and gas piping are at operating temperature, 24 hr/day, 256 day/year and are at ambient temperature the remainder of the time.

**Costs are as of June, 1978.

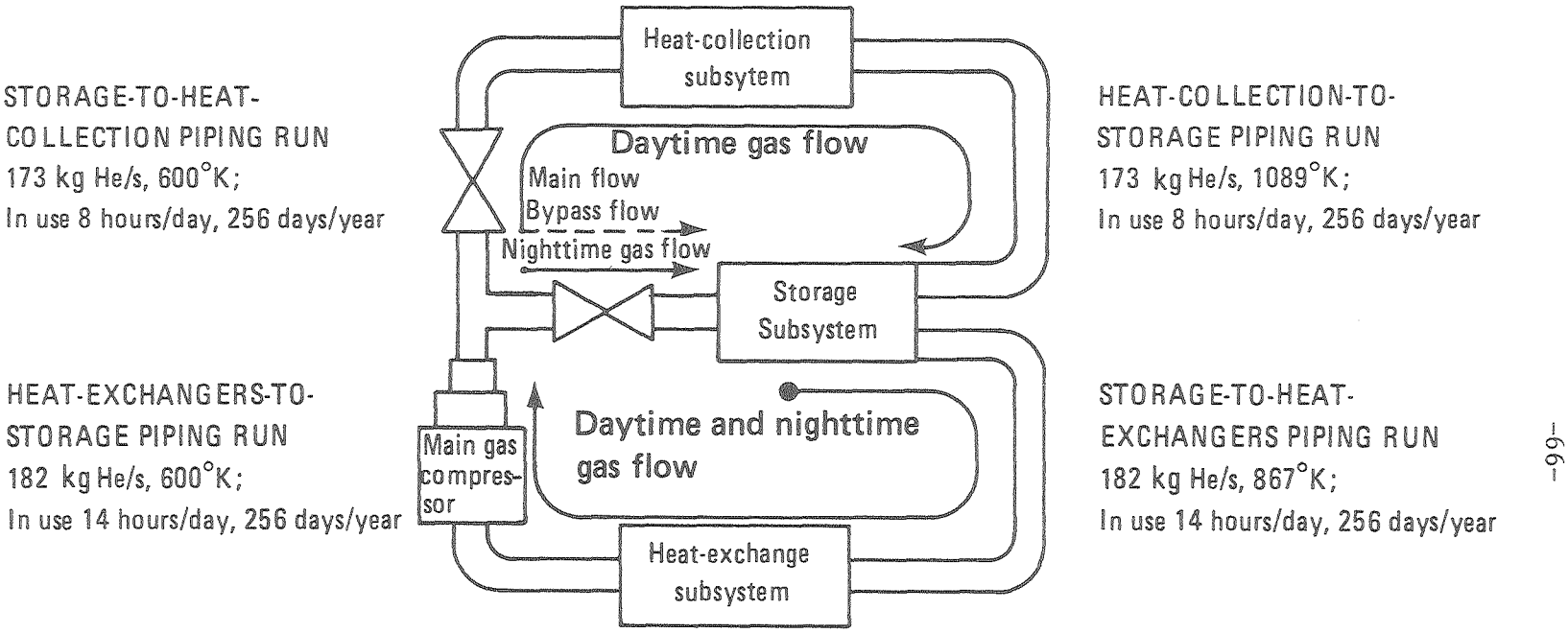

XBL 797-2193

Fig. 4-6. The proposed piping arrangement for the gas-circulation subsystem.

type of compressor typically has external losses of about 2% of the drive power, and internal losses of about 11% of the drive power.[31] The compressor can be steam driven or driven by a three-phase electric motor. An electric motor of the required size will have a drive efficiency of about 92% [23, p. 460], or external losses of about 8% of electric power required. Combining these estimates shows that about 10% of the electric power supplied to the drive motor is externally dissipated due to frictional losses. An additional 10% of the electric power supplied to the drive motor is internally dissipated raising the gas temperature, but not compressing the gas. The remaining 80% of the electric drive power provides useful gas compression, as well as heating the gas. It is assumed that decreasing the compressor head during discharge to about 40% of the compressor head during charge will not affect the efficiency of compression. If the error in this assumption is too large, separate compressors may be desirable to handle daytime and nighttime operations. Addition of a second compressor will not have a significant effect on the solar power plant since cost of a gas compressor is only about 0.5% of the total cost of the power plant.

Piping selection involves determining the effects of important piping parameters on the sum of the annual fixed charges and the annual value of energy losses for an incremental length of piping for each expected set of operating conditions. The annual fixed charges for capitalization, operating, and maintenance were estimated to be 18% of the total installed costs. This estimate included 14% of the total installed cost per year for capitalization and 4% per year of the total

installed cost for operating and maintenance costs. For these piping design studies, electric energy and thermal energy were assumed to be worth \$100 per MW_e-hr and \$40 per MW_t-hr respectively. These energy values are in good agreement with the predicted electric energy cost discussed in Chapter 4.6.

Figure 4-7 shows graphically how the insulation thickness was chosen for the storage-to-heat-collection piping. A kaowool-blanket insulation thickness of 120 mm was chosen, although the graph shows that any insulation thickness between 60 mm and 120 mm would very likely be acceptable. This graph does not consider gas pumping power, which should not change since the pipe diameter available for flow remains fixed.

Selection of the flow diameter for the storage-to-heat-collection piping was based upon an attempt to minimize the sum of the annual fixed charges, the annual value of the thermal losses, and the annual value of parasitic pumping energy required for an incremental length of straight pipe. Figure 4-8 shows that the chosen flow diameter of 1.8 m is well within the range of reasonable flow diameters (~1.6 m to ~2.0 m).

The calculations shown graphically in Figs. 4-7 and 4-8 were carried out for all four piping runs. The details of the proposed designs for the gas-circulation piping are shown in Table 4-8. Table 4-8 also contains information on the expected heat losses and expected pressure drops for incremental lengths of piping along each piping run.

The operation of the gas-circulation subsystem is summarized in Table 4-9. Compressor operation requires an average of 6.0 MW_e during

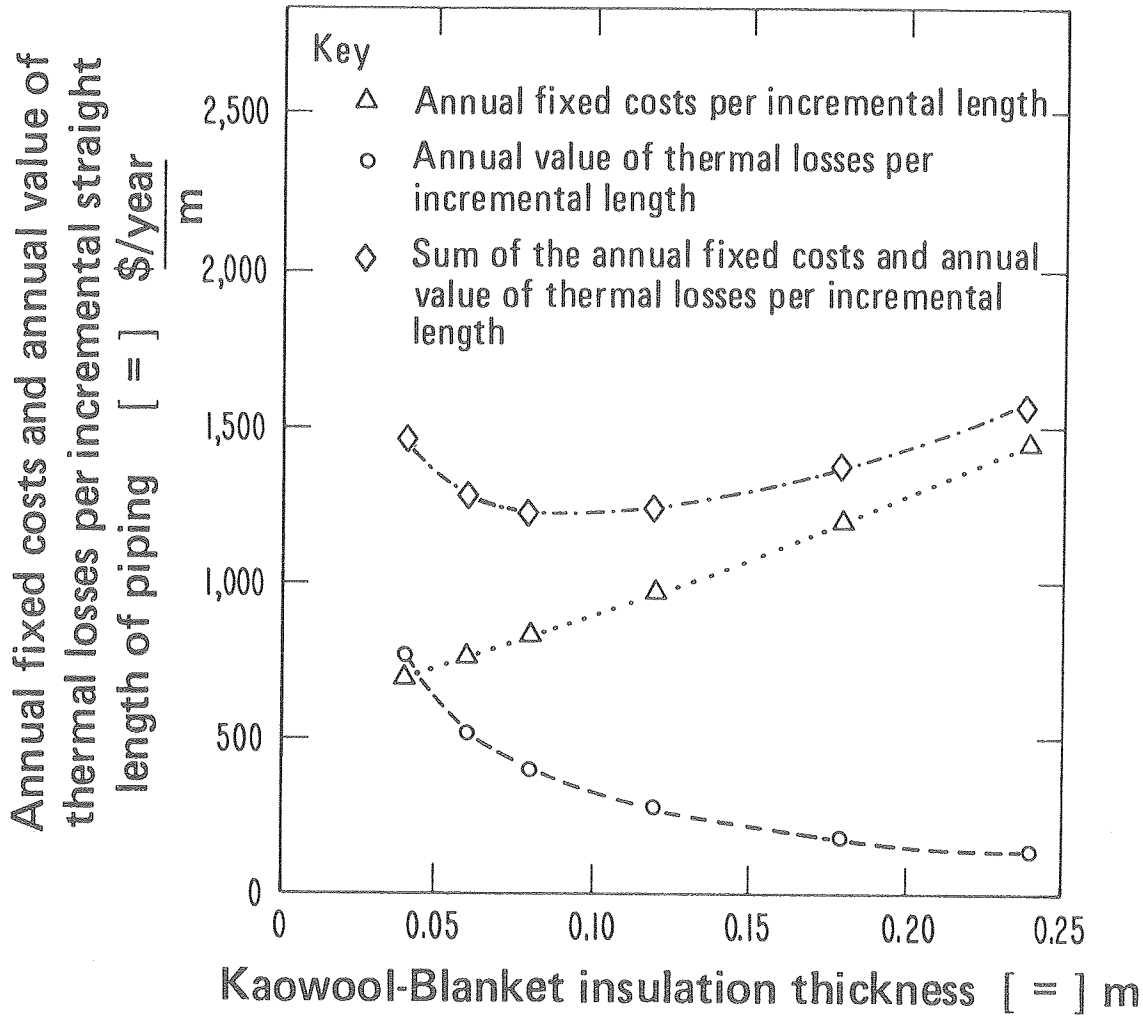

XBL 797-2182

Fig. 4-7. Determination of the range of reasonable piping insulation thicknesses for the storage-to-heat-collection piping run. This figure was prepared for a pipe with a 1.8 m flow diameter. Helium gas at a temperature of 600°K flows through the pipe. This piping run is in use 8 hours per day, 256 days per year. Thermal losses from the pipe are calculated assuming the pipe wall temperature is approximately ambient temperature (300°K) and assuming that the thermal conductivity of kaowool-blanket insulation filled with helium equals the thermal conductivity of helium. Thermal energy is assumed to have a value of $40 per MW_t-hr. The annual fixed costs per incremental length of piping for capitalization, operating and maintenance are estimated to total 18% of the incremental installed costs.

Fig. 4-8. Determination of the range of reasonable piping flow diameters for the storage-to-heat-collection piping run. Piping insulation was 120 mm thick for this study. Helium flows through this piping run at a temperature of 600°K and a mass flow rate of 173 kg per second. This piping run is in use 8 hours per day, 256 day per year. The electric energy usage for parasitic gas pumping is estimated assuming gas recompression at 600°K and assuming an equivalent roughness for insulation lined pipes of 10 mm. Thermal energy losses are calculated as described in Fig. 4-7. The values of energy losses have been estimated to be \$100 per MW_e-hr and \$40 per MW_t-hr. The annual fixed costs per incremental length of piping for capitalization, operating, and maintenance are estimated to total 18% of the incremental installed costs.

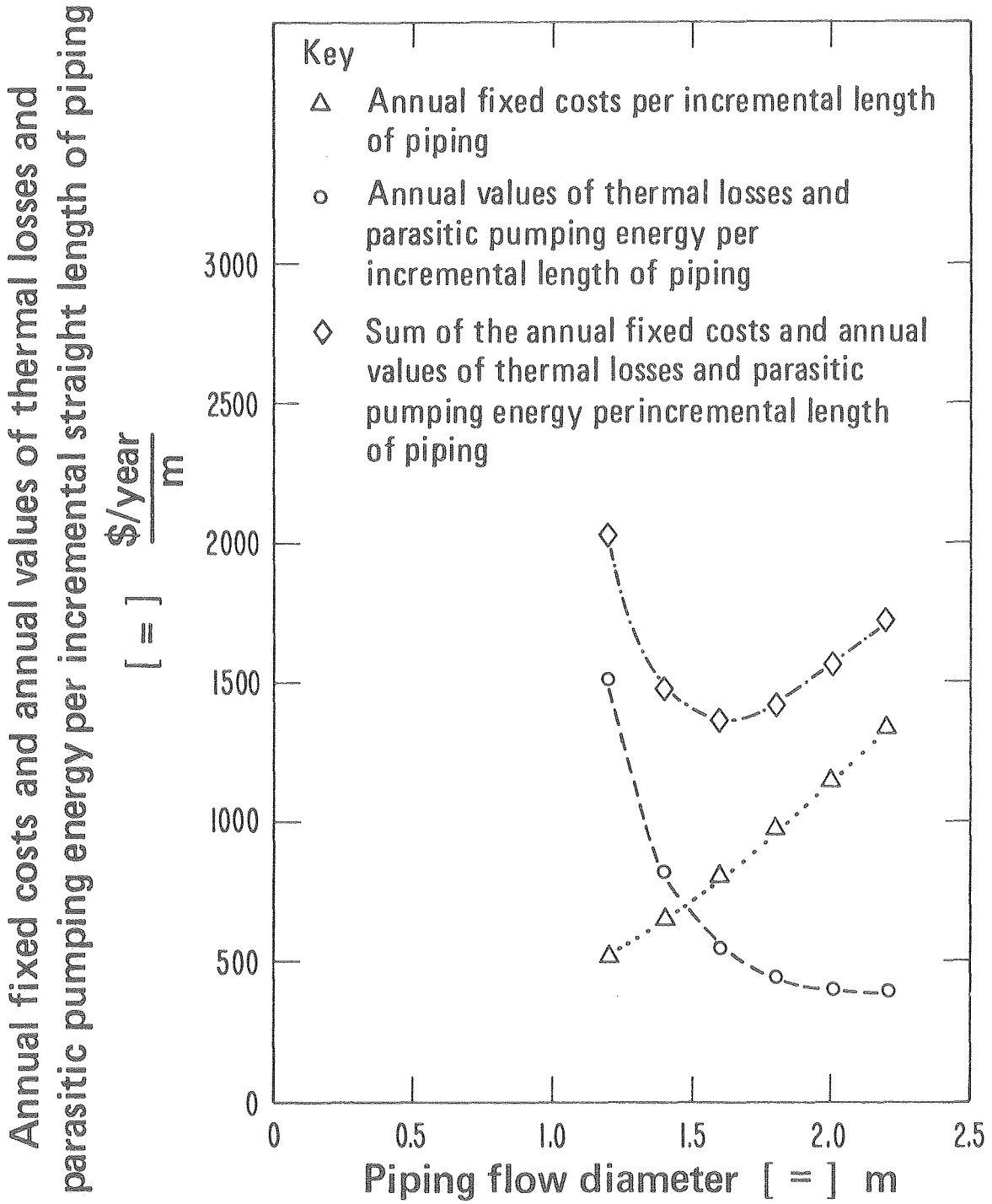

XBL 797-2180

Fig. 4-8.

Table 4-8. Gas-circulation Piping Design Details

	Heat-Exchangers-to-Storage	Storage-to-Heat-Collection	Heat-Collection-to-Storage	Storage-to-Heat-Exchangers
Piping Operational Conditions				
Helium Mass Flow Rate, kg/s	182	173	173	182
Helium Temperature, °K	600	600	1089	867
Assumed Pipe Temperature, °K	300	300	300	300
Daily Length of Operation, hr.	14.0	8.0	8.0	14.0
Days of Operation Expected Annually	256	256	256	256
Proposed Piping Design*				
Pipe Flow Diameter, m	1.80	1.80	1.80	1.80
Kaowool-Blanket Insulation Thickness, mm	120	120	180	180
Pipe Inside Diameter, m	2.04	2.04	2.16	2.16
Pipe Wall Thickness, mm	39	39	41	41
Installed Piping Cost per Length, $/m	5400	5400	6700	6700
Piping Length, m	50	350	350	50
Number of 90° Bends	2	3	3	2
Equivalent Length for Calculation of Pressure Drop, m	165	520	520	165
Piping Operational Details				
Expected Heat Loss Per Length, MW_t/m	0.0034	0.0034	0.0081	0.0052
Expected Pressure Drop per Equivalent Length, Pa/m	18	17	31	27

*Pipes are constructed of SA-516, Grade 70 carbon steel.

Table 4-9. Gas-Circulation Subsystem Summary

Compressors

Compressor Design -	Single Stage, Axial Compressor
Gas Mass Flow Rate -	182 kg He/s
Gas Temperature -	600 °K
Gas Volumetric Flow Rate -	66 m^3 He/s
Required Compression Head Range Charging -	0.066 MPa - 0.088 MPa
Average Total Compressor Power, Charging -	6.0 MW_e
Required Compression Head Range, Discharging -	0.025 MPa - 0.037 MPa
Average Total Compressor Power, Discharging -	2.4 MW_e
Annual Electric Energy Usage by Compressors -	15,200 MW_e-hr
Annual Thermal Energy Added by Compressors to the Gas -	14,000 MW_t-hr

Piping and Valves

	Heat-Exchanger-to-Storage Piping Run	Storage-to-Heat-Collection Piping Run	Heat-Collection-to-Storage Piping Run	Storage-to-Heat-Exchangers Piping Run	Total
Gas Flow Rate, kg/s	182	173	173	182	-
Gas Velocity, m/s	25.7	24.6	44.8	37.4	-
Reynolds Number	4,200,000	4,000,000	2,600,000	3,200,000	-
Pressure Drop, MPa	0.0030	0.0089	0.0162	0.0045	Charge-0.0326 Discharge-0.0075
Parasitic Pumping Power, MW_e	0.25	0.74	1.33	0.37	Charge-2.7 Discharge-0.6
Annual Parasitic Pumping Energy, MW_e-hr.	800	1,500	2,700	1,200	6,200
Annual Heat Losses, MW_t-hr	600	2,400	5,800	900	10,000

Installed Costs as of June, 1978

Piping Installed	$4,800,000
Flow Control Valves Installed Cost -	$400,000
Gas Compressor Installed Cost -	$400,000
Total Installed Gas-Circulation Subsystem Cost -	$5,600,000

the daytime and an average of 2.4 MW_e at night. Pumping the gas through the piping is responsible for almost half of the daytime recompression head. About 1% of the total annual thermal energy collected by the receiver is dissipated from gas-circulation piping, but this is compensated for by annual addition of 14,000 MW_t-hr to the gas by the compressors. Gas piping costs are estimated to be $4,800,000. Flow-control valves and the main gas compressor are each estimated to cost $400,000. The installed cost for the gas-circulation subsystem is $5,600,000 based on June, 1978 prices.

4.5 THE POWER-GENERATION SUBSYSTEM

The proposed solar power plant generates electricity by use of a Rankine-cycle turbine-generator, condenses the exhaust steam in an indirect condenser and rejects heat from a natural-draft, dry-cooling tower. The turbine selected is a high-backpressure, reheat design compatible with the higher condenser temperature expected for a dry-cooled unit. Turbine inlet steam conditions are 811°K (1000°F) and 12.4 MPa (1800 psia) for superheated steam and 811°K (1000°F) and 3.2 MPa (460 psia) for reheated steam. Feedwater is preheated with extraction steam to improve the cycle efficiency of electric generation. Layout of the power-generation subsystem discussed above is displayed in Fig. 4-9.

A high-backpressure turbine with a dry-cooling tower was used in the proposed solar power plant to reduce the overall water requirements. A number of recent water-availability studies indicate that most of the southwestern United States will be short of water before the year

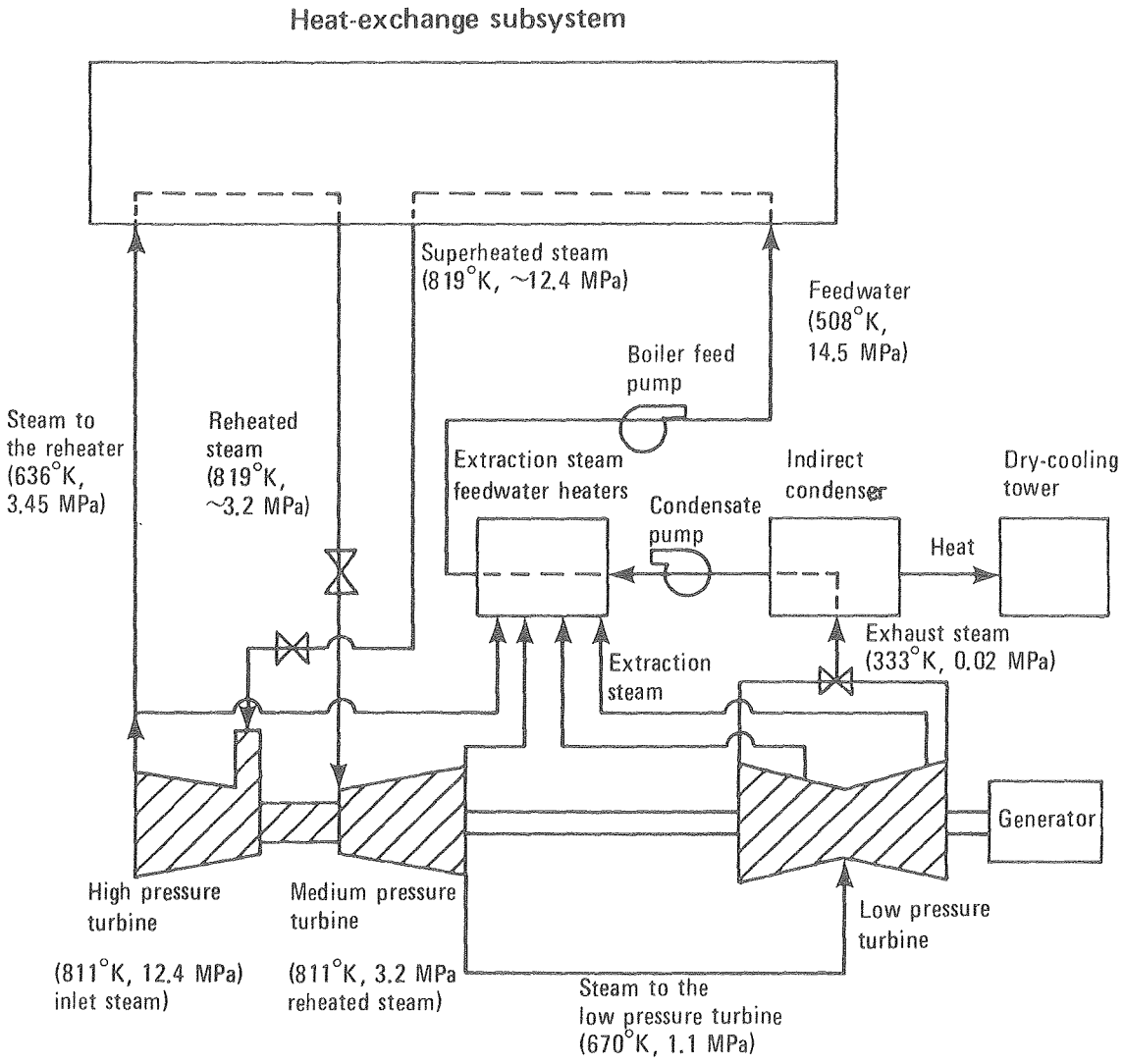

XBL 797-2172

Fig. 4-9. Layout of the power-generation subsystem.

2000.[8] Acceptable water-usage levels for power plants built in water-limited regions will be very low. A comparison of the relative advantages of wet-cooled and dry-cooled solar power plants is given in Chapter 5.7.

The present status of dry-cooling tower development and acceptance is discussed in detail by Rossie and Cecil.[28] Dry-cooling towers have seen only limited use in the United States, but are more common in Europe. GEA Airexchangers, Inc. has discussed building dry-cooling towers with several United States utility companies. The dry-cooling tower cost estimate was based on their price formula (28, p.127). The approximate size of a natural-draft cooling tower to meet the required heat duty of 152 MW_t is given in Table 4-10. Cooling tower dimensions were estimated by interpolation from dimensions given for a cooling tower capable of rejecting 800 MW_t (28, p.318).

The design of high-backpressure turbines is an area which has only recently received attention. General Electric announced plans in 1971 to develop designs for a series of high-backpressure turbines suitable for generating 250 MW_e to 750 MW_e.[19,20] It was hoped that these turbines would be ready for shipping in 1976. Substantial design effort may still be required before a suitable 100 MW_e turbine design is developed. Since a suitable turbine design in the 100 MW_e range has not been developed, turbine performance and steam turbine flow arrangements were estimated based on the heat balance prepared for the 330 MW_e, high-backpressure "Black Hills" turbine.[12]

Overnight shutdowns of the turbine complicate the design. Peaking

Table 4-10. Approximate Size of the Natural-Draft Dry-Cooling Tower*

Heat Rejection from the Cooling Tower -	152 MW_t
Initial Air/Water Temperature Difference in the Dry-Cooling Tower -	28 °K
Diameter of the Cooling Tower Stack -	45 m
Total Height of the Dry-Cooling Tower -	115 m
Diameter of the Cooling Delta Skirt -	50 m
Distance from the Turbine to the Tower -	90 m

* - Cooling tower dimensions have been estimated by interpolation from dimensions given for a cooling tower capable of rejecting 800 MWt (28, p.318).

turbines suitable for daily, cold startups were deemed unacceptable for the proposed design because of their low efficiencies. This decision mandated that the turbine must be kept hot overnight, either by continuously discharging storage at a moderate rate, or by discharging most of the stored energy rapidly and saving a small fraction of the stored energy to keep the turbines warm the remainder of the night. The proposed solar power plant discharges most of the stored energy rapidly. Maintaining the turbines at "hot standby" is estimated to require about 5% of the design heat input or about 13 MW_t. The turbine must be kept hot for 10 hours, so this heat loss reduces the length of the discharge cycle by about one-half hour per day. Chapter 5 discusses the possibility of discharging storage overnight at a constant rate.

Table 4-11 contains the power-generation subsystem summary. The gross efficiency of the turbine-generator is 39.7%, converting 252 MW_t into 100 MW_e. Most of the remaining 152 MW_t must be rejected by the dry-cooling tower. Energy losses from the power-generation subsystem are relatively high. Thermal losses associated with maintaining the turbines at "hot standby" amount to 3.5% of the energy absorbed in the central receiver, and parasitic power to run the turbine feed pumps and circulate cooling water decreases the net electric generation by 3.5 MW_e. The total installed cost of the power-generation subsystem is estimated to be $10,000,000 based on June, 1978 prices.

4.6 AN OVERVIEW OF THE SOLAR POWER PLANT

Previous sections in this chapter have discussed operational

Table 4-11. Power-Generation Subsystem Summary

Heat Input to the Turbine-Generator -	252 MW_t
Turbine Description -	12.4 MPa, 811 K/811 K; high back pressure turbine
Gross Turbine-Generator Efficiency -	0.397 MW_e/MW_t
Gross Electric Power Generation -	100.0 MW_e
Heat Rejection from the Cooling Tower -	152 MW_t
Cooling Tower and Condenser Description -	Indirect condenser with heat rejection from a natural-draft dry-cooling tower.
Initial Air-Water Temperature Difference in the Dry-Cooling Tower -	28°K
Estimated Heat Requirement to Maintain the Turbine at Warm Standby -	13 MW_t
Annual Heat Loss from Turbine at Warm Standby -	32,000 MW_t-hr
Parasitic Power to Run Turbine Feed Pumps -	2.3 MW_e
Parasitic Power for Cooling Water Circulation -	1.2 MW_e
Annual Parasitic Energy Use for Power Generation -	11,000 MW_e-hr
Installed cost of the Turbine-Generator, Pumps, and Extraction Steam Feedwater Heaters* -	$6,500,000
Installed Cost of the Dry-Cooling Tower and Condenser* -	$3,500,000
Total Installed Cost of the Power-Generation Subsystem* -	$10,000,000

*- Costs are as of June, 1978.

details and costs for each of the solar power plant subsystems. This section examines the operation and cost of the entire solar power plant, and attempts to determine the impact of the sensible-heat storage unit on the cost of electricity generated by the solar power plant.

Table 4-12 gives an overall summary of the proposed solar power plant design. The annual net thermal energy absorbed by the heat-transfer gas is 906,000 MW_t-hr. This figure includes heat absorbed in the central receiver and heat absorbed during gas compression. Assorted thermal losses reduce the annual thermal energy available for power generation by 12% to 792,000 MW_t-hr. This is sufficient energy to allow an average of 12.3 hours of operation at full capacity per day, 256 days per year. Since the power plant is in operation whenever heat is available from the central receiver, the average length of the charge period is 8.0 hours per day, and the average length of the discharge period is 4.3 hours per day. The gross electric generation is 100.0 MW_e whenever the power plant is operating at full capacity. Parasitic power losses during charging total 9.6% of the gross generation, leaving 90.4 MW_e net electric power generation. At nighttime, no gas is pumped through the receiver, cutting parasitic power losses to 5.9 MW_e and providing a net electric generation of 94.1 MW_e.

The proposed solar power plant provides 288,000 MW_e-hr net annual electric energy generation. Adding the installed costs for each subsystem gives a total installed solar power plant cost of $139,000,000 based on June, 1978 prices. Assuming that capitalization, operating, and maintenance costs total 18% of the installed cost each year, the

Table 4-12. An Overall Summary of the Proposed Solar Power Plant Design

Annual Net Thermal Energy Input to the Central Receiver -	892,000 MW_t-hr
Annual Thermal Energy Input by the Gas Compressor -	14,000 MW_t-hr
Annual Thermal Energy Losses -	-114,000 MW_t-hr
Storage Subsystem -	-60,000 MW_t-hr
Heat-Exchange Subsystem -	-12,000 MW_t-hr
Gas-Circulation Subsystem -	-10,000 MW_t-hr
Power-Generation Subsystem -	-32,000 MW_t-hr
Annual Thermal Energy Available for Power Generation -	792,000 MW_t-hr
Number of Days of Operation Annually -	256 Days
Average Length of Daily Operation at Full Capacity -	12.3 hours
Average Length of Daily Charging Period -	8.0 hours
Average Length of Daily Discharging Period -	4.3 hours
Gross Electric Generation, Charging and Discharging -	100.0 MW_e
Parasitic Power Losses, Charging -	9.6 MW_e
Heat-Collection Subsystem -	1.8 MW_e
Storage Subsystem -	0.7 MW_e
Heat-Exchange Subsystem -	0.9 MW_e
Gas-Circulation Subsystem -	2.7 MW_e
Power-Generation Subsystem -	3.5 MW_e
Net Electric Power Generation, Charging -	90.4 MW_e
Parasitic Power Losses, Discharging -	5.9 MW_e
Storage Subsystem -	0.9 MW_e
Heat-Exchange Subsystem -	0.9 MW_e
Gas-Circulation Subsystem -	0.6 MW_e
Power-Generation Subsystem -	3.5 MW_e
Net Electric Power Generation, Discharging -	94.1 MW_e
Subsystem Installed Costs (June, 1978)	
Heat-Collection Subsystem -	$80,300,000
Storage Subsystem -	$36,200,000
Heat-Exchange Subsystem -	$ 7,000,000
Gas-Circulation Subsystem -	$ 5,600,000
Power-Generation Subsystem -	$10,000,000
Net Thermal Efficiency of the Solar Power Plant -	0.323 MW_e-hr/MW_t-hr
Net Annual Electric Energy Generation -	288,000 MW_e-hr
Total Installed Cost of the Solar Power Plant -	$139,000,000
Estimated Annual Cost of the Solar Power Plant for Capitalization, Operating, and Maintenance* -	$ 25,000,000
Estimated Annual Cost per Net Annual Electric Generation -	$ 87 per MW_e-hr

* - Capitalization costs are estimated to be 14% per year of the total installed cost. Operating and maintenance costs are estimated to be 4% per year of the total installed cost.

annual cost of this solar power plant is estimated to be $25,000,000. Dividing the annual solar power plant cost by the net annual electric energy generation gives an estimated electric cost of $87 per MW_e-hr.

The impact of sensible-heat storage on the cost of electricity generated by the proposed solar power plant is examined in Table 4-13. A comparison is made between the operations and costs for this solar power plant and for a similar solar power plant with "ideal" storage. "Ideal" storage is used to describe a best-possible storage unit which experiences negligible energy losses and can be installed for a negligible cost. "Ideal" storage provides a goal against which proposed storage unit designs can be compared. A solar power plant with "ideal" storage can provide 8% more net annual electric energy for a total installed cost which is 25% lower than the total installed cost of the proposed solar power plant design. Comparing the annual costs per net annual electric generation, the solar power plant with "ideal" storage produces electricity for $59 per MW_e-hr while the proposed solar power plant produces electricity for $87 per MW_e-hr. Increased capital costs represent 75% of this difference, while the decrease in electric production for the proposed storage unit raises the cost of electricity by $7 per MW_e-hr. It must be noted that the solar power plant with "ideal" storage produces electricity at a lower cost than any real solar power plant. Even if the storage unit could be completely eliminated, increased costs would still be incurred due to the increased size of the heat-exchange subsystem and the increased

Table 4-13. The Impact of Sensible-Heat Storage on the Cost of Electricity Generated by this Solar Power Plant.

	The Proposed Solar Power Plant Design	Solar Power Plant with "Ideal" Storage; Energy Losses from Storage and Cost of Storage assumed Negligible.
Annual Net Thermal Energy Input to the Central Receiver, MW_t-hr	892,000	892,000
Annual Thermal Energy Input by the Gas Compressor, MW_t-hr	14,000	12,000
Annual Thermal Energy Losses, MW_t-hr	-114,000	-54,000
Annual Thermal Energy Available for Power Generation, MW_t-hr	792,000	850,000
Average Length of Daily Operation at Full Capacity, hours	12.28	13.17
Average Length of Daily Charging Period, hours	8.00	8.00
Average Length of Daily Discharging Period, hours	4.28	5.17
Gross Electric Generation, MW_e	100.0	100.0
Parasitic Power Losses, Charging, MW_e	9.6	8.9
Net Electric Power Generation, Charging, MW_e	90.4	91.1
Parasitic Power Losses, Discharging, MW_e	5.9	5.0
Net Electric Power Generation, Discharging, MW_e	94.1	95.0
Net Thermal Efficiency of the Solar Power Plant, MW_e-hr/MW_t-hr	0.323	0.350
Net Annual Electric Energy Generation, MW_e-hr	288,000	312,000
Total Installed Cost of the Solar Power Plant, $	139,000,000	103,000,000
Estimated Annual Cost of the Solar Power Plant for Capitalization, Operating, and Maintenance,* $	25,000,000	18,500,000
Annual Cost per Net Annual Electric Generation, $/$MW_e$-hr	87	59

*-Capitalization, operating, and maintenance costs are estimated to be 18% of the total installed costs annually.

size of the power-generation subsystem required to utilize all of the solar energy as it becomes available.

5. THE EFFECTS OF SEVERAL MAJOR DESIGN PARAMETERS ON COST AND OPERATION OF THE SOLAR POWER PLANT

The proposed design for the solar power plant required specification of a series of design parameters to meet the requirements of the study guidelines that were discussed in Chapter 2. This chapter examines how well these design parameters were chosen by studying the impact of several major design parameters on the cost and operation of the solar power plant.

5.1 STORAGE-VESSEL DESIGN

The proposed solar power plant uses welded carbon-steel pressure vessels for brick containment in the sensible-heat storage units. Chapter 4.2 discusses the decision to use shop-fabricated vessels in an attempt to reduce storage-vessel costs. This vessel design is backed by years of experience and should be easily adaptable to storage unit requirements.

Siempelkamp Giesserei KG is presently developing a design for economical high-pressure/large-volume prestressed cast-iron storage vessels.[13] Prefabricated, interlocking cast-iron blocks form the walls of a storage vessel that can readily be assembled on site. These blocks are held together by axial and tangential cables. The cables are prestressed to keep the walls under compression even when the vessel is pressurized. An internal liner is provided to prevent gas leaks from the vessel.

Table 5-1 compares the use of welded carbon-steel storage vessels to the use of prestressed cast-iron vessels in the sensible-heat storage

Table 5-1. The Impact of Storage Vessel Design on the Sensible-Heat Storage Subsystem.

	Proposed Design: Welded Carbon-Steel Storage Vessels	Prestressed Cast-Iron Storage Vessels
Number of Storage Tanks	48	2
Number of Storage Tanks in Series	6	2
Inside Diameter of Storage Tanks, m	3.36	8.86
Length of Storage Tanks, m	21.0	59.0
Volume of each Storage Tank, m^3	190	3,600
Total Required Storage Volume, m^3	9,000	7,300
Thermal Energy Stored per Cycle, MW_t-hr	1,510	1,510
Thermal Energy Released per Cycle, MW_t-hr	1,280	1,440
Annual Thermal Energy Input to Storage, MW_t-hr	387,000	387,000
Annual Heat Losses from Storage, MW_t-hr	60,000	19,000
Annual Parasitic Pumping Energy, MW_e-hr	2,500	2,700
Installed Storage Tanks Cost*, $	19,500,000	6,400,000
Installed Magnesia Brick Cost*, $	9,200,000	9,200,000
Installed Storage Tank Insulation Cost*, $	5,800,000	2,000,000
Installed Storage Piping, Headers, and Valves Cost*, $	1,700,000	700,000
Total Installed Sensible-Heat Storage Subsystem Cost*, $	36,200,000	18,300,000

* - Costs are as of June, 1978.

subsystem. Prestressed cast-iron vessels can be field-assembled allowing the use of larger diameters and greater lengths for the storage tanks than could be done for shop-fabricated vessels. This reduces the number of storage tanks from 48 to 2. Larger storage vessel diameters decrease the annual storage heat losses from 15% of the stored energy for the welded carbon-steel tanks to 5% of the stored energy for prestressed cast-iron vessels. Use of the prestressed cast-iron vessels also reduces costs for both the storage tanks and the storage-tank insulation by 65%, cutting the total installed sensible-heat storage subsystem cost from $36,200,000 to $18,300,000.

The impact of storage-vessel design on the solar power plant is reviewed in Table 5-2. Decreased thermal losses increase both the average length of daily operation at full capacity and the net annual electric energy generation for the solar power plant with prestressed cast-iron storage vessels. The increase in electric generation combined with the decrease in the total installed cost for the energy storage unit drops the cost of solar electricity from $87 per MW_e-hr for the proposed plant to $72 per MW_e-hr when prestressed cast-iron storage vessels are used.

5.2 CROSS-SECTIONAL AREA FOR GAS FLOW THROUGH THE STORAGE CHECKERWORK

Design of the sensible-heat storage unit requires deciding on the number of channels for gas flow through the storage unit. Increasing the cross-sectional area for gas flow through storage decreases gas velocity and results in a lower pressure drop in the storage unit. However, at lower gas velocities the gas-film heat-transfer coefficient

Table 5-2. The Impact of Storage Vessel Design on the Solar Power Plant

	Proposed Solar-Power Plant	Solar-Power Plant with Prestressed Cast-Iron Storage Vessels
Annual Net Thermal Energy Input to the Central Receiver, MW_t-hr	892,000	892,000
Annual Thermal Energy Input by the Gas Compressor, MW_t-hr	14,000	14,000
Annual Thermal Energy Losses, MW_t-hr	-114,000	-73,000
Annual Thermal Energy Available for Power Generation, MW_t-hr	792,000	833,000
Average Length of Daily Operation at Full Capacity, hours	12.3	12.9
Gross Electric Generation, MW_e	100.0	100.0
Parasitic Power Losses, Charging, MW_e	9.6	9.6
Net Electric Generation, Charging, MW_e	90.4	90.4
Parasitic Power Losses, Discharging, MW_e	5.9	6.0
Net Electric Generation, Discharing, MW_e	94.1	94.0
Net Annual Electric Energy Generation, MW_e-hr	288,000	303,000
Total Installed Cost of the Solar Power Plant,* $	139,000,000	121,000,000
Estimated Annual Cost of the Solar Power Plant for Capitalization, Operating and Maintenance,*,** $	25,000,000	21,800,000
Annual Cost per Net Annual Electric Generation,* $/$MW_e$-hr	87	72

* - Costs are as of June, 1978.

** - Capitalization, operating, and maintenance costs are estimated to be 18% of the total installed costs annually.

will drop, resulting in an increase in the mass of bricks required to store the specified amount of thermal energy. Figure 5-1 shows the effects of the cross-sectional area for gas flow on net annual electric energy generation and cost. A large increase in the net annual electric energy generation is experienced when the cross-sectional area is changed from 3.0 m^2 to 6.0 m^2. Only minimal changes are noted for cross-sectional areas between 6.0 m^2 and 18.0 m^2. No alternative design for a solar power plant was found in this study that allows generation of electricity at an appreciably lower cost than the proposed solar power plant with 12.0 m^2 of flow-channel cross-sectional area through storage.

5.3 OPERATING PRESSURE OF THE HEAT-TRANSFER FLUID

The operating pressure of the gas used as a heat-transfer medium affects the economics of the solar power plant. Low operating pressures reduce wall thicknesses required for the gas piping, storage tanks, and heat exchangers. Capital costs are increased at high operating pressures, but less parasitic energy is used for pumping the gas, so that the net annual electric energy generation is also increased. Figure 5-2 displays the effects of the operating pressure of the heat-transfer fluid on electric energy generation and cost. The proposed solar power plant operating at a pressure of 3.45 MPa (500 psia) generated electricity for \$87 per MW_e-hr. Alternative designs operating at pressures of 1.72 MPa (250 psia) and 5.17 MPa (750 psia) both generated electricity for \$91 per MW_e-hr.

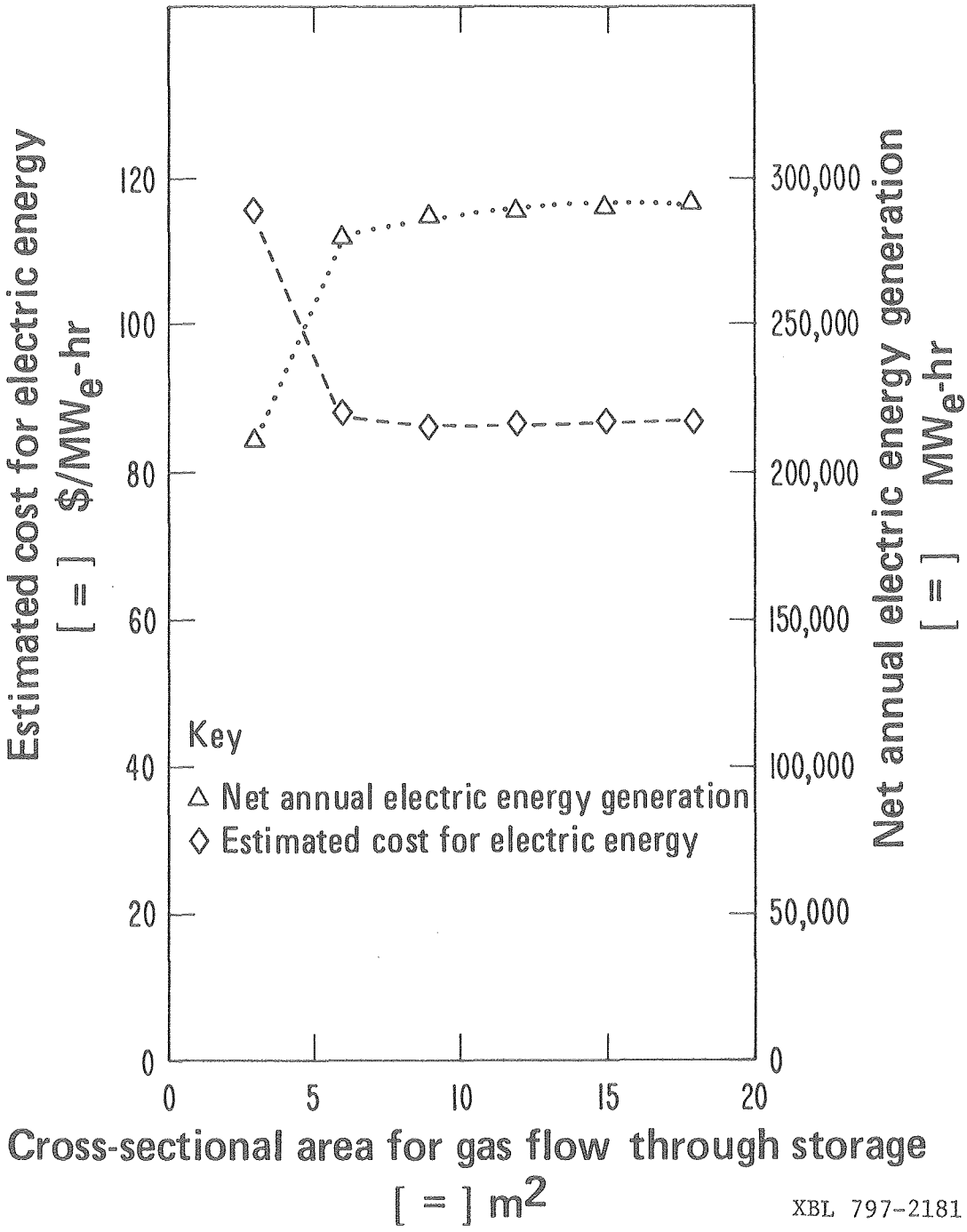

Fig. 5-1. A parametric study on the effects of the cross-sectional area for gas flow through storage on the amount of electric energy generated and its cost. The values of other independent parameters are identical with the design parameters for our proposed solar power plant. The annual fixed costs for capitalization, operating, and maintenance are assumed to be 18% of the installed solar power plant costs. The costs for electric energy were estimated by dividing the annual fixed costs by the net annual electric energy generation.

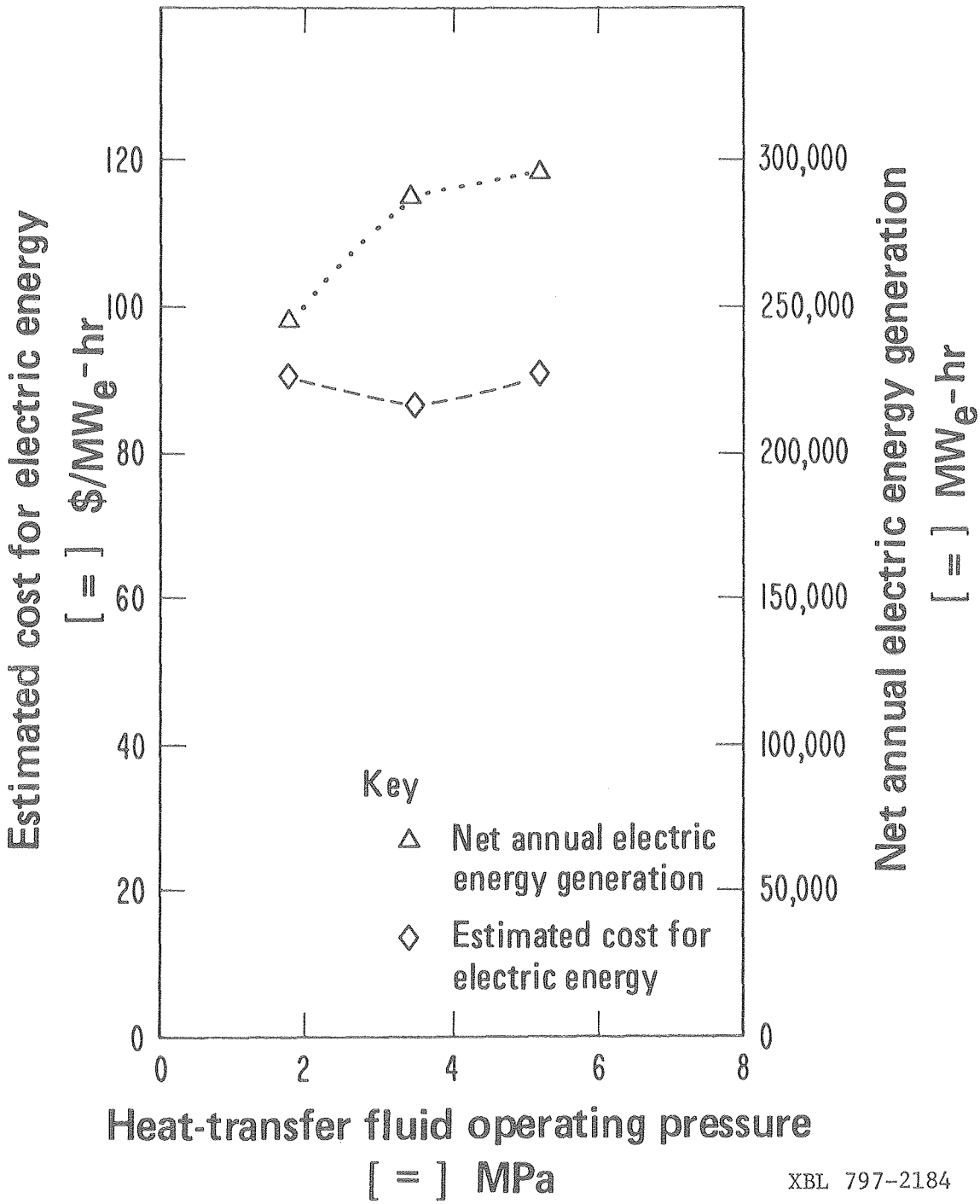

Fig. 5-2. A parametric study on the effects of heat-transfer fluid operating pressure on the amount of electric energy generated and its cost. Other major design parameters are identical with the design parameters for our proposed solar power plant. The cost for electric energy was estimated based on the procedure discussed for Fig. 5-1.

5.4 ELIMINATION OF NIGHTTIME ELECTRIC GENERATION

The solar power plant can be designed to generate electricity only during the daytime. Such a design would require a small sensible-heat storage unit to keep the turbines hot overnight, and would require larger heat exchangers and a larger power-generation subsystem to convert all of the available thermal energy into electricity during the eight hours of daylight. Table 5-3 compares a solar power plant without nighttime electric generation to the proposed solar power plant. The solar power plant which generates all its electricity during the daytime produces electricity for \$76 per MW_e-hr. The electricity cost for the proposed solar power plant, which generates 36% of its net electric energy overnight, is \$87 per MW_e-hr.

5.5 DURATION OF THE STORAGE DISCHARGE

The proposed solar power plant stores enough thermal energy to produce 100.0 MW_e gross power generation for 4.3 hours. A study showing the effect of varying the duration of storage discharge is summarized in Table 5-4. Annual thermal-energy input to storage is held constant. Longer storage discharge times are obtained by reducing the rate of storage discharge. Lower discharge rates adversely affect the thermal efficiency of the turbine-generator, but also reduce the thermal losses associated with keeping the turbine hot overnight. The net effect is that solar power plants with longer storage discharge times produce only slightly less electric energy and electricity costs are therefore only slightly higher.

Table 5-3. The Effect of Eliminating Nighttime Electric Generation on the Solar Power Plant

	Proposed Solar Power Plant	Solar-Power Plant without Nighttime Electric Generation
Annual Net Thermal Energy Input to the Central Receiver, MW_t-hr	892,000	892,000
Annual Thermal Energy Input by Gas Compressor, MW_t-hr	14,000	11,000
Annual Thermal Energy Losses, MW_t-hr	-114,000	-122,000
Storage Subsystem, MW_t-hr	-60,000	-16,000
Heat-Exchange Subsystem, MW_t-hr	-12,000	-18,000
Gas-Circulation Subsystem, MW_t-hr	-10,000	-10,000
Power-Generation Subsystem, MW_t-hr	-32,000	-78,000
Annual Thermal Energy Available for Power Generation, MW_t-hr	792,000	781,000
Annual Thermal Energy Input to Storage, MW_t-hr	387,000	106,000
Average length of the Daily Charging Period, hours	8.0	8.0
Steam-Turbine Heat Rate, Charging, MW_t	252	381
Gross Thermal Efficiency of Generation, Charging, MW_e/MW_t	0.40	0.40
Gross Electric Generation Charging, MW_e	100.0	151.4
Parasitic Power Losses, Charging, MW_e	9.6	11.4
Net Electric Generation, Charging, MW_e	90.4	140.0
Average Length of the Daily Discharging Period, hours	4.28	
Steam-Turbine Heat Rate, Discharging, MW_t	252	
Gross Thermal Efficiency of Generation, Discharging, MW_e-MW_t	0.40	
Gross Electric Generation, Discharging, MW_e	100.0	
Parasitic Power Losses, Discharging, MW_e	5.9	
Net Electric Generation, Discharging, MW_e	94.1	
Subsystem Installed Costs (as of June, 1978)		
Heat-Collection Subsystem, $	80,300,000	80,300,000
Storage Subsystem, $	36,200,000	9,900,000
Heat-Exchange Subsystem, $	7,000,000	10,600,000
Gas-Circulation Subsystem, $	5,600,000	5,600,000
Power-Generation Subsystem, $	10,000,000	15,100,000
Net Annual Electric Energy Generation, MW_e-hr	288,000	287,000
Total Installed Solar Power Plant Cost, $	139,000,000	121,000,000
Estimated Annual Cost of the Solar Power Plant for Capitalization, Operating, and Maintenance,* $	25,000,000	21,900,000
Annual Cost per Net Annual Electric Generation, $/MW-hr$_e$	87	76

* - Capitalization, operating, and maintenance costs are estimated to be 18% of the total installed solar power plant costs annually.

Table 5-4. The Effect of Varying Storage Discharge Time on the Solar Power Plant

	Proposed Solar Power Plant 4.3 hr Discharge	Solar-Power Plant with Storage Discharging in 10 hours	Solar Power Plant with Storage Discharging in 16 hours
Annual Net Thermal Energy Input to the Central Receiver, MW_t-hr	892,000	892,000	892,000
Annual Thermal Energy Input by Gas Compression, MW_t-hr	14,000	13,000	12,000
Annual Thermal Energy Losses, MW_t-hr	-114,000	-107,000	-97,000
Storage Subsystem, MW_t-hr	-60,000	-66,000	-75,000
Heat-Exchange Subsystem, MW_t-hr	-12,000	-12,000	-12,000
Gas-Circulation Subsystem, MW_t-hr	-10,000	-10,000	-10,000
Power-Generation Subsystem, MW_t-hr	-32,000	-19,000	-
Annual Thermal Energy Available for Power Generation, MW_t-hr	792,000	798,000	807,000
Annual Thermal Energy Input to Storage, MW_t-hr	387,000	387,000	387,000
Average Length of the Daily Charging Period, hours	8.0	8.0	8.0
Steam Turbine Heat Rate, Charging, MW_t	252	252	252
Gross Thermal Efficiency of Generation, charging, MW_e/MW_t	0.40	0.40	0.40
Gross Electric Generation, Charging, MW_e	100.0	100.0	100.0
Parasitic Power Losses, Charging, MW_e	9.6	9.6	9.6
Net Electric Generation, Charging, MW_e	90.4	90.4	90.4
Average Length of the Daily Discharging Period, hours	4.3	10.0	16.0
Steam Turbine Heat Rate, Discharging, MW_t	252	110	71
Gross Thermal Efficiency of Generation, Discharging, MW_e/MW_t	~0.40	~0.34	~0.31
Gross Electric Generation, Discharging, MW_e	100.0	37.0	22.0
Parasitic Power Losses, Discharging, MW_e	5.9	2.1	1.2
Net Electric Generation, Discharging, MW_e	94.1	34.9	20.8
Subsystem Installed Costs (as of June, 1978)			
Heat-Collection Subsystem, $	80,300,000	80,300,000	80,300,000
Storage Subsystem, $	36,200,000	35,300,000	34,700,000
Heat-Exchange Subsystem, $	7,000,000	7,000,000	7,000,000
Gas-Circulation Subsystem, $	5,600,000	5,600,000	5,600,000
Power-Generation Subsystem, $	10,000,000	10,000,000	10,000,000
Net Annual Electric Energy Generation, MW_e-hr	288,000	274,000	270,000
Total Installed Solar-Power Plant Cost, $	139,000,000	138,000,000	138,000,000
Estimated Annual Cost of the Solar-Power Plant for Capitalization, Operating, and Maintenance,* $	25,000,000	24,900,000	24,800,000
Annual Cost per Net Annual Electric Generation, $/$MW_e$-hr	87	91	92

* - Capitalization, operating, and maintenance costs are estimated to be 18% of the total installed solar power plant costs annually.

5.6 CHOICE OF GAS USED AS HEAT-TRANSFER MEDIUM

The properties of three possible heat-transfer gases are compared in Table 5-5. Helium has the highest heat capacity per unit mass and the lowest relative mass flow per unit of heat-transport capacity. Nitrogen and water vapor both require higher mass flows but lower volumetric flows than helium to carry a specified amount of heat. Parasitic pumping power requirements would be highest for a solar power plant with nitrogen as the heat-transfer medium and lowest for one with water vapor. Helium has the highest relative gas-film heat-transfer coefficient if gas flows with equal heat-transport capacities are passed through identical cross sections, but this gas-film heat-transfer coefficient is only about 50% higher than the gas-film heat-transfer coefficients of either nitrogen or water vapor.

Consideration of the temperature of condensation at the working pressure led to the elimination of water vapor as a possible heat-transfer medium, even thought it compares very favorably with nitrogen and helium in other respects. There appeared to be no practical and economically feasible method of avoiding condensation of water at the walls of the storage-containment vessels.

Table 5-6 shows model predictions for the effect of changing the heat-transfer fluid on central receiver operation. The model used to make these predictions is discussed in Chapter 4.1. This model predicts effective cavity temperatures for Boeing's central receiver design and for the proposed central receiver design, both of which use helium, and the alternative central receiver design using nitrogen. A lower

Table 5-5. Heat-Transfer Gas Properties

	Helium	Nitrogen	Water Vapor
Working Pressure, MPa	3.45	3.45	3.45
Condensation Temperature$\|_{\text{working pressure}}$, °K	< 300	< 300	514[1]
Density$\|^{600°K}_{\text{working pressure}}$, kg/m^3	2.77	19.3	13.2[1]
Density$\|^{1089°K}_{\text{working pressure}}$, kg/m^3	1.52	10.6	6.9[1]
Thermal Conductivity$\|^{1089°K}$, W/m°K	0.377[2]	0.070[2]	0.107[2]
Heat Capacity$\|^{1089°K}$, J/kg°K	5200[3]	1100[3]	2300[3]
Gas Viscosity$\|^{1089°K}$, N-s/m^2	4.8×10^{-5}[4]	4.6×10^{-5}[4]	4.2×10^{-5}[4]
Prandlt Number	0.64	0.72	0.92
Relative Mass Flows for Equal Heat Carrying Capacities$\|^{1089°K}_{\text{working pressure}}$	1.00	4.73	2.26
Relative Volumetric Flows for Equal Heat Carrying Capacities$\|^{1089°K}_{\text{working pressure}}$	1.00	0.68	0.50
Relative Gas Film Heat Transfer Coefficients for Gas Flows with Equal Heat Carrying Capacities through Identical Cross-sections	1.00	0.69	0.68

References for Gas Properties:

(1) Reference 15
(2) Reference 22, p. 3-215
(3) Reference 22, pp. 3-120 to 3-122
(4) Reference 22, pp. 3-210 & 3-211

Table 5-6. Model Predictions for the Effect of Changing the Heat Transfer Fluid on Central Receiver Operation*

	Boeing's Central Receiver Design	Proposed Central Receiver Design	Central Receiver Design with Nitrogen as the Heat-Transfer Fluid
Heat-Transfer Gas	Helium	Helium	Nitrogen
Gas Flow Rate per Tube, kg/s	0.0436	0.0248	0.117
Heat Flux to Gas per Tube, W	63,000	63,000	63,000
Inlet Gas Temperature, °K	811	600	600
Outlet Gas Temperature, °K	1089	1089	1089
Central Receiver Operating Pressure, MPa	3.45	3.45	3.45
Overall Heat-Transfer Coefficient, Tube Wall to Gas, $W/m^2°K$	1420	1010	750
Model Prediction for the Effective Cavity Temperature, °K	1276	1254	1270
Model Prediction for the Maximum Tube-Wall Temperature, °K	1133	1137	1156
Model Prediction for Pressure Drop Through the Heat-Exchange Tubing, kPa	46	15	42

* - This table summarizes conditions found for the lowest row of heat-exchange tubes in the central receiver. These tubes have the highest heat flux per tube.

overall heat-transfer coefficient between the tube wall and the gas results in a higher predicted maximum tube-wall temperature when nitrogen is used. This increase in the tube-wall temperature could be avoided, if necessary, by decreasing the gas temperature at the outlet of the receiver.

The effect of the heat-transfer fluid on the solar power plant is examined in Table 5-7. The lower thermal conductivity of nitrogen reduces annual thermal energy losses and increases the average length of daily operation at full capacity. Higher parasitic power losses for nitrogen partially offset this increased gross electric generation. Total installed costs for both solar power plants are an identical $139,000,000. Electricity costs are $87 per MW_e-hr when helium is used and $83 per MW_e-hr for the case with nitrogen. These estimates do not include the capital costs for establishing a heat-transfer medium inventory or the annual make-up costs to replace heat-transfer medium inventory losses.

5.7 CHOICE OF METHOD OF HEAT DISSIPATION

The choice of how the condensers of the solar power plant will eventually be cooled will depend largely on the availability of water. The proposed solar power plant is designed for a region where water is in short supply. This situation requires use of a high-backpressure turbine with heat rejection from a dry-cooling tower. Regions with greater water availability could use a conventional turbine with heat rejection from a wet-cooling tower. The proposed solar power plant is compared with one using cooling water in Table 5-8. The higher gross

Table 5-7. The Effect of the Heat-Transfer Fluid on the Solar Power Plant*

	Proposed Solar Power Plant	Solar Power Plant with Nitrogen as the Heat-Transfer Fluid
Annual Net Thermal Energy Input to the Central Receiver, MW_t-hr	892,000	887,000
Annual Thermal Energy Input by Gas Compressor, MW_t-hr	14,000	21,000
Annual Thermal Energy Losses, MW_t-hr	-114,000	-66,000
Annual Thermal Energy Available for Power Generation, MW_t-hr	792,000	842,000
Average Length of Daily Operation at Full Capacity, hours	12.3	13.05
Gross Electric Generation, MW_e	100.0	100.0
Parasitic Power Losses, Charging, MW_e	9.6	12.0
Net Electric Generation, Charging, MW_e	90.4	88.0
Parasitic Power Losses, Discharging, MW_e	5.9	7.7
Net Electric Generation, Discharging, MW_e	94.1	92.3
Net Annual Electric Energy Generation, MW_e-hr	288,000	300,000
Total Installed Cost of the Solar Power Plant***, $	139,000,000	139,000,000
Estimated Annual Cost of the Solar Power Plant for Capitalization, Operating and Maintenance**,*** $	25,000,000	25,000,000
Annual Cost per Net Annual Electric Generation***, $/$MW_e$-hr	87	83

* - Heat-transfer fluid inventory capital and make-up costs have not been included in this study.

** - Capitalization, operating, and maintenance costs are estimated to be 18% of the total installed costs annually.

***- Cost are as of June, 1978.

Table 5-8. A Comparison of Wet-Cooled and Dry-Cooled Solar Power Plant Designs

	Proposed Solar Power Plant	Wet-Cooled Solar-Power Plant
Cooling Tower Type	Dry-Cooling Tower	Wet-Cooling Tower
Turbine Type	12.4 MPa, 811K/811K; High-Back pressure Turbine	12.4 MPa, 811K/811K; Conventional Turbine
Turbine Backpressure, kPa	20	9
Average Length of Daily Operation at Full Capacity, hours	12.3	12.3
Gross Thermal Efficiency of Generation, MW_e/MW_t	0.40	0.425
Gross Electric Generation, MW_e	100.0	107.1
Parasitic Power Losses, Charging, MW_e	9.6	9.3
Net Electric Generation, Charging, MW_e	90.4	97.8
Parasitic Power Losses, Discharging, MW_e	5.9	5.6
Net Electric Generation, Discharging, MW_e	94.1	101.5
Net Annual Electric Energy Generation, MW_e-hr	288,000	311,000
Total Installed Cost of the Solar Power Plant*, $	139,000,000	138,000,000
Estimated Annual Cost of the Solar Power Plant for Capitalization, Operating and Maintenance*,**, $	25,000,000	24,800,000
Annual Cost per Net Annual Electric Generation,* $/$MW_e$-hr	87	80
Estimated Annual Water Consumption for Cooling, m^3	-	500,000

* - Costs are as of June, 1978.

** - Capitalization, operating, and maintenance costs are estimated to be 18% of the total installed costs annually.

thermal efficiency for a conventional turbine and lower cost of a wet-cooling tower reduce the cost of electricity for a wet-cooled solar power plant to \$80 per MW_e-hr. Wet cooling will consume an estimated 500,000 m^3 of water annually.

6. ALTERNATIVE FLOWSHEETS FOR A SOLAR POWER PLANT WITH SENSIBLE-HEAT STORAGE

The previous chapters dealt with a single process configuration for a Rankine-cycle solar power plant with sensible-heat storage. Several alternative configurations were considered during the course of this work. This chapter outlines two of the more interesting flowsheet modifications and details preliminary estimates of the effects that these modifications would have on solar power plant operation.

6.1 DIVISION OF THE STORAGE UNIT INTO SEVERAL STORAGE TANK SETS

The introduction, Chap. 1.1, lists two major benefits that should be derived from the storage subsystem of the solar power plant. The storage subsystem is expected to provide energy storage and also to allow thermal buffering between the receiver and the steam boiler. The proposed storage subsystem is satisfactory in providing energy storage. However, continuous adjustments of the flow of the heat-transfer medium through storage will be required in order to maintain uniform steam conditions during a period of flucuating insolation. This need for continual adjustments to the flow through storage can be avoided during at least part of the charging cycle by division of the storage unit into several storage tank sets.

An alternative flowsheet for a solar power plant with the sensible-heat storage unit broken into two storage tanks sets is shown in Fig. 6-1. At the start of the charging cycle there will be no gas flow through storage tank set #2. A small flow of cool gas bypasses the receiver and then passes through storage flow control valve #3. The

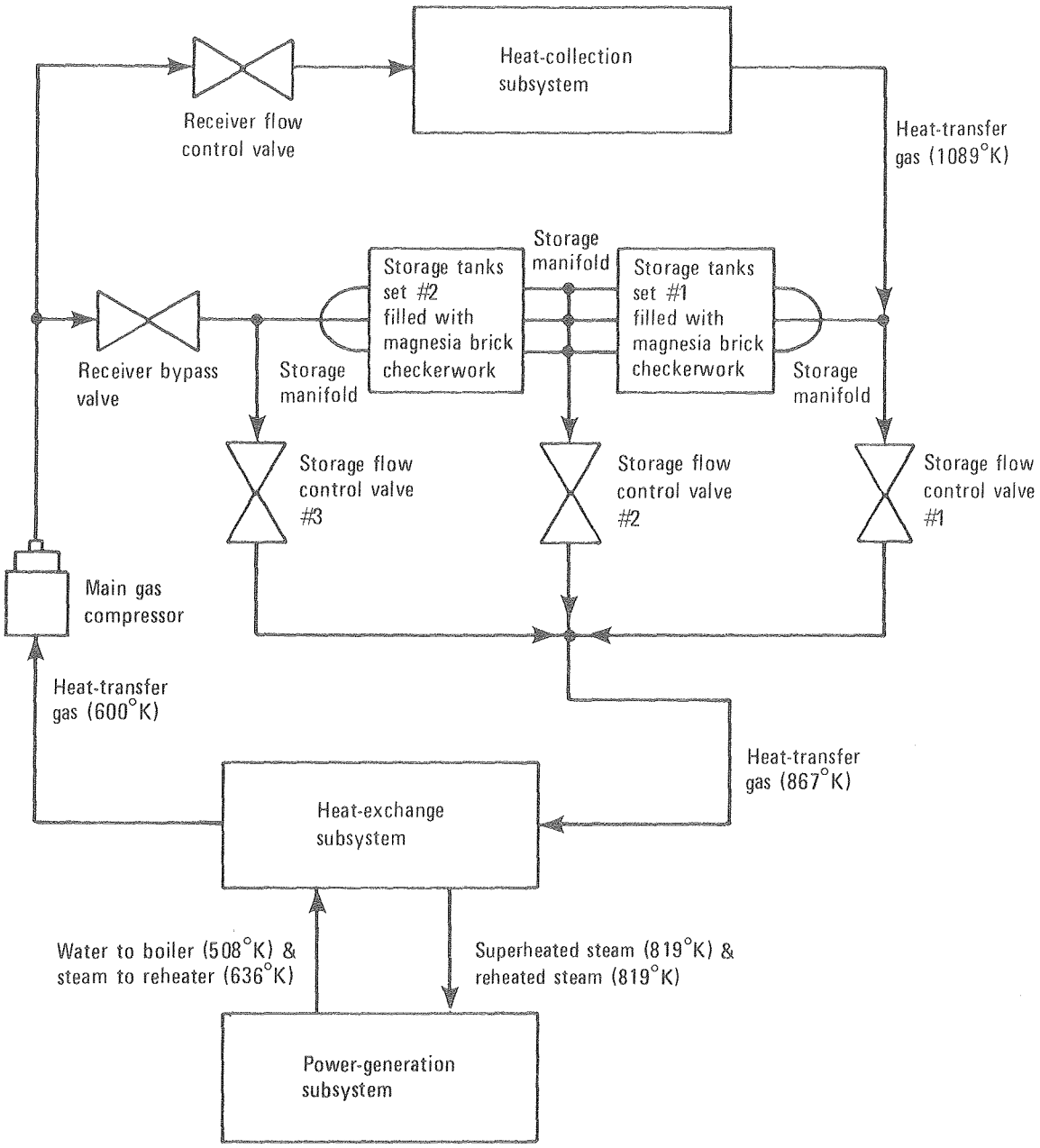

XBL 797-2174

Fig. 6-1. An alternative flowsheet for a solar power plant with the sensible-heat storage unit broken into two storage tank sets.

stream of hot gas from the receiver is split. Part of the receiver gas is routed through storage tank set #1 then out of the storage unit via storage flow control valve #2. The remaining hot gas bypasses the storage unit through storage flow control valve #1. These three streams are then mixed and sent to the heat exchangers in the steam generation system. The gas temperature out of storage tank set #1 is initially about 600°K but increases during charging. The temperature of the heat transfer gas sent to the heat exchangers is maintained constant by increasing the gas flow through storage and decreasing the fraction of the stream that is bypassed until all the hot gas passes through storage tank set #1. Gas flow through storage tank set #2 and storage flow control valve #3 is then initiated. Storage is completely charged when the mixed gas temperature through storage flow control valve #3 reaches 867°K. Figure 6-2 shows the actual gas mass flow rates during charging for this storage configuration.

Gas flow through storage is reversed during discharge. Discharging begins with part of the gas bypassing storage and the remaining gas flowing backwards through storage tank set #2 and then out storage flow control valve #2. The gas flow rate through storage tank set #2 is increased as the outlet gas temperature falls. When the outlet gas temperature from storage tank set #2 drops below 867°K, all of the gas flows into the storage unit. Gas flow backwards through storage tank set #1 is next initiated. As the gas outlet temperature from storage tank set #1 drops, the fraction of gas flowing through it is increased. Storage discharge is complete when all the heat-transfer gas is flowing

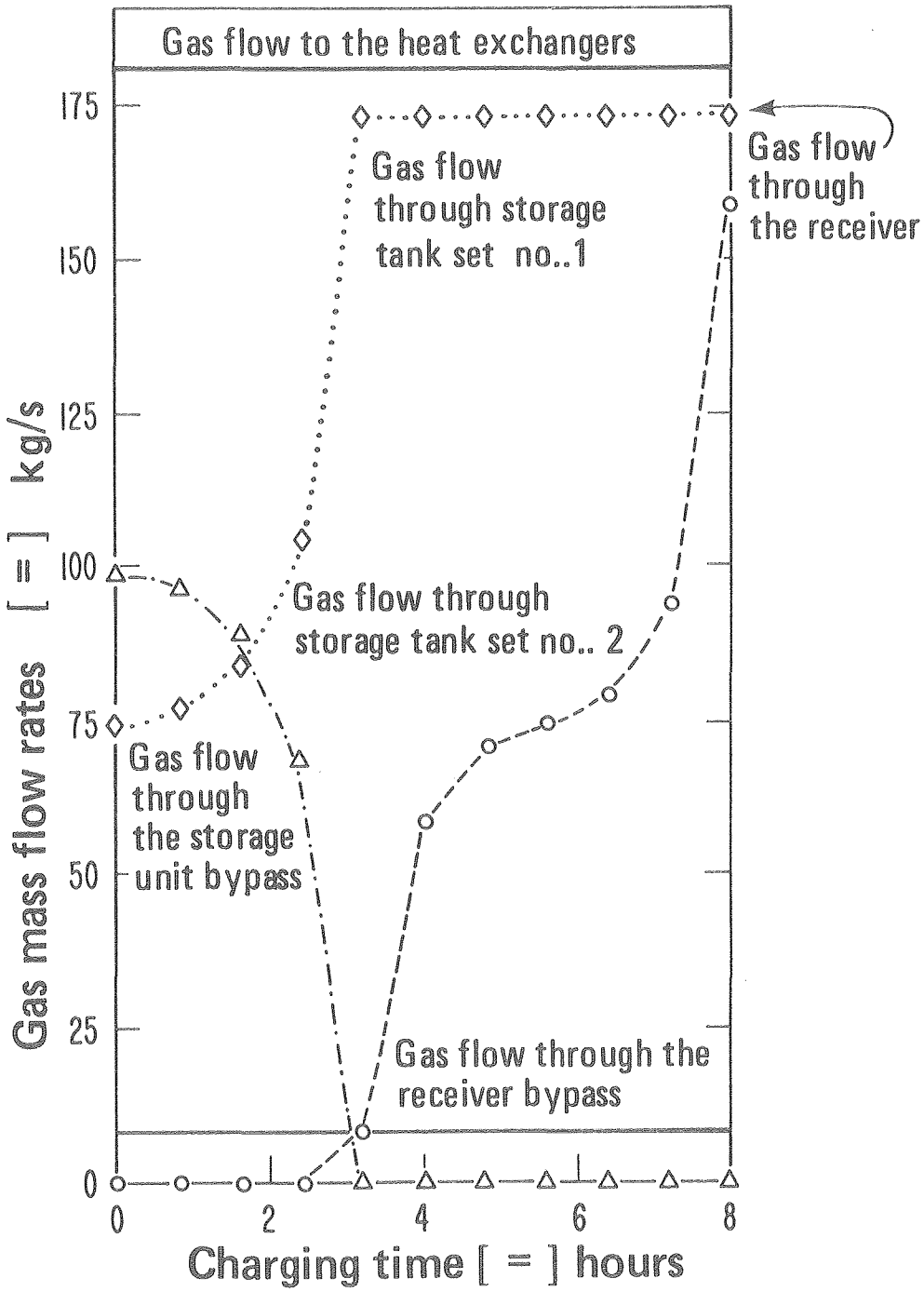

XBL 797-2183

Fig. 6-2. Charging gas mass flow rates for an alternate solar power plant with the storage unit divided into two storage tank sets.

backwards through both storage tank sets and the gas inlet temperature to the heat exchangers of 867°K can no longer be maintained.

Table 6-1 shows the effects on performance of dividing the storage unit into 1, 2, or 4 storage tank sets. Dividing the storage unit into several tank sets achieves the desired result of reducing the length of time during the charge cycle when the buffering of insolation transients requires variation in the flow rate through storage. Storage units with multiple storage tank sets also require fewer bricks, although this saving will be offset by increased costs for additional storage manifolds and additional storage flow control valves. No estimates were made of the cost of dividing the storage unit into several tank sets. However, this design modification appears to offer the possibility of slightly improved power plant performance.

6.2 BRAYTON-CYCLE TOPPING OF THE STEAM-CYCLE POWER PLANT

The proposed solar power plant has heat available from the central receiver at 1089°K. The highest gas temperature required for steam generation is 867°K. Figure 6-3 shows the flowsheet for an alternative solar power plant that takes advantage of this difference in temperature levels through the use of Brayton-cycle topping. High temperature gas is first expanded through a gas turbine, then generates steam for a Rankine-cycle turbine, and finally is recompressed to complete the cycle. An alternate flow path has been included which bypasses the gas turbine, for use when the gas temperature out of storage drops below an acceptable level.

Table 6-1. The Effects on Performance of Dividing the Storage Unit into Several Storage Tank Sets

	1 Storage Tank Set	2 Storage Tank Sets	4 Storage Tank Sets
Average Time per Charge Cycle during which insolation transient buffering requires varying storage flow rates, hr.	8.0	3.1	1.1
Average Brick Temperature after Charging, °K	1039	1052	1060
Average Brick Temperature after Discharging, °K	669	652	641
Brick Mass Required for Storage Unit, MM kg	13.8	12.7	12.2
Relative Required Brick Mass	1.00	0.92	0.88
Relative Average Pressure Drop, Charging	1.0	1.8	2.0
Relative Average Pressure Drop, Discharging	1.0	1.0	1.0

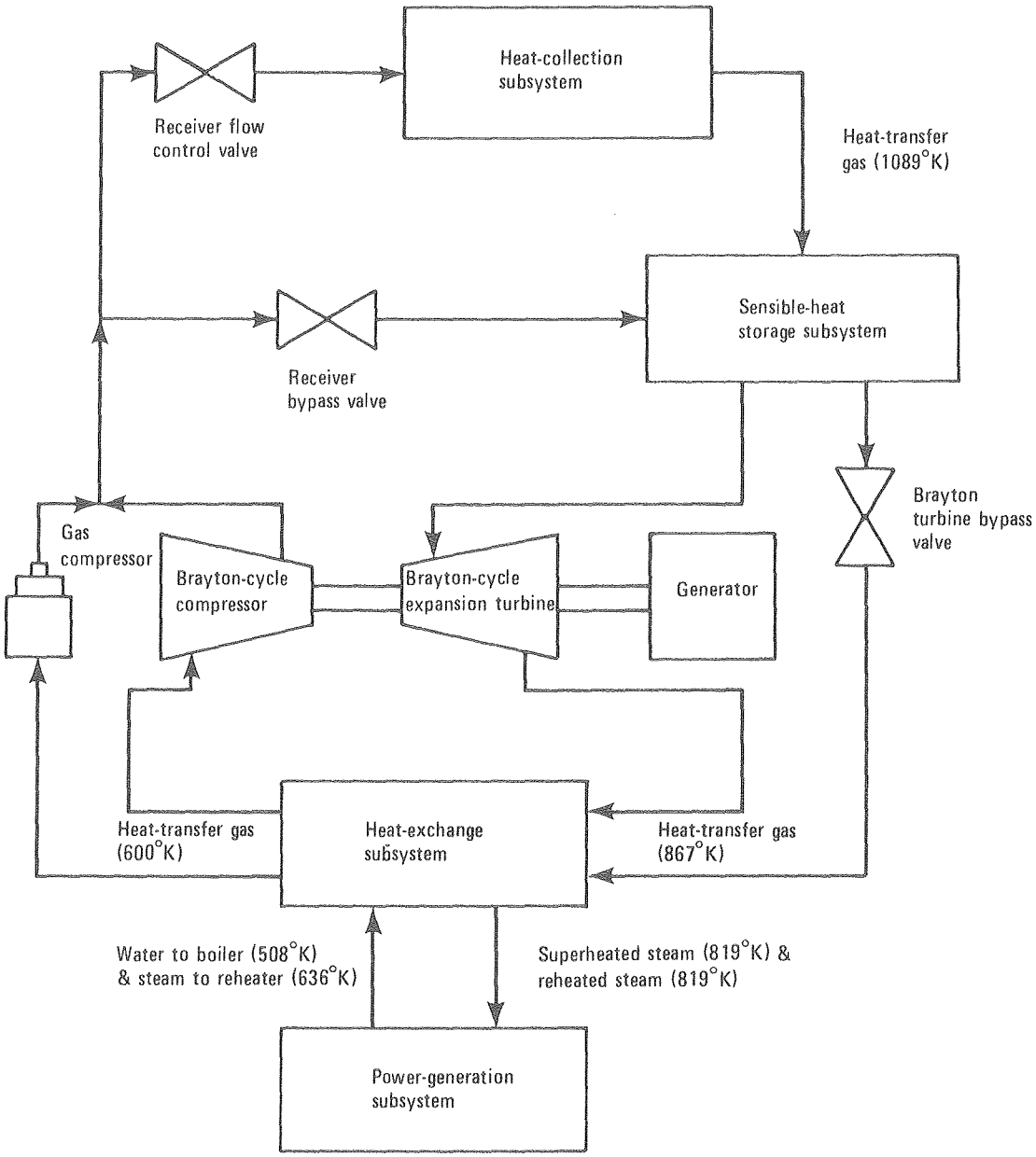

XBL 797-2173

Fig. 6-3. An alternative flowsheet for a solar power plant with Brayton-cycle gas turbine topping.

The effect of Brayton-cycle topping on the solar power plant is shown in Table 6-2. If the efficiencies of the expansion turbine and compressor are assumed to be 100%, gas-turbine topping can improve the gross thermal efficiency of generation to 0.479 MW_e per MW_t. However, if the efficiencies of the expansion turbine and compressor are 80%, the gross thermal efficiency of a solar power plant with gas-turbine topping will be less than the gross thermal efficiency of the proposed solar power plant. Brayton-cycle topping also adversely effects circulating gas temperature. Incorporation of a gas topping turbine in the solar power plant could also be expected to increase the required gas flow rate through the receiver and decrease the storage capacity of the sensible-heat storage unit, although the magnitude of these effects has not been examined.

Table 6-2. The Effect of Brayton Cycle, Gas Turbine Topping on the Gross Thermal Efficiency of a Solar Power Plant

	Proposed Solar Power Plant	Solar Power Plant with Ideal Gas Turbine Topping	Solar Power Plant with 80% Efficient Gas Turbine Topping
Brayton Cycle, Gas Turbine Generator Included	No	Yes	Yes
Isentropic Turbine-Generator Efficiency Assumed,	-	100%	80%
Gas Temperature to Turbine, °K	-	1005	1005
Gas Temperature to Heat Exchangers, °K	867	867	867
Heat Transfer Gas Pressure, High Pressure Side, MPa	3.45	3.45	3.45
Heat Transfer Gas Pressure, Low Pressure side, MPa	-	2.38	2.15
Gas Temperature out of Heat Exchangers, °K	600	600	600
Gas Temperature out of Compressor, °K	-	696	756
Electric Energy Produced per Unit Gas Flow, MJ/kg	0.55	0.77	0.46
Gas Expansion Turbine, MJ/kg	-	0.72	0.72
Gas Compressor, MJ/kg	-	-0.50	0.81
Steam Turbine, MJ/kg	0.55	0.55	0.55
Thermal Energy Released Per Gas Flow, MJ/kg	1.39	1.61	1.30
Gross Thermal Efficiency of Generation, MW_e/MW_t	0.397	0.479	0.355

7. A COMPARISON OF SENSIBLE-HEAT STORAGE WITH CHEMICAL-HEAT STORAGE FOR A STEAM SOLAR ELECTRIC PLANT

This work was undertaken to provide a basis for economic and operational comparisons between the sulfur oxide chemical-heat storage process described by Dayan, Lynn, and Foss[9] and the proposed sensible-heat storage process. Table 7-1 compares these two methods of energy storage. The chemical-heat storage process requires storage of a very large volume of pressurized oxygen. Underground caverns were chosen for this application. Above-ground storage of oxygen in the least costly vessels (prestressed cast iron) would increase the total chemical-heat storage costs by 80%. This large incentive for underground oxygen storage may limit the choice of sites suitable for a solar plant with sulfur oxide chemical-heat storage.

Table 7-1 shows that the installed cost per unit of energy stored and recovered each day is substantially lower for the chemical-heat storage process than for the proposed process of sensible-heat storage. Much of the difference in installed cost is due to the fact that the storage medium for chemical-heat storage (sulfur oxide) is much less expensive than the storage medium for sensible-heat storage (magnesia bricks). This reduction in the installed storage cost does not translate into a lower electric cost for a solar power plant with chemical-heat storage for two reasons. First, the reactants in the sulfur oxide system pose corrosion problems which will increase the annual operating and maintainance costs. These increased costs in the chemical system are reflected in the 25% annual charge for capital; in the sensible-

Table 7-1. A Comparison of the Proposed Sensible-Heat Storage Subsystem with a Sulfur Oxide Chemical-Heat Storage Process

	Proposed Sensible-Heat Storage Subsystem	Sulfur Oxide, Chemical-Heat Storage Process Described by Dayan, Lynn, and Foss[9]	
Storage Media	Magnesia Bricks	SO_3 or SO_2	O_2
Mass per Daily Energy Recovered, kg/MW_t-hr	10,800	3,000[SO_3]	800
Cost per Daily Energy Recovered, $\$/MW_t$-hr	7,200	500[SO_3]	None
Volume per Daily Energy Recovered, m^3/MW_t-hr	7.0	1.8	18.9
Storage Pressure, MPa	3.45	1.11	4.05
Storage Design	Cylindrical, Welded Carbon Steel Tanks	Spherical, Welded Carbon Steel Tanks	Underground Cavern Storage
Volumetric Cost, $\$/m^3$	2,200	600	200
Cost per Daily Energy Recovered, $\$/MW_t$-hr	15,400	1,100	3,800
Storage Insulation	Kaowool Block	None	None
Cost per Daily Energy Recovered, $\$/MW_t$-hr	4,500	-	-
Miscellaneous Storage Capacity Related Items	Storage Piping, Tank Manifolds, and Valves	None	None
Cost per Daily Energy Recovered, $\$/MW_t$-hr	1,300	-	-
Miscellaneous Storage Charging/Discharging Rate Related Items	None	Heat Exchangers, Distillation Column, Low Temperature Reactor, and Catalyst	
Cost per Daily Energy Recovered, $\$/MW_t$-hr	-	13,800	
Total Installed Storage Costs per Daily Energy Recovered, $\$/MW_t$-hr	28,000	19,000	

heat system the annual charge is only 18%. Second, the energy storage process chosen for a solar power plant greatly influences the plant energy balance, which changes the sizes of the remaining solar power plant components.

A comparison of the two energy storage processes for a solar power plant is given in Table 7-2. The solar power plant energy balances have been normalized based on equal net electric energy generation. About 20% more heat must be collected in the central receiver of a power plant with chemical-heat storage in order to provide the same amount of electric energy generation as a power plant with sensible-heat storage. The most striking difference between the two power plant designs is the large amount of waste heat which must be rejected from the chemical-heat storage system. More thermal energy losses are incurred by a solar power plant with sensible-heat storage since the chemical-heat storage process stores reactants at ambient temperature. Also, the solar power plant with chemical-heat storage has a much lower parasitic energy usage since all pumping is done on liquids. The estimated cost of electricity for the proposed plant of \$87 per MW_e-hr is about 20% lower than the estimated cost of electricity for the solar power plant with chemical-heat storage proposed by Dayan, Lynn and Foss.[9] This difference in electricity costs is caused primarily by the need for a larger heliostat field and central receiver when the chemical-heat storage process is used.

Both the chemical-heat storage process and the sensible-heat storage process are fairly well suited to the short-term storage

Table 7-2. A Comparison of Two Energy Storage Processes for a Solar Power Plant

	Proposed Solar Power Plant with Sensible-Heat Storage	Solar Power Plant with Sulfur Oxide Chemical-Heat Storage (9)
Normalized Solar Power Plant Energy Balances Based on the Net Electric Energy Generation		
Energy Input to the Central Receiver	309%	379%
Energy Input due to Gas Compression	5%	-
Waste Heat Rejected by the Steam Turbine	165%	137%
Waste Heat Rejected by the Storage System	-	132%
Thermal Energy Losses from the Turbine Overnight	11%	7%
Thermal Energy Losses from Storage	21%	-
Miscellaneous Thermal Energy Losses	8%	-
Total Energy Input	314%	379%
Total Waste Heat Rejected	165%	269%
Total Thermal Energy Losses	40%	7%
Electric Energy Usage for Parasitic Pumping	9%	3%
Net Electric Energy Generation	100%	100%
Fraction of the Electric Energy Generated at Night	36%	51%
Duration of the Discharge Period, hours	4.3	16.0
Estimated Electricity Costs* Prorated over Sections of the Plant		
Heat-Transfer Loop, Power Plant Boilers, and Storage, $/MW$_e$-hr	31	31
Heat-Collection Section, Turbine Generators, and Cooling Towers, $/MW$_e$-hr	56	76
Estimated Cost* of Electricity from the Solar Power Plant $/MW$_e$-hr	87	107

*- The electricity cost is estimated by dividing the Annual Costs for capitalization, operating and maintenance by the Net Annual Electric Energy Generation.

usages needed to store energy for nighttime discharge. However, chemical-heat storage is definitely superior for medium-term storage applications where energy is gradually accumulated for discharge perhaps once a week. The process for sulfur oxide chemical-heat storage stores reactants at ambient temperatures, avoiding the serious thermal losses that will be incurred if an attempt is made to store energy as sensible heat for an extended period of time. Also, since the costs related to charging and discharging rates dominate the cost of chemical-heat storage, expanding storage capacity is relatively inexpensive as long as maximum charging and discharging rates are not changed.

The provision of ambient-temperature storage for the chemical-heat storage process even though heat is absorbed and released at high temperatures greatly complicates design of a solar power plant. Large amounts of energy must be exchanged between streams over a wide range of temperatures in order to achieve the best possible thermal efficiency. Chemical-heat storage requires central receiver reactor tubes that are internally costed with catalyst to facilitate dissociation of SO_3 into SO_2 and O_2, technology that is not now available. The sulfur-oxide system components, SO_3, SO_2, and O_2, pose severe corrosion and toxicity problems under many of the proposed operating conditions. These factors combine to make the solar power plant design with sensible-heat storage the more desirable alternative unless a very large incentive for medium-term storage exists.

8. CONCLUSIONS AND RECOMMENDATIONS

This thesis presents a sensible-heat storage unit which will provide reasonable daily energy storage for a solar power plant. The operating temperature of the storage unit is sufficiently high to insure that steam can be supplied to the turbine at design conditions throughout discharge. High thermal losses and high capital costs make weekly or seasonal energy storage in a sensible-heat storage unit impractical. The major conclusions reached in studying the proposed solar power plant and several other power plants with different design parameters are:

1) Charging the storage unit in series with the power plant steam boilers and operating the storage unit at temperatures higher than those required by the steam boilers insures that the thermodynamic availability of energy supplied to the power turbines does not decrease during discharge. This is an important consideration in maximizing the efficiency of power generation and reducing the costs of the heliostat field and the central receiver.
2. The sensible-heat storage unit provides reasonable daily energy storage for a solar power plant. Energy storage for much longer periods of time would be impractical due to high capital costs and high thermal losses from storage.
3. The availability of cheap storage vessels will greatly influence the economic feasibility of sensible-heat storage. The use of prestressed cast-iron vessels for brick storage

cuts the cost of the storage subsystem in half and reduces the estimated cost of solar electricity by 17% compared with brick storage in welded carbon-steel tanks.

4) Nitrogen is an acceptable alternative to helium as the heat-transfer medium. A solar power plant using nitrogen will have lower thermal losses but will require higher parasitic power for gas circulation. The lower cost of nitrogen may prove to be the deciding factor.

5) The cross-sectional area for gas flow through the storage medium has little effect on the estimated cost of electricity for storage units having areas between 9 m^2 and 18 m^2. Consideration should be given to minimizing storage vessel costs before final selection of the configuration of the storage medium.

6) The nominal pressure of operation has little effect on the cost of electricity for operating pressures between 2 MPa and 5 MPa.

7) The duration of discharge of a given amount of stored energy has little effect on the estimated electric cost. How storage is to be discharged should be based on the anticipated night-time electricity demand.

8) In areas where sufficient water is available, wet cooling methods can increase the net electric generation by about 8%.

9) There is only a minimal difference between the cost of electricity produced by a solar power plant with sensible-heat storage using prestressed cast-iron vessels for brick

storage and that for a solar power plant without any nighttime electricity generation. The increased cost for the larger turbines and steam boiler system required when all of the collected solar energy must be converted into electricity during the daytime offsets the cost of the thermal energy storage that permits part of the electricity to be generated at night. The choice between these two power plants must be made on the basis of when the electricity can be most effectively utilized.

Two alternative flowsheets for a solar power plant with sensible-heat storage have been suggested. The process modification to allow Brayton-cycle topping offers little potential for improving operation of the solar power plant. Modification of the storage unit by dividing it into several storage-tank sets is a more promising idea. Although the complexity of storage piping increases, the storage unit will now adequately buffer variations in insolation without adjustments to storage flow rates for a substantial portion of the charge cycle. Further development of the solar power plant should examine this flowsheet modification in more detail.

A solar power plant with sensible-heat storage offers a number of advantages over a solar power plant with a sulfur-oxide chemical-heat storage process. These include a lower estimated electricity cost, a less complicated process flowsheet, more flexibility in site selection, and less corrosion and toxicity problems. Sulfur-oxide chemical-heat storage should only be pursued if the potential it offers for medium-term energy storage outweighs all of these disadvantages. Sensible-heat

storage can provide solar power plant energy storage for a reasonable price using technology that is presently available. It appears to be the most appropriate choice for the first solar power plants.

NOTATION

A_{brick} = Total brick cross-sectional area through storage; m^2

$A_{channel}$ = Total cross-sectional area for gas flow through storage; m^2

C_{brick} = Brick heat capacity; J/(kg·°K)

$C_{p,gas}$ = Gas heat capacity at a constant pressure; J/(kg·°K)

$C_{v,gas}$ = Gas heat capacity at a constant volume; J/(kg·°K)

D = Effective diameter of the gas flow channels through storage; m

D_i = Inside diameter of the receiver heat-exchange tubes; m

D_o = Outside diameter of the receiver heat-exchange tubes; m

h_{brick} = Brick-side heat transfer coefficient; $W/(m^2 \cdot °K)$

h_{gas} = Gas film heat transfer coefficient; $W/(m^2 \cdot °K)$

K_{brick} = Thermal conductivity of the brick; W/(m·K)

K_{gas} = Thermal conductivity of the gas; W/(m·°K)

K_{wall} = Thermal conductivity of the receiver heat-exchange tube walls; W/(m·°K)

L = Length of a receiver heat-exchange tube; m

$\dot{M}_{gas}$ = Gas mass flow rate through storage; kg/s

$\dot{M}_{gas\ per\ tube}$ = Gas mass flow rate through a receiver heat-exchange tube; kg/s

P_{eff} = Effective heat transfer perimeter between the gas and the bricks; m

Pr = Prandlt number.

q = Heat flux density through a receiver heat-exchange tube based on the outer surface area of the tube; W/m^2

$q_{cavity\ to\ tube\ wall}$ = Heat flux density from the cavity to the outer wall of a receiver heat-exchange tube based on the outer surface area of the tube; W/m^2

q_{eff} = Effective local heat flux density; W/m^2

$q_{tube\ wall\ to\ gas}$ = Heat flux density from the outer wall of a receiver heat-exchange tube to the bulk gas based on the outer surface area of the tube; W/m^2

Q_{tube} = Total heat flux to a single receiver heat-exchange tube; W

Re = Reynolds number.

t_{wall} = Wall thickness for a receiver heat-exchange tube; m

$T_{avg,brick}$ = Mass-averaged brick temperature for an incremental volume of bricks; °K

T_{brick} = Local brick temperature; °K

$T_{eff,cavity}$ = Effective cavity temperature to be used in modeling the receiver; °K

T_{gas} = Bulk gas temperature; °K

$T_{gas,in}$ = Gas temperature at the inlet to the receiver; °K

$T_{gas,out}$ = Gas temperature at the outlet from the receiver; °K

$T_{interface}$ = Temperature of the brick/gas interface; °K

$T_{tube\ wall}$ = Outer temperature of the receiver tube wall; °K

U_o = Overall heat-transfer coefficient; $W/(m^2 \cdot °K)$

W = Brick width; m

X = Distance into the brick perpendicular to a vertical flow channel wall; m

Z = Distance into the storage unit or receiver heat-exchange tube; m

α_{12} = Tube absorptance.

ΔZ = An incremental length of the storage unit; m

$\Delta\theta$ = An incremental amount of time; s

ε_1 = Tube emittance.

θ = Time; s

ρ_{brick} = Brick density; kg/m^3

σ = Stefan-Boltzmann constant; 5.67×10^{-8} $W/(m^2 \cdot K^4)$

REFERENCES

1. American Society of Mechanical Engineers, ASME BOILER AND PRESSURE VESSEL CODE, An American National Standard, SECTION VIII, Rules for Construction of Pressure Vessels, Division 1, 1974 Edition, New York.

2. Boeing Engineering and Construction, ADVANCED THERMAL ENERGY STORAGE CONCEPT DEFINITION STUDY FOR SOLAR BRAYTON POWER PLANT: Final Technical Report, Volumes 1,2,3, and 4, ERDA Contract No. EY-76-C-03-1300, July 1, 1976-December 31, 1976, U.S. Energy Research and Development Administration, Washington.

3. Boeing Engineering and Construction, CLOSED CYCLE, HIGH-TEMPERATURE CENTRAL RECEIVER CONCEPT FOR SOLAR ELECTRIC POWER: Interim Report, Report No. EPRI ER-183, February, 1976, National Technical Information Service, Springfield, VA.

4. Boeing Engineering and Construction, TECHNICAL AND ECONOMIC ASSESSMENT OF PHASE CHANGE AND THERMOCHEMICAL ADVANCED THERMAL ENERGY STORAGE (TES) SYSTEMS, EPRI EM-256, (Research Project 788-1), Final Report, Volume 1, December 1976, Electric Power Research Institute, Palo Alto, CA.

5. CE Plant Cost Index, Chem. Eng., Volumes 67 to 85, (1960 to 1978).

6. Clark, F. D. and Fermi, S. D., Jr., "Thick-wall Pressure Vessels", Chem. Eng., 79, No. 7, pp. 112-116, (1972).

7. Clerk, J., "Multiplying Factors Give Installed Costs of Process Equipment", Chem. Eng., 70, No. 4, pp. 182-184, (1963).

8. Davidson, M., and Grether, D., The Central Reciever Power Plant: An Environmental, Ecological, and Socioeconomic Analysis, Report No. LBL-6329, June, 1977, National Technical Information Service, Springfield, VA.

9. Dayan, J., Foss, A. S., and Lynn, S., Evaluation of a Sulfer Oxide Chemical Heat Storage Process for a Steam Solar Electric Plant, Report No. LBL-7868, 1979, Lawrence Berkeley Laboratory, Berkeley, CA.

10. Foust, Wenzel, Clump, Maus, and Anderson, Principles of Unit Operations, John Wiley & Sons, New York, (1960).

11. General Electric Company, Steam Turbine-Generator Products Division, Heat Rates For Fossil Reheat Cycles Using General Electric Steam Turbine-Generators 150,000 KW and Larger, General Electric Company Reprint GET-2050 C, February, 1974, Schenectady, NY.

12. General Electric Company, Steam Turbine-Generator Products Division, "Turbine Design Drawing 414 HB 725," November 8, 1972, Schenectady, NY.

13. Gilli, P. V., Beckmann, G., and Schilling, F. E., Thermal Energy Storage Using Prestressed Cast Iron Vessels (PCIV), Final Report, ERDA Contract No. EY-76-C-02-2886, June, 1977, National Technical Information Service, Springfield, VA.

14. Hill, S. A., Adaptation of the Sulfer Oxide System for Chemical Storage of Solar Energy, UC Berkeley, M.S. Thesis, (1978).

15. Keenan, J. H., and Keyes, F. G., Thermodynamic Properties of Steam, John Wiley & Sons, New York, (1936).

16. Larsen, F. W., "Rapid Calculation of Temperature in a Regenerative Heat Exchanger Having Arbitrary Initial Solid and Entering Fluid Temperatures," Int. J. Heat Mass Transfer, Volume 10, pp. 149-168, (1967).

17. Martin Marietta Corporation, CENTRAL RECEIVER SOLAR THERMAL POWER SYSTEM, PHASE 1, Progress Report for Period Ending December 31, 1975, ERDA Contract E(04-3)1110, National Technical Information Service, Springfield, VA.

18. Martin Marietta Corporation, CENTRAL RECEIVER SOLAR THERMAL POWER SYSTEM, PHASE 1, Quarterly Progress Report for Period Ending June 30, 1976, ERDA Contract E(04-3)1110, National Technical Information Service, Springfield, VA.

19. Morrison, M.K., "Turbines for High Exhaust Pressures," General Electric Marketing Information Letter No. 922, June 28, 1971, Schenectady, NY.

20. Morrison, M. K., "Turbine-Generators for High Exhaust Pressures", General Electric Marketing Information Letter No. 946, November 29, 1971, Schenectady, NY.

21. Norton, R.C., Westre, W. J., and Larsen, G. L., "Dry Cooling Design Characteristics of a Large Power Plant," Stone & Webster Engineering Corporation, Boston.

22. Perry, R. H., and Chilton, C. H., Editors, Chemical Engineers' Handbook, Fifth Edition, McGraw-Hill, San Francisco, (1973).

23. Peters, M. S., and Timmerhaus, K. D., Plant Design and Economics for Chemical Engineers, Second Edition, McGraw-Hill, San Francisco, (1968).

24. Popper, H., Editor, Modern Cost-Engineering Techniques, McGraw-Hill, San Francisco, (1970).

25. Private communication with General Electric Company, Power Generation Sales Division, San Francisco, (1978).

26. Private Communication with Mr. H. M. Mikami, Manager, Basic Refractories Research, Kaiser Aluminum and Chemical Corporation, Pleasanton, CA, August 10, 1978.

27. Private communication with Westinghouse Corporation; (1978).

28. Rossie, J. P., and Cecil, E. A., Research on Dry-Type Cooling Towers for Thermal Electric Generation: Part I, EPA Contract 14-12-823, November, 1970, U.S. Government Printing Office, Washington.

29. Skimrod, A. C., Brumleve, T. D., Schafer, C. T., Yokomizo, C. T., and Leonard, C. M., Jr., Status Report on a High Temperature Solar Energy System, Report No. SAND 74-8017, September, 1974, Sandia Laboratories, Livermore, CA.

30. Spencer, R. C., Cotton, K. C., and Cannon, C. N., "A Method for Predicting the Performance of Steam Turbine Generators...16,500 KW and Larger, General Electric Company Reprint GER-2007C, July, 1974, Schenectady, NY.

31. Stepanoff, A. J., TURBOBLOWERS: Theory, Design, and Application of Centrifugal and Axial Flow Compressors and Fans, John Wiley & Sons, New York, (1955).

32. Woodard, J. B., "Role of Storage in Determining the Value of a Solar Electric Plant in an Electric Power Grid", Talk given at the 1978 DOE Workshop on System Studies for Central Solar Thermal Electric, March, 1978, Houston.

APPENDIX I

Cost Estimation Methods

Valid cost estimation techniques are mandatory for an accurate assessment of the feasibility of sensible-heat storage. The techniques that were used for estimating the solar power plant installed costs are outlined in this appendix. An attempt was made to balance cost estimation detail and the influence that individual items have upon the cost of energy storage. For this reason, sensible-heat-storage-unit components were examined in much greater detail than components of other power plant subsystems. Cost data from a variety of sources were adjusted to estimated price levels for June, 1978 by use of the CE Plant Cost Index published in each issue of Chemical Engineering.

I.1 STORAGE SUBSYSTEM COSTS

Storage subsystem component costs were examined in great detail. This examination included separate cost estimates for the storage tanks, the storage-tank insulation, the magnesia-brick checkerwork, and piping, headers, and valves for the storage subsystem. Costing procedures for piping, headers, and valves are developed in section I.2, which explains cost estimation for the gas-circulation subsystem. Costing procedures for the remaining items are explained below.

I-1a Storage Tanks: Welded Carbon-Steel Pressure Vessel Cost

The costs of welded carbon-steel pressure vessels were determined by estimating the vessel weights and by estimating costs per kilogram of steel for vessel fabrication, for shipping the vessel to location,

and for installing the vessel. Pressure vessel weights and dimensions were calculated using general methods presented in the ASME Boiler and Pressure Vessel Code, Section VIII, Division 1.[1]

Vessel fabrication costs were determined using the cost data presented by Clark and Fermi for shop fabrication of presure vessels with 5-cm to 23-cm thick walls.[6] The tanks for the proposed storage unit have 5.4-cm thick walls and were estimated to cost $3.1 per kilogram steel. Shipping the vessels to location was estimated to add 10¢ per kilogram steel to the delivered vessel cost.[6] Tank installation costs were assumed to be 40% of the purchased tank cost or about $1.3 per kilogram steel (23, p. 109). Adding fabrication, delivery, and installation charges resulted in an installed tank cost of $4.5 per kilogram steel. The installed cost for a 3.36-m ID tank, 21-m long, with a total volume of 190 m^3, that can withstand internal pressures up to 3.80 MPa was estimated to $400,000. This represents a volumetric storage cost of about $2,200 per cubic meter.

I.1b Storage Tanks: Prestressed Cast-Iron Vessel Cost

Siempelkamp Giesserei KG is presently involved in development of prestressed cast-iron vessels. This design concept promises to reduce the costs of large-volume, high-pressure storage tanks. In a report to ERDA on the possibilities of using prestressed cast-iron vessels for thermal-energy storage,[13] Gilli, Beckmann, and Schilling present a detailed analysis indicating the expected effects of pressure and vessel dimensions on the costs of various vessel components, vessel installation, and startup. This analysis was used to estimate a cost

of $3,200,000 for a 59 m long tank with an inside diameter of 8.86 m and a total volume of 3600 m^3 designed to withstand an internal pressure of 3.80 MPa. The volumetric storage cost for these prestressed cast-iron vessels of $880 per m^3 is only 40% of the volumetric storage cost for welded carbon-steel vessels.

I-1c Magnesia Brickwork Cost

Communication with Mr. Mikami of Kaiser Aluminum and Chemical Corporation[26] has revealed that the cost of Kaiser brand K-98B magnesia bricks is $2.92 per standard size brick (76 mm × 114 mm × 229 mm) or $0.50 per kilogram brick. Shipping costs are estimated to add 10¢ per kilogram of brick,[6] and laying the brick checkerwork inside the storage tanks is expected to cost about 7¢ per kilogram brick (2, p. 2-23). Based on these estimates, the total cost of installed magnesia-brick checkerwork is $0.67 per kilogram of brick.

I.1d Kaowool Insulation Cost

The installed cost of kaowool insulation was estimated to be $12.8 per kilogram kaowool (2, p. 2-23). This estimate was used in determining costs of both kaowool-blanket insulation and kaowool-block insulation.

I.2 GAS-CIRCULATION SUBSYSTEM COSTS

1.2a Gas Piping Cost

Gas circulation for the solar power plant requires several long runs of very large diameter (~2 m) piping. Fabrication of this piping will most closely resemble fabrication of a thin-walled pressure vessel. Based on this observation and on cost data for thin-walled pressure

vessels gathered from variety of sources (22, p. 6-104; 23, p. 477; 24, pp. 90-91), the fabricated cost of welded carbon-steel piping was estimated to be $1.0 per kilogram of carbon-steel. Delivering the pipes to location was estimated to cost $0.1 per kilogram steel.[6] Pipe installation was estimated to be about 46% of the total installed piping cost or $0.9 per kilogram of steel (23, p.111). This results in an installed steel piping cost of $2.0 per kilogram of carbon steel. Pipe dimensions and weight were determined following the ASME Boiler and Pressure Vessel Code, Section VIII, Division 1.[1] The total installed piping cost is obtained by adding the cost of kaowool insulation to the cost of the steel piping. Kaowool-blanket insulation installed cost was estimated to be $12.8 per kilogram (2, p. 2-23) or about $1640 per m^3 based on a density of 130 kg/m^3 (3, p. 43).

I.2b Flow Control Valve Costs

No satisfactory method was found for determining the cost or even the feasibility of a valve suitable for controlling flow of a high-temperature (1089°K), high-pressure (3.45 MPa) gas through a 1.8 m pipe. An order-of-magnitude cost estimate was obtained by hypothesizing that the cost of the valve is proportional to the valve flow area and scaling up from the cost of a 10-inch ID butterfly valve (23, p. 452). This estimation procedure suggested a cost of $70,000 per m^2 of valve flow area or a cost of $200,000 for a 1.8-m ID flow control valve.

I.2c Gas Compresor Cost

The cost of a single-stage axial compressor with motor-gear drive was extrapolated from a graph in Peters and Timmerhaus showing the costs

of five-stage to twelve-stage axial compressors over a wide range of capacities (23, p. 468). A cost of $400,000 was estimated for a single-stage axial compressor with a capacity of 66 m^3/s.

I.3 HEAT-COLLECTION SUBSYSTEM COSTS

The heat-collection subsystem has been adapted directly from work that Boeing Engineering and Construction did on a high-temperature central receiver.[3] In another report, Boeing presents the costs (2, p. 1-6) and amount of heat which will be absorbed (2, p. 5-8) if such a receiver is used to provide thermal energy for their proposed Brayton-cycle solar power plant. These data were used to estimate costs under the assumption that central receiver and heliostat field costs are proportional to the amount of heat absorbed. Heliostats were predicted to cost $136,000 per MW_t absorbed by the gas. The central receiver including heat exchangers tubes and the tower it is mounted upon was estimated to cost $48,000 per MW_t absorbed by the gas.

I.4 HEAT-EXCHANGE SUBSYSTEM COSTS

A detailed heat exchangers correlation (24, p. 88) was used to estimate the costs of individual heat exchangers and associated piping. This correlation is based upon costs of typical heat exchangers and may predict unrealistically low costs. In this study, exchangers were designed to reduce shell-side pressure drop by using a very large pitch between tubes. This reduced the number of tubes per cross-sectional area in this design to well below the typical value. In addition, part of the shell is filled with insulation further reducing the number of tubes which can be put into the shell. However, since the total projected

cost of the heat-exchange subsystem is only $7,000,000 or 5% of the total installed solar power plant cost, this is not anticipated to be a major source of error.

I.5 POWER-GENERATION SUBSYSTEM COSTS

1.5a Steam Turbine-Generator Cost

The Power Generation Sales Division of General Electric Company was contacted about anticipated costs for 100 MW_e conventional and high-backpressure steam turbine-generators.[25] They were unable to provide a firm cost estimate, but indicated that they expected prices for both types of turbine-generators to be in the range of six to seven million dollars. An installed cost for a 100 MW_e turbine-generator of $6,500,000 was assumed.

I.5b Dry-Cooling Tower Costs

Dry-cooling tower costs were estimated using a price formula suggested by Mr. Von Cleve of GEA Airexchangers, Inc. (28, p. 127). Mr. Von Cleve has used this price formula to quote dry-cooling tower prices to United States utilities. The installed cost of an indirect (Heller) dry-cooling system with a natural-draft cooling tower was estimated to be $23,000 per MW_t of heat load for a tower with a 50°F difference between inlet gas and inlet water temperatures.

I.5c Wet-Cooling Tower Costs

The installed cost of a mechanical-draft wet-cooling tower with 24°F difference between the inlet water temperature and the wet bulb temperature of the inlet air was estimated to be $13,000 per MW_t heat load (28, p. 204).

Table I-1. Important Sources of Cost Estimation Data

Component	References	Unit Cost: June, 1978
Welded, Carbon Steel Pressure Vessels		$2200/m^3 for a 190 m^3 tank
Vessel Dimensions	1	
Fabricated Cost	6	3.1 $/Kg Steel (based on costs for thick walled vessels)
Shipping Cost	6	0.1 $/Kg Steel
Installation Cost	23,p.109	1.3 $/Kg Steel
Prestressed Cast-Iron Vessels	13	$880/m^3 for a 3600 m^3 Tank
Magnesia Brick		0.67 $/Kg Brick
F.O.B. Cost of Bricks	26	0.50 $/Kg Brick
Shipping Cost	6	0.10 $/Kg Brick
Installation Cost	2,p.2-23	0.07 $/Kg Brick
Kaowool Insulation	2,p.2-23	12.8 $/Kg Kaowool
Welded, Carbon-Steel Piping		2.0 $/Kg Steel
Piping Dimensions	1	
Fabricated Cost	22,p.6-104 23,p.477 24,pp.90-91	1.0 $/Kg Steel (estimated from typical costs of thin walled Pressure Vessels)
Shipping Cost	6	0.1 $/Kg Steel
Installation Cost	23,p.111	0.9 $/Kg Steel
Flow Control Valves	23,p.452	70,000 $/square meter of value flow area (linear scale up based on area from 10" ID to 1.8 m ID and from normal conditions to very harsh conditions [550 psi, 1089°K])
Gas Compressor	23,p.468	400,000 $ for a single stage axial compressor with a capacity of 66 cubic meters per second.
Heliostats	2,pp.1-685-8	136,000 $/MW Heat Absorbed
Central Receiver, Heat Exchange, & Tower	2,pp.1-685-8	48,000 $/MW Heat Absorbed
Heat Exchangers	24,p.88	Detailed Correlation
Steam Turbine	25	6,500,000 $/100 MWE Turbine
Dry-Cooling Tower	28,p.127	23,000 $/MW Heat Load (50°F ITD assumed)
Wet-Cooling Tower	28,p.204	13,000 $/MW Heat Load (24°F ITD assumed)

APPENDIX II

Storage Unit Modeling Program - HREGEN

The computer program used for modeling the storage unit is reviewed in this appendix. A discussion is contained in Chapter 3 on how the storage unit model was developed. This appendix contains program flowcharts, a listing of definitions for the physical variables used, a directory explaining program subroutines, a program listing and a sample program output. The numerical values of parameters set by data cards have been included in the listing of definitions for physical variables.

II.1 SUBROUTINE DIRECTORY FOR PROGRAM HREGEN

		Program Flowchart (Figure #)	Program Listing (Page #)
HREGEN	- Main program, calls other subroutines.	II-1	148
BCKGR	- Reads input variables.	II-2	148
IJSET	- Sets variables.	II-2	149
CRGINPT	- Reads input variables.	II-2	149
DISINPT	- Reads input variables.	II-2	150
GSPROP	- Calculates gas properties.	II-2	150
DESIGN	- Uses our model to design the storage unit	II-3	151
HRGCRG	- Calculates storage unit performance during charging based on input parameters	II-4	152
HRGDIS	- Calculates storage unit performance during discharging based on input parameters.	II-5	154

	Program Flowchart (Figure #)	Program Listing (Page #)
PRINTBG - Prints output data.	II-6	156
PRINTCH - Prints output data.	II-6	157
PRINTDS - Prints output data.	II-6	158
PDROPCH - Calculates storage pressure drop during charging.	II-6	159
PRNPRS - Prints output data.	II-6	159
PDROPDS - Calculates storage pressure drop during discharging and prints output data.	II-6	160

II.2 DEFINITIONS OF THE PHYSICAL VARIABLES USED IN PROGRAM HREGEN

COMMON/BCKGR/

CPBRIK - Brick heat capacity; 1067.0 J/(kg•°K)

CTGINF - Normal inlet temperature of gas to the storage unit during charging; °K

DIGINF - Normal inlet temperature of gas to the storage unit during discharging; °K

FLOWA - Cross-sectional gas flow area through storage; m^2

IGAS - Heat transfer gas symbol (1 represents H_2O, 2 represents He, and 3 represents N_2)

NTANKT - Total number of separately manifolded storage tank sets in series.

PERIM - Effective heat transfer perimeter through storage; m

TDSOSC - Desired outlet temperature of gas from the storage unit at the end of charging; °K

TEQD - Equivalent diameter of gas flow channels through storage; 0.0348 m

COMMON/CRGINPT/

DTHETC - Length of one time increment during charging; sec.

HTHETC - Total length of the storage charging cycle; hours

QHEC(360) - Heat transferred by the heat exchangers during a specified time increment; W

QR(360) - Heat absorbed by the central receives during a specified time increment; W

QRMAX(360) - Maximum amount of heat which could be absorbed by the central receiver during a specified time increment; W

THETC - Total length of the storage charging cycle; sec

TINHEC(360)- Gas temperature into the heat exchangers during a specified time increment; °K

TOUTHEC(360) - Gas temperature out of the heat exchangers during a specified time increment; °K

TOUTRM - Maximum allowable gas temperature out of the central receiver; °K

COMMON/DISINPT/

DTHETD - Normal length of one time increment during discharging; sec.

ESTDT - Estimated total length of the storage discharging cycle; sec.

HESTDT - Estimated total length of the storage discharging cycle; hours

QHED(360) - Heat transferred by the heat exchangers during a specified time increment; W

TDSOHE(360) - Desired outlet temperature of gas from the heat exchangers during a specified time increment; °K

TINHED(260) - Inlet temperature of gas to the heat exchangers during a specified time increment; °K

PROGRAM HREGEN

ENERGYC - Thermal energy accumulated in storage during charging; MW-hr

ENERGYD - Thermal energy released from storage during discharging; MW-hr

STORCAP - Energy accumulated in storage during each charge cycle per total mass of storage bricks; MW-hr/kg

SUBROUTINE BCKGR

No variables.

COMMON/ITSET/

IX12 - The total number of length increments storage is divided into.

JX10 - The estimated number of time increments charge and discharge cycles are divided into.

SUBROUTINE IJSET

No variables.

SUBROUTINE CRGINPT

ISTART(20) - First time increment within an interval over which the charging conditions are constant.

ISTOP(20) - Last time increment within an interval over which the charging conditions are constant.

N - Total number of particular sets of charging conditions.

SUBROUTINE DISINPT

ISTART(20) - First time increment within an interval over which the discharging conditions are constant.

ISTOP(20) - Last time increment within an interval over which the discharging conditions are constant.

N - Total number of particular sets of discharging conditions.

COMMON/GSPROP/

CPGAS - Gas heat capacity; J/(kg•°K)

KG - Gas thermal conductivity; W/(m•°K)

MU - Gas viscosity; Pa•s

PR - Prandtl number

SUBROUTINE GSPROP

No variables.

COMMON/SIZE/

DZ - Incremental length of the storage bed; m

MBRIK - Total storage brick mass; kg

Z - Total length of the storage bed; m

COMMON/PROFILE/

CTW(2,351) - Brick temperature averaged over brick thickness and averaged over a particular incremental length of the storage bed at the start of a particular time increment; °K

CTWBAR(361) - Brick temperature averaged over brick thickness and averaged over the entire length of the storage bed at the start of a particular time increment; °K

DTW(2,351) - Brick temperature averaged over brick thickness and averaged over a particular incremental length of the storage bed at the strat of a particular time increment; °K

DTWBAR(361) - Brick temperature averaged over brick thickness and averaged over the entire length of the storage bed at the start of a particular time increment; °K

SUBROUTINE DESIGN

DDEVDP1 - Estimate for the change in DEVIA with a change in P1

DEVIA(20) - Normalized deviation of the estimated gas temperature out of storage at the end of charging from the desired value for a particular attempted storage model.

ENDT12C - Gas temperature out of storage at the end of charging; °K

FRACSTR(20) - Normalized thermal energy accumulation in storage over a complete charge/discharge cycle for a particular attempted storage model.

ITDREM - The last time increment in the discharge cycle.

P1(20) - Dimensionless parameter used to estimate the spatial and thickness averaged brick temperature at the end of charging for a particular attempted storage model.

ROBRIK - Brick density; 2930.0 kg/m^3

COMMON/HRGCRG/

ACUMCT(360) - Accumulated charging time at the end of a particular time increment; s

CMDOT(360,12) - Gas mass flow rate through storage for a particular time increment and for a particular storage tank set; kg/s

CTG(360,2) - Gas temperature at the start of a particular length increment and the start of a particular time increment; °K

CTGI(351) - Gas temperature of a particular length increment; °K

CTGSTR(360,12) - Storage array for gas temperatures at the start of a particular time increment and the start of a selected length increment; °K

CTWSTR(10,350) - Storage array for brick temperatures averaged over brick thickness and averaged over a particular length increment at the start of a selected time increment; °K

ESTTGC(361,12) - Extrapolated gas temperature at the start of a future time increment and at the start of a selected length increment; °K

FB1(360) - Gas mass flow through the heat exchanger bypass during a particular time increment; kg/s

FB2(360) - Gas mass flow through the receiver/storage bypass during a particular time increment; kg/s

FHEC(360) - Heat exchanger gas mass flow during a particular time increment; kg/s

FMIXS(360) - Gas mass flow from storage to the heat exchangers during a particular time increment; kg/s

FR(360) - Receiver gas mass flow during a particular time increment; kg/s

HC(360,12) - Gas film heat transfer coefficient for a particular time increment and a particular storage tank set; $W/(m^2\ °K)$

IBEGIN(12) - First length increment in a particular storage tank set.

IEND(12) - Last length increment in a particular storage tank set.

ITCREM - Last time increment in the charge cycle.

NTANKC(360) - The storage tank set in which gas temperature drops from above TMIXS to less than or equal to TMIXS for a particular time increment.

QEQVR(360) - Equivalent receiver heat absorbtion based on a cumulative energy balance for a particular time increment; W

QSC(360) - Heat stored in storage during a particular time increment; W

REC(360,12) - Gas Reynolds number for a particular time increment and for a particular storage tank set

TINR(360) - Gas temperature to the receiver for a particular time increment; °K

TMIXS(360) - Mixed temperature of gas leaving and bypassing storage for a particular time increment; °K

TOUTR(360) - Gas temperature out of the receiver for a particular time increment; °K

UOC(360,12) - Overall heat transfer coefficient for a particular time increment and a particular storage tank set; $W/(m^3\ °K)$

SUBROUTINE HRGCRG

CTGIN - Gas temperature into storage; °K

IBEGIN1 - First length increment in a storage tank set.

IEND1 - Last length increment in a storage tank set.

ISEG - Last storage segment in the storage tank set of interest.

ISEGM1 - Last storage segment in the storage tank set before the one of interest.

KBRIK - Brick thermal conductivity; 5.48 W/(m•°K)

NTANKC1 - The storage tank set in which gas temperature drops from above TMIXS to less than or equal to TMIXS.

ZCENTER - Brick half width; 0.0381 m

COMMON/HRGDIS/

ACUMDT(361) - Accumulated discharging time at the end of a particular time increment; s

DMDOT(360,12) - Gas mass flow rate through storage for a particular time increment and for a particular storage tank set; kg/s

DTG(360,2) - Gas temperature at the start of a particular length increment and the start of a particular time increment; °K

DTGI(351) - Gas temperature of a particular length increment; °K

DTGSTR(360,12) - Storage array for gas temperatures at the start of a particular time increment and the start of a selected length increment; °K

DTHETD1(361) - Adjusted length of a particular time increment; s

DTWSTR(10,350) - Storage array for brick temperatures averaged over brick thickness and averaged over a particular length increment at the start of a selected time increment; °K

ESTTGD(361,12) - Extrapolated gas temperature at the start of a future time increment and at the start of a selected length increment; °K

ESTTGP2(362) - Extrapolated temperature of gas leaving storage two time increments in the future; °K

FHED(360) - Heat exchanger gas mass flow during a particular time increment; kg/s

HD(360,12) - Gas film heat transfer coefficient for a particular time increment and a particular storage tank set; $W/(m^2\ °K)$

IBEGIN(12) - First length increment in a particular storage tank set.

IEND(12) - Last length increment in a particular storage tank set.

ITDREM - Last time increment in the discharge cycle.

NTANKD(360) - The storage tank set in which gas temperature rises from less than TMIXS to greater than or equal to TMIXS for a particular time increment.

QEQVHE(360) - Equivalent heat transferred by the exchangers based on a cumulative energy balance for a particular time increment; W

QSD(360) - Heat released from storage during a particular time increment; W

RED(360,12) - Gas Reynolds number for a particular time increment and for a particular storage tank set

TOUTHED(360) - Gas temperature out of the heat exchangers for a particular time increment; °K

UOD(360,12) - Overall heat transfer coefficient for a particular time increment and a particular storage tank set; $W/(m^2\ °K)$

SUBROUTINE HRGDIS

DTGIN - Gas temperature into storage; °K

IBEGIN1 - First length increment in a storage tank set.

IEND1 - Last length increment in a storage tank set.

ISEG - Last storage segment in the storage tank set of interest.

ISEGM1 - Last storage segment in the storage tank set before the one of interest.

KBRIK - Thermal conductivity of brick, 5.48 W/(m·°K)

NTANKD1 - The storage tank set in which gas temperature rises from less than TMTXS to greater than or equal to TMIXS

ZCENTER - Brick half width; 0.0381 m

SUBROUTINE PRINTBG

No physical variables.

SUBROUTINE PRINTCH

No physical variables.

SUBROUTINE PRINTDS

No physical variables

COMMON/PDROPC/

DPBARC - Time averaged storage pressure drop; Pa

GASVOLC(360,12)- Gas volume for a particular time increment and a particular storage segment; kg/m^3

PDROPC(360,13) - Pressure drop at particular time increments and the start of particular storage segments.

SUBROUTINE PDROPCH

No physical variables.

SUBROUTINE PRNTPRS

No physical variables.

COMMON/PDROPD/

GASVOLD(360,12) - Gas volume for a particular time increment and a particular storage segment; kg/m^3

PDROPD(360,13) - Pressure drop at a particular time increment and the start of a particular storage segment.

SUBROUTINE PDROPDS

DPBAR - Time averaged storage pressure drop; Pa

II.3 HREGEN PROGRAM LISTING

PROGRAM HREGEN 7600-7600 OPT=1 FTN 4.6+452/034

```
      PROGRAM HREGEN(INPUT,OUTPUT)
      COMMON/BCKGR/NTANKT,     FLOWA,     TEQD,
     1             CPBRIK,     PERIM,     IGAS,
     2             CTGINF,     DTGINF,    TDSOSC
      COMMON/CRGINPT/THETC,    DTHETC,    HTHETC,
     1               QR(360),  QHEC(360), TINHEC(360),
     2               TOUTHEC(360), QRMAX(360), TOUTRM
      COMMON/DISINPT/ESTDT,    DTHETD,    QHED(360),
     1               TDSOHE(360), TINHED(360), HESTDT
      DO 30 I=1,2
      CALL BCKGR(I1,J1)
C     *BCKGR IS A READING SUBROUTINE
      CALL IJSET(I1,J1)
      CALL CRGINPT(ENERGYC)
      CALL DISINPT(ENERGYD)
      CALL GSPROP
      PERIM=97.6*FLOWA
      CALL DESIGN(ENERGYC,ENERGYD,STORCAP)
      CALL PRINTBG(STORCAP)
      CALL PRINTCH(ENERGYC)
      CALL PRINTDS(ENERGYD)
      CALL PDROPCH
      CALL PRNTPRS
      CALL PDROPDS
      PRINT 2
   2  FORMAT(1H1)
  30  CONTINUE
      CONTINUE
      CALL EXIT
      END
```

SUBROUTINE BCKGR 7600-7600 OPT=1 FTN 4.6+452/034

```
      SUBROUTINE BCKGR(I1,J1)
      COMMON/BCKGR/NTANKT,     FLOWA,     TEQD,
     1             CPBRIK,     PERIM,     IGAS,
     2             CTGINF,     DTGINF,    TDSOSC
      DATA TEQD,CPBRIK/0.0348,1067.0/
C     *SET NUMBER OF TIME INCREMENTS (JX10) AND LENGHT
C     *****INCREMENTS(IX12).  FOR 300 INCREMENTS OF EACH
C     *****I1=25 AND J1=3 .
      I1=25
      J1=30
C     *READ FLOWA IN M**2, CTGINF,DTGINF,AND TDSOSC IN DEG K.
      READ 10,NTANKT,FLOWA,IGAS,CTGINF,DTGINF,TDSOSC
   10 FORMAT(I2,8X,F10.2,I1,9X,3F10.2)
C     *PERIM, THE EFFECTIVE HEAT TRANSFER PERIMETER IS CALCULATED
C     *****AS FOLLOWS.  A SINGLE CHANNEL IN THE REGENERATOR
C     *****IS 0.0205M*0.0762M OR 1.56E-.3M**2/CHANNEL.
C     *****ONLY THE SIDES OF THE CHANNEL ARE ASSUMED TO TRANSFER
C     *****HEAT SO PERIM IS 2*0.0762M/CHANNEL.  THUS,
C     *****THE RATIO OF EFFECTIVE PERIMETER TO FLOW AREA IS
C     *****97.6M PERIMETER PER M**2 FLOW AREA.
      PERIM=97.6*FLOWA
      PRINT 15
   15 FORMAT(1H1)
      PRINT 20,NTANKT,FLOWA,CTGINF,DTGINF,TDSOSC
   20 FORMAT(///,5X,*NTANKT=*, I2,* FLOWA=*,F10.2,* CTGINF=*,
     1       F10.2,/,5X,*DTGINF=*,F10.2,* TDSOSC=*,F10.2,///)
      RETURN
      END
```

```
SUBROUTINE IJSET     7600-7600 OPT=1                    FTN 4.6+452/534
      SUBROUTINE IJSET(I1,J1)
      COMMON/IJSET/I,IADJUST,IX12,IX12P1,IX6,J,JX10,JX10P1,JX5,
     1             RI,RIX12,RJ,RJX10
      I=I1
      J=J1
      IADJUST=1/2
      IX12=I*12
      IX12P1=I*12+1
      IX6=6*I
      RI =I
      RIX12=I*12.
      JX10=J*10
      JX10P1=J*10+1
      JX5=5*J
      RJ=J
      RJX10=RJ*10.
      PRINT 10,IX12,JX10
   10 FORMAT(//,5X,*LENGTH INCREMENTS=*,I4,* TIME INCREMENTS=*,I4,//)
      RETURN
      END
```

```
SUBROUTINE CRGINPT   7600-7600 OPT=1                    FTN 4.6+452/534
      SUBROUTINE CRGINPT(ENERGYC)
     *THIS SUBROUTINE READS CONDITIONS FOR CHARGING.
      COMMON/CRGINPT/THETC,          DTHETC,          HTHETC,
     1               QR(360),        QHEC(360),       TINHEC(360),
     2               TOUTHEC(360),   QRMAX(360),      TOUTRM
      COMMON/IJSET/I,IADJUST,IX12,IX12P1,IX6,J,JX10,JX10P1,JX5,
     1             RI,RIX12,RJ,RJX10
      DIMENSION ISTART(20),     ISTOP(20),     RQRMW(20),
     1          RQHEMW(20),     RTINHE(20),    RTOUTHE(20),
     2          RQRMXMW(20)
     *READ THE NUMBER OF CHANGES IN CHARGE CONDITIONS (N),
     *****THE CHARGE TIME IN HOURS(HTHETC) (300 TIME INCREMENTS),
     *****AND THE MAXIMUM TEMPERATURE FROM THE RECEIVER (TOUTRM).
      READ 10,N,HTHETC,TOUTRM
   10 FORMAT(I2,8X,2F10.4)
      THETC=HTHETC*3600.
      DTHETC=THETC/RJX10
      PRINT 20,HTHETC,TOUTRM
    2 FORMAT(//,5X,*INPUT FOR CHARGE CYCLE*,//,5X,
     1       *HTHETC=*,F10.4,* HOURS,     TOUTRM=*,F10.2,* K*)
      DO 30 K=1,N
     *READ THE DESIRED HEAT RATES IN MW AND TEMPERATURES
     *****IN DEG K OVER THE TIME INTERVAL FROM INCREMENT
     *****ISTART(K) TO INCREMENT ISTOP(K).  STORE THE
     *****DESIRED HEAT RATES IN WATTS AND TEMPERATURES IN
     *****DEG K FOR EACH TIME INCREMENT OVER THE INTERVAL.
      READ 4 ,ISTART(K),ISTOP(K),RQRMW(K),RQHEMW(K),
     1        RTINHE(K),RTOUTHE(K),RQRMXMW(K)
   40 FORMAT(I3,7X,I3,7X,5F10.2)
      I1=ISTART(K)
      I2=ISTOP(K)
      I3=(I1+I2)/2
      DO 50 L=I1,I2
      QR(L)=RQRMW(K)*1.0E+06
      QHEC(L)=RQHEMW(K)*1.0E+06
      TINHEC(L)=RTINHE(K)
      TOUTHEC(L)=RTOUTHE(K)
   50 QRMAX(L)=RQRMXMW(K)*1.0E+06
     *PRINT BACK THE INPUT DATA FOR VERIFICATION.
      PRINT 60 ,ISTART(K),ISTOP(K),TINHEC(I3),TOUTHEC(I3),
     1          QR(I3),QHEC(I3),QRMAX(I3)
   60 FORMAT(5X,*ISTART=*,I4,* ISTOP=*,I4,* TINHEC=*,F10.2,
     1       * K,   TOUTHEC=*,F1 .2,* K*,/,5X,*QR=*,F15.2,
     2       * W,   QHEC=*,F15.2,* W,   QRMAX=*,F15.2,*W*)
   30 CONTINUE
     *CALCULATE THE ENERGY CHARGED IN MW-HR.
      ENERGYC=0.0
      DO 70 M=1,JX10
   70 ENERGYC=ENERGYC+((QR(M)-QHEC(M))/1.0E+06)*(DTHETC/3600.0)
      RETURN
      END
```

SUBROUTINE DISINPT 7600*7600 OPT=1 FTN 4.6+452/034

```
      SUBROUTINE DISINPT(ENERGYD)
*THIS SUBROUTINE READS CONDITIONS FOR DISCHARGE
     .COMMON/DISINPT/ESTDT,      DTHETD,      QHED(36),
     1               TDSOHE(360),   TINHED(360),   HESTDT
     OCOMMON/IJSET/I,IADJUST,IX12,IX12P1,IX6,J,JX1 ,JX1 P1,JX5,
     1             KI,RIX12,RJ,RJX10
      DIMENSION RQHEMW(20),    RTDSOHE(20),    RTINHE(20),
     1          ISTART(20),    ISTOP(20)
*READ THE NUMBER OF CHANGES IN DISCHARGE CONDITIONS (N) AND
*****THE ESTIMATED DISCHARGE TIME IN HOURS (HESTDT).  WHICH CORRESPONDS
*****TO 3.. TIME INCREMENTS.  DISCHARGE MAY CONTINUE FOR UP
*****TO 20 PERCENT LONGER THAN ESTIMATED (360 TIME INCREMENTS).
      READ 10,N,HESTDT
   10 FORMAT(I2,8X,F10.4)
      ESTDT=HESTDT*3600.0
      DTHETD=ESTDT/RJX1
      PRINT 15,HESTDT,DTHETD
  150FORMAT(//,5X,*INPUT FOR DISCHARGE CYCLE*,//,5X,
     1       *HESTDT=*,F10.4,* HOURS,   DTHETD=*,F10.4,* SECONDS*)
      DO 20 K=1,N
*READ THE DESIRED HEAT RATE IN MW AND TEMPERATURES IN
*****DEG K OVER THE TIME INTERVAL FROM INCREMENT
*****ISTART(K) TO INCREMENT ISTOP(K).  STORE THE DESIRED
*****HEAT RATE IN WATTS AND TEMPERATURES IN DEG K FOR
*****EACH TIME INCREMENT OVER THE INTERVAL.
      OREAD 30,ISTART(K),ISTOP(K),RQHEMW(K),
     1       RTDSOHE(K),RTINHE(K)
   30 FORMAT(I3,7X,I3,7X,3F10.2)
      I1=ISTART(K)
      I2=ISTOP(K)
      I3=(I1+I2)/2
      DO 40 L=I1,I2
      QHED(L)=RQHEMW(K)*1.0E+06
      TDSOHE(L)=RTDSOHE(K)
    4 TINHED(L)=RTINHE(K)
*PRINT BACK THE INPUT DATA FOR VERIFICATION.
      PRINT 50,ISTART(K),ISTOP(K),QHED(I3),TDSOHE(I3),TINHED(I3)
   50 FORMAT(5X,*ISTART=*,I4,* ISTOP=*,I4,* QHED=*,
     1       F15.2,* W*,/,5X,*TDSOHE=*,F10.2,* K,  TINHED=*,F10.2,* K*)
   20 CONTINUE
*CALCULATE THE MAXIMUM ENERGY WHICH MAY BE DISCHARGED IN MW-HR.
      ENERGYD=0.0
      DO 60 M=1,360
   60 ENERGYD=ENERGYD+(QHED(M)/1.0E+06)*(DTHETD/3600.0)
      RETURN
      END
```

SUBROUTINE GSPROP 7600*7600 OPT=1 FTN 4.6+452/034

```
      SUBROUTINE GSPROP
      COMMON/GSPROP/KG,MU,PR,CPGAS
      OCOMMON/BCKGR/NTANKT,      FLOWA,      TEQD,
     1              CPBRIK,      PERIM,      IGAS,
     2              CTGINF,      DTGINF,     TDSOSC
      REAL KG,MU
* SPECIFY IGAS, 1=WATER,2=HELIUM
*PROPERTIES AT CTGINF
      IF (IGAS.EQ.1)GO TO 3
      IF(IGAS.EQ.2) GO TO 40
      IF(IGAS.EQ.3) GO TO 60
    3 PRINT 32
   32 FORMAT(/,10X,*  RECEIVER GAS IS WATER*,//)
      KG=0.00011*(CTGINF-120.)
      MU=4.1E-08*(CTGINF-70.)
      PR=0.92
      CPGAS=23..
      GO TO 90
   40 PRINT 42
   42 FORMAT(/,10X,*  RECEIVER GAS IS HELIUM*,//)
      KG=0.00026*(CTGINF+360.)
      MU=3.5E-08*(CTGINF+270.)
      PR=0.64
      CPGAS=5200
      GO TO 90
   60 PRINT 62
   62 FORMAT(/,10X,*  RECEIVER GAS IS NITROGEN*,//)
      KG=5.2E-05*(CTGINF+260.)
      MU=3.3E-08*(CTGINF+300.)
      PR=0.72
      CPGAS=1100.0
   90 RETURN
      END
```

```
SUBROUTINE DESIGN   76..-76..  OPT=1          FTN 4.6+452/...4
      1         SUBROUTINE DESIGN(ENERGYC,ENERGYD,STORCAP)
                OCOMMON/BCKGR/NTANKT,     FLOWA,     TEQD,
                1             CPBRIK,     PERIM,     IGAS,
                2             CTGINF,     DTGINF,    TDSOSC
      5         COMMON/SIZE/DZ,Z,MBRIK
                REAL MBRIK
                COMMON/PROFILE/DTW(2,351),    DTWBAR(361),
                1              CTW(2,351),    CTWBAR(361)
                OCOMMON/IJSET/I,IADJUST,IX12,IX12P1,IX6,J,JX10,JX10P1,JX5,
     10         1              RI,RIX12,RJ,RJX10
                DIMENSION DEVIA(20),     FRACSTR(20),    P1(20)
                DATA ROBRIK/2930.0/
               *MAKE A PRELIMINARY ESTIMATE OF THE LENGTH AVERAGED WALL TEMPERATURE
               *****AT THE END OF DISCHARGE.
     15         ITDREM=JX1
                DTWBAR(ITDREM+1)=0.8*DTGINF+0.2*CTGINF
                DO 10 IZC=1,IX12P1
             10 DTW(2,IZC)=DTWBAR(ITDREM+1)
               *MAKE A PRELIMINARY ESTIMATE OF P1 (CTWBAR=
     20        *****  P1*(CTGINF-DTGINF)+DTGINF
                P1(1)=0.9
               *START OF THE IT LOOP.  DURING EACH PASS THROUGH
               *****THE LOOP ESTIMATES FOR DTW(2,IZC) (THE WALL
               *****PROFILE AT THE END OF DISCHARGE) AND P1 (RELATES
     25        *****CTWBAR TO CTGINF AND DTWBAR) IMPROVE.
               *****ITERATION THROUGH THE LOOP IS DISCONTINUED WHEN THE
               *****ENERGY STORED IS SUFFICIENTLY CLOSE TO THE ENERGY
               *****DISCHARGED AND WHEN THE ESTIMATED AND DESIRED GAS
               *****TEMPERATURES AT THE END OF THE CHARGE CYCLE ARE
     30        *****ALSO SUFFICIENTLY CLOSE.
                DO 2 IT=1,20
               *ESTIMATE THE LENGTH AVERAGED WALL TEMPERATURE AT THE END OF CHARGE,
               *****MASS OF BRICKS, BED LENGTH, AND BED INCREMENT LENGTH
               *****FOR EACH NEW ESTIMATE OF P1 AND DTWBAR
     35         CTWBAR(JX10P1)=P1(IT)*(CTGINF-DTGINF)+DTGINF
                MBRIK=ABS(ENERGYC*1.0E+06*361)./((CPBRIK*
                1       (DTWBAR(ITDREM+1)-CTWBAR(JX10P1))))
                Z=MBRIK/(ROBRIK*(3.72*FLOWA))
                DZ=Z/RIX12
     40         CALL HRGCRG(ENERGYC,ENDT12C)
                CALL HRGDIS(ENERGYD,ITDREM)
               *CALLING HRGDIS IMPROVES THE ESTIMATES FOR DTW AND DTWBAR(THE WALL
               *****PROFILE AT THE END OF DISCHARGE) BY DISCHARGING A STORAGE UNIT
               *****OF ROUGHLY THE NEEDED SIZE UNTIL THE REQUIRED OUTLET
     45        *****TEMPERATURE CAN NO LONGER BE MAINTAINED.
               *CALCULATE STORAGE CAPACITY IN MW-HRS/KG BRICK
                STORCAP=ENERGYC/MBRIK
               *CALCULATE THE NORMALIZED DEVIATIONS OF THE ESTIMATED
               *****GAS TEMPERATURE AT THE END OF CHARGE (ENDT12C) AND THE
     50        *****ENERGY DISCHARGED (ENERGYD) FROM THEIR DESIRED VALUES.
                DEVIA(IT)=(ENDT12C-TDSUSC)/(CTGINF-DTGINF)
                FRACSTR(IT)=(ENERGYC+ENERGYD)/ENERGYC
               *AFTER THE THIRD TRIP THROUGH THE LOOP CHECK TO SEE
               *****IF A SOLUTION HAS BEEN REACHED AND CHECK
     55        *****THAT THE LOOP IS NOT DIVERGING EACH TIME THROUGH.
                IF(IT.LT.3) GO TO 30
                IF(ABS(DEVIA(IT)).GE.0.004.OR.ABS(FRACSTR(IT)).

SUBROUTINE DESIGN   7600-7600 OPT=1          FTN 4.6+452/...4
                1   GE.0.004) GO TO 40
                    RETURN
     60         4  IF(ABS(DEVIA(IT)).LE.ABS(DEVIA(IT-1)).OR.ABS(FRACSTR(IT)).
                1   LE.ABS(FRACSTR(IT-1))) GO TO 30
                    PRINT 50
                5. FORMAT(///,3X,*SUBROUTINE DESIGN DIVERGES*,///)
                    RETURN
     65        *THE CHANGE IN DEVIA WITH P1 IS ESTIMATED FROM
               *****PAST EXPERIENCE.  THIS DIFFERENTIAL IS THEN USED
               *****TO ESTIMATE A NEW VALUE FOR P1.
                30 DDEVDP1=5.0
                    P1(IT+1)=P1(IT)-DEVIA(IT)/DDEVDP1
     70             IF(P1(IT+1).GE.1.0) P1(IT+1)=(P1(IT)+1.0)/2.0
                    IF(P1(IT+1).LE.0. ) P1(IT+1)=P1(IT)/2.
                    PRINT 60,IT,P1(IT),ENDT12C,FRACSTR(IT),
                1           DEVIA(IT),DDEVDP1
                6. FORMAT(/,5X,*IT=*,I3,* P1(IT)=*,F8.6,
     75         1        *ENDT12C=*,F10.2,/,5X,*FRACSTR(IT)=*,
                2        F8.6,* DEVIA(IT)=*,F8.6,* DDEVDP1=*,F10.2)
                2) CONTINUE
                    END
```

```
SUBROUTINE HRGCRG   76 .*76.0 OPT=1                    FTN 4.6+452/ 34
      SUBROUTINE HRGCRG(ENERGYC,ENDT12C)
      COMMON/CTWSTR1/CTWSTR1(35)
      COMMON/BCKGR/NTANKT,        FLOWA,        TEQD,
     1             CPBRIK,        PERIM,        IGAS,
     2             CTGINF,        DTGINF,       TDSOSC
      COMMON/SIZE/DZ,Z,MBRIK
      REAL MBRIK
      COMMON/HRGCRG/CTGI(351),    ESTTGC(361,12),ACTW(361),
     1             QEQVR(360),    FHEC(360),    FB2(360),
     2             FMIXS(360),    TMIXS(360),   FR(360),
     3             FB1(360),      TINR(360),    TOUTR(360),
     4             NTANKC(360),   CMDOT(360,12),REC(360,12),
     5             HC(360,12),    UOC(360,12),  IBEGIN(12),
     6             IEND(12),      CTG(360,2),   CTGSTR(360,12),
     7             CTWSTR(1),35 ),QSC(360),     ACUMCT(36 ),
     8             ITCREM
      COMMON/CRGINPT/THETC,       DTHETC,       HTHETC,
     1             QR(360),       QHEC(360),    TINHEC(361),
     2             TOUTHEC(360),  QRMAX(360),   TOUTRM
      COMMON/PROFILE/DTW(2,351),  DTW8AR(361),
     1             CTW(2,351),    CTW8AR(361)
      COMMON/GSPROP/KG,MU,PR,CPGAS
      REAL KG,MU
      COMMON/IJSET/I,IADJUST,IX12,IX12P1,IX6,J,JX10,JX10P1,JX5,
     1             RI,RIX12,RJ,RJX10
      REAL KBRIK
      DATA ZCENTER,KBRIK/0.0381,5.48/
*INITIALIZE ENERGYC
      ENERGYC=0.0
*ESTIMATE THAT FOR THE FIRST TIME INCREMENT, GAS TEMPERATURES
*****WILL MATCH THE WALL TEMPERATURES AT THE END OF THE
*****PREVIOUS DISCHARGE (DTW(2,*))
      DO 20 IZC=1,IX12
      CTGI(IZC)=DTW(2,IX12P1-IZC)
      CTGI(IX12P1)=DTW(2,1)
      ISGEND=IZC/I
      SGEND=IZC/RI
      IF((ISGEND-SGEND).NE.0) GO TO 20
      ESTTGC(1,ISGEND)=DTW(2,IX12P1-IZC)
   20 CONTINUE
*START OF THE MAIN ITC LOOP. CALCULATES HEAT REGENERATOR
*****PERFORMANCE THROUGHOUT THE CHARGE CYCLE
      DO 30 ITC=1,JX10
*INITIALIZE ACTW(ITC+1) AND QSC(ITC).
      ACTW(ITC+1)=0.0
      QSC(ITC)=0.0
*THIS SECTION CALCULATES SYSTEM OPERATION. QS(ITC-1)
*****AND ESTTGC(ITC,12) ARE CALCULATED ELSEWHERE. SUBROUTINE
*****CRGINPT PROVIDES QR,QHEC,TINHEC,TOUTHEC,QRMAX,AND TOUTRM VALUES.
*WHEN ESTTGC(ITC,12) IS LESS THAN TINHE(ITC), BYPASS TWO IS CLOSED
*****(FB2(ITC)=0.0)
*HEAT AVAILABLE FROM THE RECEIVER AT AN INSTANT OF TIME (QEQVR)
*****IS ASSUMED TO DEPEND ON A CUMULATIVE ENERGY BALANCE.
      QEQVR(1)=QR(1)
      IF(ITC.NE.1) QEQVR(ITC)=QR(ITC)+(QEQVR(ITC-1)-QHEC(ITC-1)-
     1                                 QSC(ITC-1))
      FHEC(ITC)=QHEC(ITC)/(CPGAS*(TINHEC(ITC)-TOUTHEC(ITC)))
```

```
SUBROUTINE HRGCRG   7600+7600 OPT=1                    FTN 4.6+452/034   1
      IF((ESTTGC(ITC,12)-TINHEC(ITC)).LE.0.0) FB2(ITC)=0.0
      OIF((ESTTGC(ITC,12)-TINHEC(ITC)).GT.0.0) FB2(ITC)=FHEC(ITC)*
     1      (ESTTGC(ITC,12)-TINHEC(ITC))/(ESTTGC(ITC,12)-TOUTHEC(ITC))
      FMIXS(ITC)=FHEC(ITC)-FB2(ITC)
      OFMIXS(ITC)=(FHEC(ITC)*TINHEC(ITC)-FB2(ITC)*TOUTHEC(ITC))/
     1            FMIXS(ITC)
      OFR(ITC)=(QRMAX(ITC)/CPGAS+FMIXS(ITC)*(TOUTHEC(ITC)-
     1      ESTTGC(ITC,12)))/(TOUTRM-ESTTGC(ITC,12))
      FB1(ITC)=FR(ITC)-FMIXS(ITC)
      OTINR(ITC)=(TOUTHEC(ITC)*(FHEC(ITC)-FB2(ITC))+
     1      FB1(ITC)*ESTTGC(ITC,12))/FR(ITC)
      TOUTR(ITC)=TINR(ITC)+QEQVR(ITC)/(FR(ITC)*CPGAS)
*FB1 MUST BE A POSITIVE FLOW
      IF(FB1(ITC).GE.0.0) GO TO 35
      FB1(ITC)=0.0
      TINR(ITC)=TOUTHEC(ITC)
      FR(ITC)=QRMAX(ITC)/(CPGAS*(TOUTRM-TINR(ITC)))
      TOUTR(ITC)=TINR(ITC)+QEQVR(ITC)/(FR(ITC)*CPGAS)
      FMIXS(ITC)=FR(ITC)
      FB2(ITC)=FHEC(ITC)-FMIXS(ITC)
      OTMIXS(ITC)=(FHEC(ITC)*TINHEC(ITC)-
     1            FB2(ITC)*TOUTHEC(ITC))/FMIXS(ITC)
   35 CONTINUE
      CTGIN=TOUTR(ITC)
*MOVE THE CALCULATED WALL TEMPERATURES FOR TIME ITC
*****INTO THE FIRST LINE OF THE ARRAY CTW(1,IZC)
      DO 40 IZC=1,IX12
      IF(ITC.EQ.1) CTW(1,IZC)=DTW(2,IX12P1-IZC)
   40 IF(ITC.NE.1) CTW(1,IZC)=CTW(2,IZC)
*DETERMINE MASS FLOW THROUGH EACH TANK IN THE STORAGE UNIT
*****CASE 1,GAS TEMPERATURE AT THE END OF ONE TANK
*****MATCHES TMIXS(ITC), INCLUDES OVER FLOW CONDITION.
      DO 50 NTANK=1,NTANKT
      ISEG=12*NTANK/NTANKT
      IF(ABS(ESTTGC(ITC,ISEG)-TMIXS(ITC)).GE.1.0) GO TO 50
      NTANKC(ITC)=NTANK
      DO 60 NTANKA=1,NTANKT
      IF(NTANKA.LE.NTANKC(ITC)) CMDOT(ITC,NTANKA)=FR(ITC)
   60 IF(NTANKA.GT.NTANKC(ITC)) CMDOT(ITC,NTANKA)=FB1(ITC)
     1            *FR(ITC)/1000.0
      GO TO 70
   50 CONTINUE
*****CASE 2,GAS TEMPERATURE DROPS FROM ABOVE TO BELOW TMIXS(ITC)
***** IN THE FIRST TANK
      ISEG=12/NTANKT
      IF(CTGIN.LE.TMIXS(ITC).OR.ESTTGC(ITC,ISEG).GE.TMIXS(ITC))
     1      GO TO 80
      NTANKC(ITC)=1
      DO 90 NTANKA=1,NTANKT
      CMDOT(ITC,1)=FB1(ITC)+FMIXS(ITC)*(CTGIN-TMIXS(ITC))/
     1            (CTGIN-ESTTGC(ITC,ISEG))
   90 IF(NTANKA.GT.NTANKC(ITC)) CMDOT(ITC,NTANKA)=FB1(ITC)
     1            *FR(ITC)/1000.0
      GO TO 70
   80 CONTINUE
*****CASE 3, GAS TEMPERATURE DROPS FROM ABOVE TO BELOW
*****TMIXS(ITC) IN A LATER TANK
```

```
      IF(NTANKT.EQ.1) GO TO 100
      DO 110 NTANK=2,NTANKT
      ISEG=12*NTANK/NTANKT
      ISEGM1=ISEG-12/NTANKT
     0IF(ESTTGC(ITC,ISEGM1).LE.TMIXS(ITC).OR.
     1     ESTTGC(ITC,ISEG).GE.TMIXS(ITC)) GO TO 110
      NTANKC(ITC)=NTANK
      NTANK1=NTANKC(ITC)
      DO 120 NTANKA=1,NTANKT
      IF(NTANKA.LT.NTANKC(ITC)) CMDOT(ITC,NTANKA)=FR(ITC)
      CMDOT(ITC,NTANK1)=FB1(ITC)*FMIXS(ITC)*(ESTTGC(ITC,ISEGM1)-
     1     TMIXS(ITC))/(ESTTGC(ITC,ISEGM1)-ESTTGC(ITC,ISEG))
  120 IF(NTANKA.GT.NTANKC(ITC)) CMDOT(ITC,NTANKA)=FB1(ITC)
     1          *FR(ITC)/1000.0
      GO TO 70
   11 CONTINUE
*IF LOGIC IN NOT TRANSFERED TO 70, THE STORAGE UNIT HAS FAILED IN ITS
*****BUFFERING FUNCTION. OUTPUT IS PRINTED AND SUBROUTINE HRGCRG RETURN
  100 PRINT 130,ITC,CTGIN
  130 0FORMAT(///,3X,*STORAGE BUFFERING FAILS AT ITC=*,I4,/,3X,
     1     *INLET GAS TEMPERATURE=*,F1..2,2X,*DEG K*,//)
      0PRINT 140,ESTTGC(ITC,1),ESTTGC(ITC,2),ESTTGC(ITC,3),
     1     ESTTGC(ITC,4),ESTTGC(ITC,5),ESTTGC(ITC,6)
      0PRINT 140,ESTTGC(ITC,7),ESTTGC(ITC,8),ESTTGC(ITC,9),
     1     ESTTGC(ITC,10),ESTTGC(ITC,11),ESTTGC(ITC,12)
  140 FORMAT(5X,6F10.2)
      RETURN
   70 CONTINUE
*START OF THE MAIN NTANK LOOP. CALCULATES HEAT REGENERATOR
*****PERFORMANCE FOR THE TIME INCREMENT ITC.
      DO 150 NTANK=1,NTANKT
*FIND THE OVERALL HEAT TRANSFER COEFFICIENT (UOC) FOR GAS FLOW
*****IN EACH TANK OF THE HEAT REGENERATOR, A MINIMUM
*****VALUE IS SET FOR HC TO HANDLE TANKS WITH NO FLOW.
      REC(ITC,NTANK)=TEQD*(CMDOT(ITC,NTANK)/FLOWA)/MU
      HC(ITC,NTANK)=0.023*KG*REC(ITC,NTANK)**0.8*PR**0.33/TEQD
      UOC(ITC,NTANK)=1.0/(1./HC(ITC,NTANK)+(ZCENTER/2. )/KBRIK)
*DETERMINE BEGIN AND END POINTS FOR TANK-NTANK
      IBEGIN(NTANK)=(IX12*(NTANK-1))/NTANKT+1
      IEND(NTANK)=(IX12*NTANK)/NTANKT
      IBEGIN1=IBEGIN(NTANK)
      IEND1=IEND(NTANK)
*START OF THE MAIN IZC LOOP.  CALCULATES TANK-NTANK
*****PERFORMANCE FOR TIME INCREMENT ITC.
      DO 160 IZC=IBEGIN1,IEND1
*MOVE THE CALCULATED GAS TEMPERATURES FOR POSITION IZC
*****INTO THE FIRST COLUMN OF THE ARRAY CTG(ITC,1).
*****THE GAS TEMPERATURE FOR POSITION IZC+1 IS THEN CALCULATED
*****INTO THE SECOND COLUMN OF THE ARRAY CTG(ITC,2).
      IF(IZC.EQ.1) CTG(ITC,1)=CTGIN
      IF(IZC.GE.2) CTG(ITC,1)=CTG(ITC,2)
     0CTG(ITC,2)=CTG(ITC,1)+UOC(ITC,NTANK)*PERIM*
     1          DZ*(CTW(1,IZC)-CTG(ITC,1))/
     2          (CPGAS*CMDOT(ITC,NTANK))
*FILL THE CALCULATED GAS TEMPERATURES FOR TIME ITC AND
*****POSITION IYIZC=1,2,...,12 (IZC=I-1/2+1,2*I-1/2+1,...,12*I-1/2+1)
*****INTO THE ARRAY CTGSTR(ITC,IYIZC)
      IYIZC=(IZC+1/2)/1
      YIZC=(IZC+1/2)/RI
      IF((IYIZC-YIZC).EQ.0) CTGSTR(ITC,IYIZC)=CTG(ITC,1)
*ESTIMATE BY LINEAR EXTRAPOLATION THE GAS TEMPERATURE AT THE END OF
*****EACH SEGMENT FOR THE NEXT TIME INCREMENT ITC+1 (ESTTGC(ITC+1,,
*****ISGEND)).  RECALL THE GAS TEMPERATURE FOR THE TIME INCREMENT
*****ITC-1 FROM CTGI(IZC+1).
      ISGEND=IZC/I
      SGEND=IZC/RI
      0IF((ISGEND-SGEND).EQ.0) ESTTGC(ITC+1,ISGEND)=CTG(ITC,2)*2.-
     1     CTGI(IZC+1)
*MOVE THE GAS TEMPERATURES FOR TIME ITC INTO CTGI(IZC)
      CTGI(1)=CTGIN
      CTGI(IZC+1)=CTG(ITC,2)
*CALCULATE THE WALL TEMPERATURE FOR TIME ITC+1 INTO
*****THE SECOND LINE OF THE ARRAY CTW(2,IZC)
*****THE FIRST LINE OF THE ARRAY CTW(1,IZC)
*****CONTAINS THE WALL TEMPERATURES AT TIME ITC.
      0CTW(2,IZC)=CTW(1,IZC)+UOC(ITC,NTANK)*PERIM*
     1          (CTG(ITC,1)-CTW(1,IZC))*DTHETC/
     2          ((MBRIK/Z)*CPBRIK)
*ACCUMULATE THE WALL TEMPERATURES AT TIME ITC+1 FOR IX12 WALL POSITIONS
      ACTW(ITC+1)=ACTW(ITC+1)+CTW(2,IZC)
*FILL THE CALCULATED WALL TEMPERATURES FOR POSITION IZC
*****AND TIME IYITC=1,2,...,10 (ITC=J+1,2*J+1,...,10*J+1)
*****INTO THE ARRAY CTWSTR(IYITC,IZC)
      IYITC=ITC/J
      YITC=ITC/RJ
      IF(ITC.EQ.1) CTWSTR(IZC)=CTW(1,IZC)
      IF((IYITC-YITC).EQ.0) CTWSTR(IYITC,IZC)=CTW(1,IZC)
*END OF THE MAIN IZC LOOP.  TANK NTANK HAS BEEN
*****CALCULATED FOR TIME INCREMENT ITC.
  160 CONTINUE
*ACCUMULATE HEAT STORAGE
      0QSC(ITC)=QSC(ITC)+CPGAS*CMDOT(ITC,NTANK)*
     1     (CTGI(IBEGIN1)-CTGI(IEND1+1))
*END OF THE MAIN NTANK LOOP.  THE HEAT REGENERATOR HAS
*****BEEN CALCULATED FOR TIME INCREMENT ITC.
      ITCREM=ITC
  150 CONTINUE
*ACCUMULATE CHARGING TIME
      IF(ITC.EQ.1) ACUMCT(ITC)=DTHETC
      IF(ITC.GE.2) ACUMCT(ITC)=ACUMCT(ITC-1)+DTHETC
*CALCULATE THE LENGTH AVERAGED WALL TEMPERATURE AT THE START
***** OF TIME INCREMENT ITC+1, INTO CTWBAR(2,ITC+1)
      CTWBAR(ITC+1)=ACTW(ITC+1)/RIX12
*ACCUMULATE ENERGY IN MW-HR
      ENERGYC=ENERGYC+(QSC(ITC)/1.0E+06)*(DTHETC/3600.0)
*END OF THE ITC LOOP.  HEAT REGENERATOR PERFORMANCE
*****HAS BEEN CALCULATED FOR THE ENTIRE CHARGE CYCLE.
   30 CONTINUE
*STORE ESTTGC(JX10P1,12) FOR TRANSFER
*****IN ENDT12C
      ENDT12C=ESTTGC(JX10P1,12)
*PRINT SECTION
      PRINT 170, ITCREM,CTWBAR(ITCREM+1)
 1700 FORMAT(/,5X,*STORAGE CHARGED AFTER*,I4,* TIME INCREMENTS*,
```

```
SUBROUTINE HRGCRG   7600-7600 OPT=1                    FTN 4.6+452/034

     1       5X,*CTWBAR=*,F10.2)
230  WPRINT 180, CTW(2,I),CTW(2,I*2),CTW(2,I*3),
     1       CTW(2,I*4),CTW(2,I*5),CTW(2,I*6)
     WPRINT 180,CTW(2,I*7),CTW(2,I*8),CTW(2,I*9),
     1       CTW(2,I*10),CTW(2,I*11),CTW(2,I*12)
 180 FORMAT(5X,6F10.2)
235  50  RETURN
     END
```

```
SUBROUTINE HRGDIS   7600-7600 OPT=1                    FTN 4.6+452/034

      SUBROUTINE HRGDIS(ENERGYD,ITDREM1)
      COMMON/DTWSTR1/DTWSTR1(35)
      COMMON/HCKGR/NTANKT,        FLOWA,      TEQD,
     1             CPBRIK,        PERIM,      IGAS,
     2             CTGINF,        DTGINF,     TDSOSC
      COMMON/SIZE/DZ,Z,MBRIK
      REAL MBRIK
      COMMON/HRGDIS/DTGI(351),    ESTTGD(361,12),ADTW(361),
     1             QEQVHE(360),   FHED(360),  TOUTHED(360),
     2             NTANKD(360),   DMDOT(360,12), RED(360,12),
     3             HD(360,12),    UDD(360,12),  IBEGIN(12),
     4             IEND(12),      DTG(360,2),   DTGSTR(360,12),
     5             DTWSTR(10,35),QSD(36),   ACUMDT(361),
     6             ITDREM,        ESTTGP2(362), DTHETD1(361)
      LEVEL 2,DTGI
      COMMON/DISINPT/ESTDT,       DTHETD,     QHED(360),
     1             TDSOHE(360),   TINHED(360), HESTDT
      COMMON/PROFILE/DTW(2,351),  DTWBAR(361),
     1             CTW(2,351),    CTWBAR(361)
      COMMON/GSPROP/KG,MU,PR,CPGAS
      REAL KG,MU
      COMMON/IJSET/I,IADJUST,IX12,IX12P1,IX6,J,JX10,JX10P1,JX5,
     1             RI,RIX12,RJ,RJX10
      REAL KBRIK
      DATA ZCENTER,KBRIK/0.0381,5.48/
*INITIALIZE ENERGYD
      ENERGYD=0.0
*ESTIMATE THAT FOR THE FIRST TIME INCREMENT, GAS TEMPERATURES
*****WILL MATCH THE WALL TEMPERATURES AT THE END OF THE
*****PREVIOUS CHARGE(CTW(2,*))
      DO 220 IZD=1,IX12
      DTGI(IZD)=CTW(2,IX12P1-IZD)
      DTGI(IX12P1)=CTW(2,1)
      ISGEND=IZD/I
      SGEND=IZD/RI
      IF((ISGEND-SGEND).NE.0) GO TO 220
      ESTTGD(1,ISGEND)=CTW(2,IX12P1-IZD)
  220 CONTINUE
*START OF THE MAIN ITD LOOP.  CALCULATES HEAT REGENERATOR
*****PERFORMANCE THROUGHOUT THE DISCHARGE CYCLE.
      DO 230 ITD=1,360
*INITIALIZE ADTW(ITD+1) AND QSD(ITD).
      ADTW(ITD+1)=0.0
      QSD(ITD)=0.0
*THIS SECTION CALCULATES SYSTEM OPERATION.  QS(ITD-1)
*****IS CALCULATED ELSEWHERE.  SUBROUTINE DISINPT
*****PROVIDES QHE,TINHE, AND TOSOHE.
*THE EQUIVALENT HEAT TRANSFERED OUT OF THE EXCHANGERS AT AN INSTANT
*****OF TIME (QEQVHE) IS ASSUMED TO DEPEND ON A CUMULATIVE
*****ENERGY BALANCE.
      QEQVHE(1)=QHED(1)
      IF(ITD.NE.1) QEQVHE(ITD)=QHED(ITD)+(QEQVHE(ITD-1)+QSD(ITD-1))
      FHED(ITD)=QEQVHE(ITD)/((TINHED(ITD)-TDSOHE(ITD))*CPGAS)
      TOUTHED(ITD)=TINHED(ITD)-QEQVHE(ITD)/(FHED(ITD)*CPGAS)
      DTGIN=TOUTHED(ITD)
*MOVE THE CALCULATED WALL TEMPERATURES FOR TIME ITD
*****INTO THE FIRST LINE OF DTW(1,IZD)
```

```
      DO 240 IZD=1,IX12
      IF(ITD.EQ.1) DTW(1,IZD)=CTW(2,IX12P1-IZD)
  240 IF(ITD.NE.1) DTW(1,IZD)=OTW(2,IZD)
*DETERMINE MASS FLOW RATE THROUGH EACH TANK IN THE STORAGE UNIT
*****CASE 1, GAS TEMPERATURE AT THE END OF ONE TANK
*****MATCHES TINHE(ITC).
      DO 250 NTANK=1,NTANKT
      ISEG=12*NTANK/NTANKT
      IF(ABS(ESTTGD(ITD,ISEG)-TINHED(ITD)).GE.1.0) GO TO 250
      NTANKD(ITD)=NTANK
      DO 260 NTANKA=1,NTANKT
      IF(NTANKA.LE.NTANKD(ITD)) DMDOT(ITD,NTANKA)=FHED(ITD)
  260 IF(NTANKA.GT.NTANKD(ITD)) DMDOT(ITD,NTANKA)=FHED(ITD)/1000.0
      GO TO 270
  250 CONTINUE
*****CASE 2,GAS TEMPERATURE RISES FROM BELOW TO ABOVE TINHE(ITC)
*****IN THE FIRST TANK
      ISEG=12/NTANKT
      IF(ESTTGD(ITD,ISEG).LE.TINHED(ITD)) GO TO 280
      NTANKD(ITD)=1
      DO 290 NTANKA=1,NTANKT
      DMDOT(ITD,1)=FHED(ITD)*(DTGIN-TINHED(ITD))/
     1             (DTGIN-ESTTGD(ITD,ISEG))
  290 IF(NTANKA.GT.NTANKD(ITD)) DMDOT(ITD,NTANKA)=FHED(ITD)/1000.0
      GO TO 270
  280 CONTINUE
*****CASE 3, GAS TEMPERATURE RISES FROM BELOW TO ABOVE
*****TINHE(ITC) IN A LATER TANK
      IF(NTANKT.EQ.1) GO TO 300
      DO 310 NTANK=2,NTANKT
      ISEG=12*NTANK/NTANKT
      ISEGM1=ISEG-12/NTANKT
      IF(ESTTGD(ITD,ISEG).LE.TINHED(ITD)) GO TO 310
      NTANKD(ITD)=NTANK
      NTANKD1=NTANKD(ITD)
      DO 320 NTANKA=1,NTANKT
      IF(NTANKA.LT.NTANKD(ITD)) DMDOT(ITD,NTANKA)=FHED(ITD)
     .DMDOT(ITD,NTANKD1)=FHED(ITD)*(ESTTGD(ITD,ISEGM1)-
     1       TINHED(ITD))/(ESTTGD(ITD,ISEGM1)-ESTTGD(ITD,ISEG))
  320 IF(NTANKA.GT.NTANKD(ITD)) DMDOT(ITD,NTANKA)=FHED(ITD)/1000.0
      GO TO 270
  310 CONTINUE
*IF STORAGE IS DEPLETED AND THE REQUIRED INLET TEMPERATURE TO
*****THE HEAT EXCHANGERS, TINHED(ITD), CAN NOT BE MET,
*****DISCHARGE IS STOPPED.
*TRANSFER TO PRINT SECTION
      GO TO 300
  270 CONTINUE
*ADJUST THE LENGTH OF THE LAST TIME INCREMENT TO
*****STOP DISCHARGING JUST AS THE REQUIRED OUTLET TEMPERATURE
*****CAN NO LONGER BE MAINTAINED.
      DTHETD1(1)=DTHETD
      IF(ITD.LT.2) GO TO 370
      IF(TINHED(ITD).NE.TINHED(ITD+1)) GO TO 370
      IF(ESTTGP2(ITD+1).GE.TINHED(ITD)) GO TO 370
      DTHETD1(ITD+1)=
     1      DTHETD*(ESTTGD(ITD,12)-TINHED(ITD))/
     2      (ESTTGD(ITD,12)-ESTTGP2(ITD+1))
      IF(DTHETD1(ITD+1).LE.DTHETD/20.0) GO TO 300
      GO TO 380
  370 DTHETD1(ITD+1)=DTHETD
  380 CONTINUE
*START OF THE MAIN NTANK LOOP.  CALCULATES HEAT REGENERATOR
*****PERFORMANCE FOR THE TIME INCREMENT ITD.
      DO 350 NTANK=1,NTANKT
*FIND THE OVERALL HEAT TRANSFER COEFFICIENT (UOC) FOR GAS FLOW
*****IN EACH TANK OF THE HEAT REGENERATOR.  A MINIMUM
*****VALUE IS SET FOR HC TO HANDLE TANKS WITH NO FLOW.
      RED(ITD,NTANK)=TEQD*(DMDOT(ITD,NTANK)/FLOWA)/MU
      HD(ITD,NTANK)=0.023*KG*RED(ITD,NTANK)**0.8*PR**0.333/TEQD
      UOD(ITD,NTANK)=1./(1./HD(ITD,NTANK)+(ZCENTER/2.0)/KBRIK)
*DETERMINE BEGIN AND END POINTS FOR TANK-NTANK
      IBEGIN(NTANK)=(IX12*(NTANK-1))/NTANKT+1
      IEND(NTANK)=(IX12*NTANK)/NTANKT
      IBEGIN1=IBEGIN(NTANK)
      IEND1=IEND(NTANK)
*START OF THE MAIN IZD LOOP.  CALCULATES TANK-NTANK
*****PERFORMANCE FOR THE TIME INCREMENT ITD.
      DO 360 IZD=IBEGIN1,IEND1
*MOVE THE CALCULATED GAS TEMPERATURE FOR POSITION
*****IZD INTO THE FIRST COLUMN OF THE ARRAY DTG(ITD,1).
*****THE GAS TEMPERATURE FOR POSITION IZD+1 IS THEN
*****CALCULATED INTO THE SECOND COLUMN OF THE ARAY DTG(ITD,2).
      IF(IZD.EQ.1) DTG(ITD,1)=DTGIN
      IF(IZD.GE.2) DTG(ITD,1)=DTG(ITD,2)
      DTG(ITD,2)=DTG(ITD,1)+UOD(ITD,NTANK)*PERIM*
     1           DZ*(DTW(1,IZD)-DTG(ITD,1))/
     2           (CPGAS*DMDOT(ITD,NTANK))
      IF(ABS(DTG(ITD,2)-DTG(ITD,1)).GE.ABS(DTW(1,IZD)-
     1       DTG(ITD,1))) DTG(ITD,2)=DTW(1,IZD)
*FILL THE CALCULATED GAS TEMPERATURES FOR TIME ITD
*****AND POSITION IYIZD=1,2,....,12 (IZD-1=1-1/2,2*1-1/2,...,12*1-1/2)
*****INTO THE ARRAY DTGSTR(ITD,IYIZD)
      IYIZD=(IZD+1/2)/1
      YIZD=(IZD+1/2)/RI
      IF((IYIZD-YIZD).EQ.0) DTGSTR(ITD,IYIZD)=DTG(ITD,1)
*ESTIMATE BY LINEAR EXTRAPOLATION THE GAS TEMPERATURE AT
*****THE END OF EACH SEGMENT FOR THE NEXT TIME INCREMENT ITD+1
*****(ESTTGD(ITD+1,ISGEND)).  RECALL THE GAS TEMPERATURE
*****FOR THE TIME INCREMENT ITD-1 FROM DTGI(IZD+1).
      ISGEND=IZD/1
      SGEND=IZD/RI
      DIF((ISGEND-SGEND).EQ.0) ESTTGD(ITD+1,ISGEND)=DTG(ITD,2)+
     1      (DTG(ITD,2)-DTGI(IZD+1))*(DTHETD1(ITD+1)/DTHETD1(ITD))
*MOVE THE GAS TEMPERATURES FOR TIME ITD INTO DTGI(IZD)
      DTGI(1)=DTGIN
      DTGI(IZD+1)=DTG(ITD,2)
*CALCULATE THE WALL TEMPERATURE FOR TIME ITD+1 INTO THE
*****SECOND LINE OF THE ARRAY DTW(2,IZD)
*****THE FIRST LINE OF THE ARRAY DTW(1,IZD)
*****CONTAINS THE WALL TEMPERATURES AT TIME ITD.
      DDTW(2,IZD)=DTW(1,IZD)+UOD(ITD,NTANK)*PERIM*
     1      (DTG(ITD,1)-DTW(1,IZD))*(DTHETD1(ITD+1)/
     2      ((MBRIK/2)*CPBRIK)
```

```
      SUBROUTINE HRGDIS   7600-7600 OPT=1                FTN 4.6+452/034
C*ACCUMULATE THE WALL TEMPERATURES AT TIME ITD+1 FOR IX12 WALL POSITIONS
      ADTW(ITD+1)=ADTW(ITD+1)+DTW(2,IZD)
C*FILL THE CALCULATED WALL TEMPERATURES FOR POSITION IZD
C*****AND TIME IYITD=1,2,...,12 (ITD=I+1,2*I+1,...,12*I+1)
C*****INTO THE ARAY DTWSTR(IYITD,IZD)
      IYITD=ITD/J
      YITD=ITD/RJ
      IF(ITD.EQ.1) DTWSTR1(IZD)=DTW(1,IZD)
      IF((IYITD-YITD).EQ.0) DTWSTR(IYITD,IZD)=DTW(1,IZD)
C*END OF THE MAIN IZD LOOP.  TANK NTANK HAS BEEN CALCULATED
C*****FOR TIME INCREMENT ITD.
  360 CONTINUE
C*ACCUMULATE HEAT STORAGE
      QSD(ITD)=QSD(ITD)+CPGAS*DMDOT(ITD,NTANK)*
     1         (DTGI(IBEGIN)-DTGI(IEND+1))
C*END OF THE MAIN NTANK LOOP.  THE HEAT REGENERATOR HAS
C*****BEEN CALCULATED FOR THE TIME INCREMENT ITD.
  380 CONTINUE
C*EXTRAPOLATE TO ESTIMATE THE OUTLET GAS TEMPERATURE
C*****TWO TIME INCREMENTS AHEAD.
      ESTTGP2(ITD+2)=ESTTGD(ITD+1,12)+(ESTTGD(ITD+1,12)-
     1               ESTTGD(ITD,12))*(DTHETD/DTHETD1(ITD+1))
C*ACCUMULATE DISCHARGING TIME
      ACUMDT(1)=0.0
      ACUMDT(ITD+1)=ACUMDT(ITD)+DTHETD1(ITD+1)
C*CALCULATE THE LENGTH AVERAGED WALL TEMPERATURE AT
C*****THE START OF TIME INCREMENT ITD+1, INTO DTWBAR(2,ITD+1)
      DTWBAR(ITD+1)=ADTW(ITD+1)/RIX12
C*ACCUMULATE ENERGY IN MW-HR
      ENERGYD=ENERGYD+(QSD(ITD)/1.0E+06)*(DTHETD1(ITD+1)/3600.0)
C*END OF THE MAIN ITD LOOP.  IF RJX10 IS LESS THAN 360, AND
C*****ITERATION THROUGH THIS LOOP 360 TIMES IS COMPLETED,
C*****THE WALL TEMPERATURE AT THE END OF CHARGE WAS TO
C*****HIGH TO ALLOW TOTAL DISCHARGE.
      ITDREM=ITD
      ITDREM1=ITDREM
  390 CONTINUE
C*PRINT SECTION
  400 PRINT 330,ITDREM,DTWBAR(ITDREM+1)
  330 FORMAT(/,5X,*STORAGE DISCHARGED AFTER*,I4,* TIME INCREMENTS*,
     1   5X,*DTWBAR=*,F10.2)
      PRINT 340,DTW(2,1),DTW(2,I*2),DTW(2,I*3),
     1          DTW(2,I*4),DTW(2,I*5),DTW(2,I*6)
      PRINT 340, DTW(2,I*7),DTW(2,I*8),DTW(2,I*9),
     1          DTW(2,I*10),DTW(2,I*11),DTW(2,I*12)
  340 FORMAT(5X,6F10.2)
      RETURN
      END
```

```
      SUBROUTINE PRINTBG   76  -7600 OPT=1                FTN 4.6+452/034
      SUBROUTINE PRINTBG(STORCAP)
      COMMON/BCKGR/NTANKT,          FLOWA,          TEQD,
     1             CPBRIK,          PERIM,          IGAS,
     2             CTGINF,          DTGINF,         TDSOSC
      COMMON/SIZE/DZ,Z,MBRIK
      REAL MBRIK
      COMMON/IJSET/I,IADJUST,IX12,IX12P1,IX6,J,JX10,JX10P1,JX5,
     1             RI,RIX12,RJ,RJX10
      PRINT 10
   10 FORMAT(1H1,///,5X,*BACKGROUND INFORMATION*,///)
      PRINT 15,STORCAP
  150 FORMAT(5X,*THE STORAGE POTENTIAL FOR THIS DESIGN IS*,F12.7,
     1       * MW-HRS OF HEAT PER KG OF BRICK*,/)
      PRINT 20,NTANKT,2
   20 FORMAT(5X,*STORAGE IS BROKEN DOWN INTO*,I3,
     1       * TANKS IN SERIES WITH*,F6.2,* M TOTAL LENGHT*,/)
      PRINT 30,MBRIK
   30 FORMAT(5X,*STORAGE CONTAINS*,F10.0,* KG OF BRICKS*,/)
      PRINT 40,FLOWA,PERIM
  400 FORMAT(5X,* GAS FLOW AREA=*,F10.2,* M**2*,
     1       3X,*HEAT TRANSFER PERIMETER=*,F10.2,* M*,/)
      IF(IGAS.EQ.1) PRINT 41
   41 FORMAT(5X,*THE RECEIVER GAS IS WATER*,/)
      IF(IGAS.EQ.2) PRINT 42
   42 FORMAT(5X,*THE RECEIVER GAS IS HELIUM*,/)
      IF(IGAS.EQ.3) PRINT 43
   43 FORMAT(5X,*THE RECEIVER GAS IS NITROGEN*,/)
      PRINT 44,TDSOSC
  440 FORMAT(5X,*DURING CHARGE, THE MAXIMUM*,
     1       * TEMPERATURE ALLOWED AT THE STORAGE OUTLET*,
     2       * IS*,F10.2,* DEG K*,/)
      PRINT 50,JX10,IX12
  500 FORMAT(5X,*THIS PROGRAM SOLVES THE HEAT REGENERATOR EQUATIONS BY
     1       * THE METHOD OF FINITE DIFFERENCE*,/,5X,
     2       *TIME WAS DIVIDED INTO*,I4,
     3       * INCREMENTS.*,I5,* LENGHT INCREMENTS WERE USED.*,/////)
      RETURN
      END
```

```
      SUBROUTINE PRINTCH(ENERGYC)
      COMMON/CTWSTR1/CTWSTR1(350)
     0COMMON/SCKGR/NTANKT,      FLOWA,      TEQD,
     1             CPBRIK,     PERIM,      IGAS,
     2             CTGINF,     DTGINF,     TDSOSC
      COMMON/SIZE/DZ,Z,MBRIK
      REAL MBRIK
     0COMMON/HRGCRG/CTG1(351),  ESTTGC(361,12),ACTW(361),
     1             QEQVR(360),  FHEC(360),     FB2(360),
     2             FMIXS(360),  TMIXS(360),    FR(360),
     3             FB1(360),    TINR(360),     TOUTR(360),
     4             NTANKC(360), CMDOT(360,12), REC(360,12),
     5             HC(360,12),  UOC(360,12),   IBEGIN(12),
     6             IEND(12),    CTG(360,2),    CTGSTR(360,12),
     7             CTWSTR(1[illegible],350),QSC(360),    ACUMCT(360),
     8             ITCREM
     0COMMON/CRGINPT/THETC,     DTHETC,     HTHETC,
     1             QR(360),     QHEC(360),  TINHEC(360),
     2             TOUTHEC(360), QRMAX(360), TOUTRM
     0COMMON/IJSET/I,IADJUST,IX12,IX12P1,IX6,J,JX10,JX10P1,JX5,
     1             RI,RIX12,RJ,RJX10
      PRINT 10,ENERGYC
    100FORMAT(///,5X,*CONDITIONS DURING CHARGE CYCLE*,
     1       ///,5X,*ENERGY STORED=*,F10.2,* MW-HRS*,//,
     2       4X,*ITHETC*,10X,*QEQVR*,13X,*QR*,
     3       11X,*QRMAX*,12X,*QSC*,11X,*QHEC*,/)
      K=1
      PRINT 20,K,QEQVR(K),QR(K),QRMAX(K),QSC(K),QHEC(K)
   20 FORMAT(5X,I5,5F15.2)
      ITCRMM1=ITCREM-1
      DO 30 K=J,ITCRMM1,J
   30 PRINT 20,K,QEQVR(K),QR(K),QRMAX(K),QSC(K),QHEC(K)
      K=ITCREM
      PRINT 20,K,QEQVR(K),QR(K),QRMAX(K),QSC(K),QHEC(K)
      PRINT 40
   400FORMAT(///,4X,*ITHETC*,10X,*FR*,7X,*FMIXS*,9X,*FB1*,
     1       9X,*FB2*,8X,*FHEC*,6X,*NTANKC*,/)
      K=1
      PRINT 50,K,FR(K),FMIXS(K),FB1(K),FB2(K),FHEC(K),NTANKC(K)
   50 FORMAT(5X,I5,5F12.2,I12)
      DO 60 K=J,ITCRMM1,J
    6 PRINT 50,K,FR(K),FMIXS(K),FB1(K),FB2(K),FHEC(K),NTANKC(K)
      K=ITCREM
      PRINT 50,K,FR(K),FMIXS(K),FB1(K),FB2(K),FHEC(K),NTANKC(K)
      PRINT 70
   700FORMAT(///,4X,*ITHETC*,8X,*TINR*,7X,*TOUTR*,
     1       6X,*TINHEC*,5X,*TOUTHEC*,7X,*TMIXS*,6X,*ACUMCT*,/)
      K=1
     0PRINT 80,K,TINR(K),TOUTR(K),TINHEC(K),TOUTHEC(K),
     1          TMIXS(K),ACUMCT(K)
   80 FORMAT(5X,I5,6F12.2)
      DO 90 K=J,ITCRMM1,J
   90 PRINT 80,K,TINR(K),TOUTR(K),TINHEC(K),TOUTHEC(K),
     1          TMIXS(K),ACUMCT(K)
      K=ITCREM
     0PRINT 80,K,TINR(K),TOUTR(K),TINHEC(K),TOUTHEC(K),
     1          TMIXS(K),ACUMCT(K)
```



```
      DO 1[illegible] L=1,NTANKT
      M=L*12/NTANKT
      PRINT 110,L
  11[illegible]FORMAT(/,5X,*OUTPUT TABLE FOR TANK*,I3,
     1       ///,4X,*ITHETC*,7X,*CMDOT*,9X,*REC*,
     2       9X,*UOC*,6X,*ESTTGC*,/)
      K=1
      PRINT 120,K,CMDOT(K,L),REC(K,L),UOC(K,L),ESTTGC(K+1,M)
  120 FORMAT(5X,I5,4F12.2)
      DO 130 K=J,ITCRMM1,J
  130 PRINT 120,K,CMDOT(K,L),REC(K,L),UOC(K,L),ESTTGC(K+1,M)
      K=ITCREM
      PRINT 120,K,CMDOT(K,L),REC(K,L),UOC(K,L),ESTTGC(K+1,M)
  100 CONTINUE
      IX1=I
      IX3=3*I
      IX5=5*I
      IX7=7*I
      IX9=9*I
      IX11=11*I
      PRINT 140,IX1,IX3,IX5,IX7,IX9,IX11
 1400FORMAT(//,5X,*CTWSTR TABLE*,///,
     1       4X,*ITHETC*,25X,*LENGHT INCREMENT*,//,
     2       10X,6I12,/)
      ITCRMDJ=ITCREM/J
      DO 150 L=1,ITCRMDJ
      M=L*J+1
  15[illegible] PRINT 16 ,M,CTWSTR(L,IX1),CTWSTR(L,IX3),CTWSTR(L,IX5),
     1       CTWSTR(L,IX7),CTWSTR(L,IX9),CTWSTR(L,IX11)
  160 FORMAT(5X,I5,6F12.2)
      PRINT 190
  190 FORMAT(//,7X,*ITC*,7X,*IZC*,7X,*CTW*,7X,*CTG*,/)
      DO 200 IZC=1,300
      IYIZC=(IZC+I/2)/I
      YIZC=(IZC+I/2)/RI
      IF(((IYIZC-YIZC).NE.0) GO TO 200
      DO 210 ITC=1,300
      IF((ITC.EQ.1) PRINT 220,ITC,IZC,CTWSTR1(IZC),CTGSTR(1,IYIZC)
   22 FORMAT(5X,I5,I10,2F10.2)
      IYITC=ITC/J
      YITC=ITC/RJ
      IF(((IYITC-YITC).NE.0) GO TO 210
     1 PRINT 220,ITC,IZC,CTWSTR(IYITC,IZC),CTGSTR(ITC,IYIZC)
  210 CONTINUE
  200 CONTINUE
      RETURN
      END
```

```
SUBROUTINE PRINTDS  760*-7600 OPT=1                    FTN 4.6+452/034
      SUBROUTINE PRINTDS(ENERGYD)
      COMMON/DTWSTR1/DTWSTR1(350)
     1COMMON/BCKGR/NTANKT,          FLOWA,          TEQD,
     1      CPBRIK,          PERIM,          IGAS,
     2      CTGINF,          DTGINF,         TDSOSC
      COMMON/SIZE/DZ,Z,MBRIK
      REAL MBRIK
     1COMMON/HRGDIS/DTGI(351),      ESTTGD(361,12),ADTW(361),
     1      QEQVHE(360),     FHED(360),      TOUTHED(360),
     2      NTANKD(360),     DMDOT(360,12),  RED(36 ,12),
     3      HD(360,12),      UOD(360,12),    IBEGIN(12),
     4      IEND(12),        DTG(360,2),     DTGSTR(360,12),
     5      DTWSTR(1),35 ),QSD(36 ),         ACUMDT(361),
     6      ITDREM,          ESTTGP2(362),   DTHETD1(361)
      LEVEL 2,DTGI
     1COMMON/DISINPT/ESTDT,          DTHETD,         QHED(360),
     1      TDSOHE(360),     TINHED(360),    HESTDT
     0COMMON/IJSET/I,IADJUST,IX12,IX12P1,IX6,J,JX1 ,JX1 P1,JX5,
     1      RI,RIX12,RJ,RJX10
      PRINT 10,ENERGYD
  100FORMAT(//,5X,*CONDITIONS DURING DISCHARGE CYCLE*,
     1      ///,5X,*ENERGY DISCHARGED=*, F10.2,* MW-HRS*,//,
     2      4X,*ITHETD*,11X,*QHED*,9X,*QEQVHE*,
     3      12X,*QSD*,11X,*FHED*,/)
      K=1
      PRINT 20,K,QHED(K),QEQVHE(K),QSD(K),FHED(K)
   2( FORMAT(5X,I5,4F15.2)
      ITDRMM1=ITDREM-1
      DO 3( K=J,ITDRMM1,J
   3( PRINT 20,K,QHED(K),QEQVHE(K),QSD(K),FHED(K)
      K=ITDREM
      PRINT 2.,K,QHED(K),QEQVHE(K),QSD(K),FHED(K)
      PRINT 40
  400FORMAT(///,4X,*ITHETD*,6X,*TINHED*,5X,*TOUTHED*,
     1      6X,*TDSOHE*,6X,*NTANKD*,6X,*ACUMDT(ITD+1)*,/)
      K=1
      PRINT 5(,K,TINHED(K),TOUTHED(K),TDSOHE(K),NTANKD(K),ACUMDT(K+1)
   5( FORMAT(5X,I5,3F12.2,I12,F12.2)
      DO 60 K=J,ITDRMM1,J
   6( PRINT 5(,K,TINHED(K),TOUTHED(K),TDSOHE(K),NTANKD(K),ACUMDT(K+1)
      K=ITDREM
      PRINT 50,K,TINHED(K),TOUTHED(K),TDSOHE(K),NTANKD(K),ACUMDT(K+1)
      DO 70 L=1,NTANKT
      M=L*12/NTANKT
      PRINT 8( ,L
  80(FORMAT(/,5X,*OUTPUT TABLE FOR TANK*,I3,//,
     1      4X,*ITHETD*,7X,*DMDOT*,9X,*RED*,
     2      9X,*UOD*,6X,*ESTTGD(ITD+1)*,/)
      K=1
      PRINT 90,K,DMDOT(K,L),RED(K,L),UOD(K,L),ESTTGD(K+1,M)
   9( FORMAT(5X,I5,4F12.2)
      DO 100 K=J,ITDRMM1,J
  1(  PRINT 9(,K,DMDOT(K,L),RED(K,L),UOD(K,L),ESTTGD(K+1,M)
      K=ITDREM
      PRINT 90,K,DMDOT(K,L),RED(K,L),UOD(K,L),ESTTGD(K+1,M)
   7( CONTINUE
      IX1=I
      IX3=3*I
      IX5=5*I
      IX7=7*I
      IX9=9*I
      IX11=11*I
      PRINT 110,IX1,IX3,IX5,IX7,IX9,IX11
  110(FORMAT(//,5X,*DTWSTR TABLE*,///,
     1      4X,*ITHETD*,25X,*LENGHT INCREMENT*,//,
     2      10X,6I12,/)
      ITDRMDJ=ITDREM/J
      DO 120 L=1,ITDRMDJ
      M=L*J+1
  12(  PRINT 13(,M,DTWSTR(L,IX1),DTWSTR(L,IX3),DTWSTR(L,IX5),
     1      DTWSTR(L,IX7),DTWSTR(L,IX9),DTWSTR(L,IX11)
  130 FORMAT(5X,I5,6F12.2)
      PRINT 140
  14(  FORMAT(//,7X,*ITD*,7X,*IZD*,7X,*DTW*,7X,*DTG*,/)
      DO 15( IZD=1,3.0
      IYIZD=(IZD+1/2)/I
      YIZD=(IZD+I/2)/RI
      IF((IYIZD-YIZD).NE.0) GO TO 150
      DO 160 ITD=1,300
      IF(ITD.EQ.1) PRINT 17(,ITD,IZD,DTWSTR1(1ZD),DTGSTR(1,IYIZD)
  170 FORMAT(5X,I5,I10,2F10.2)
      IYITD=ITD/J
      YITD=ITD/RJ
      IF((IYITD-YITD).NE.0) GO TO 160
      PRINT 170,ITD,IZD,DTWSTR(IYITD,IZD),DTGSTR(ITD,IYIZD)
  16(  CONTINUE
  150 CONTINUE
      RETURN
      END
```

SUBROUTINE PDROPCH 7600-7600 OPT=1 FTN 4.6+452/ 34 1

```
      SUBROUTINE PDROPCH
      COMMON/PDROPC/PDROPC(360,13),GASVOLC(360,12),DPBARC
      LEVEL 2,PDROPC,GASVOLC,DPBARC
     0COMMON/BCKGR/NTANKT,      FLOWA,      TEQD,
     1             LPBRIK,      PERIM,      IGAS,
     2             CTGINF,      DTGINF,     TDSOSC
      COMMON/SIZE/DZ,Z,MBRIK
      REAL MBRIK
     0COMMON/IJSET/I,IADJUST,IX12,IX12P1,IX6,J,JX10,JX10P1,JX5,
     1             RI,RIX12,RJ,RJX10
     0COMMON/HRGCRG/CTGI(351),      ESTTGC(361,12),ACTW(361),
     1             QEQVR(360),      FHEC(360),     FB2(360),
     2             FMIXS(360),      TMIXS(360),    FR(360),
     3             FB1(360),        TINR(360),     TOUTR(360),
     4             NTANKC(360),     CMDOT(360,12), REC(360,12),
     5             HC(360,12),      UOC(360,12),   IBEGIN(12),
     6             IEND(12),        CTG(360,2),    CTGSTR(360,12),
     7             CTWSTR(10,350),QSC(360),      ACUMCT(360),
     8             ITCREM
*START OF THE MAIN ITC LOOP.  CALCULATES PRESSURE DROP THROUGH
*****THE REGENERATOR DURING CHARGING.
      PRINT 30,ITCREM
   30 FORMAT(5X,*ITCREM=*,I4)
      DPBARC=0.0
      DO 10 ITC=1,ITCREM
*INITIALIZE PDROPC(ITC,1) , THE PRESSURE DROP BEFORE THE FIRST SEGMENT.
      PDROPC(ITC,1)=0.0
*START OF THE MAIN ISEG LOOP.  CALCULATE PRESSURE DROP THROUGH
*****SEGMENT ISEG FOR THE TIME INCREMENT ITC.
      DO 20 ISEG=1,12
*DETERMINE WHICH TANK EACH SEGMENT IS IN.
      NTANK=(NTANKT*(ISEG-1))/12+1
*DETERMINE THE GAS VOLUME IN M**3/KG, MIDWAY THROUGH EACH SEGMENT.
      IF(IGAS.EQ.1) GASVOLC(ITC,ISEG)=1.42E-04*
     1      (CTGSTR(ITC,ISEG)-68.0)
       IF(IGAS.EQ.2) GASVOLC(ITC,ISEG)=CTGSTR(ITC,ISEG)/1660.0
       IF(IGAS.EQ.3) GASVOLC(ITC,ISEG)=8.62E-05*CTGSTR(ITC,ISEG)
*FOR DETERMINATION OF PRESSURE DROP THE FANNING
*****EQUATION WAS TAKEN FROM PETERS+TIMMERHAUS, P. 421.
*****THE CHANNELS WERE ASSUMED TO BE VERY ROUGH WITH
*****A FANNING FRICTION FACTOR OF 0.025.
      DPDROPC(ITC,ISEG+1)=PDROPC(ITC,ISEG)+0.25*
     1                CMDOT(ITC,NTANK)**2*(RI*DZ)*
     2                GASVOLC(ITC,ISEG)/(TEQD*FLOWA**2)
   20 CONTINUE
      DPBARC=DPBARC+PDROPC(ITC,13)/ITCREM
   10 CONTINUE
      RETURN
      END
```

SUBROUTINE PRNTPRS 76 J-760 OPT=1 FTN 4.6+452/ 34

```
      SUBROUTINE PRNTPRS
      COMMON/PDROPC/PDROPC(360,13),GASVOLC(360,12),DPBARC
      LEVEL 2,PDROPC,GASVOLC,DPBARC
     0COMMON/IJSET/I,IADJUST,IX12,IX12P1,IX6,J,JX10,JX10P1,JX5,
     1             RI,RIX12,RJ,RJX10
     0COMMON/HRGCRG/CTGI(351),      ESTTGC(361,12),ACTW(361),
     1             QEQVR(360),      FHEC(360),     FB2(360),
     2             FMIXS(360),      TMIXS(360),    FR(360),
     3             FB1(360),        TINR(360),     TOUTR(360),
     4             NTANKC(360),     CMDOT(360,12), REC(360,12),
     5             HC(360,12),      UOC(360,12),   IBEGIN(12),
     6             IEND(12),        CTG(360,2),    CTGSTR(360,12),
     7             CTWSTR(10,350),QSC(360),      ACUMCT(360),
     8             ITCREM
      PRINT 10
   10 FORMAT(///,5X,*CHARGING PRESSURE DROP TABLE*,
     1       //,4X,*ITHETC*,20X,*END OF ISEG*,//,
     2       19X,1H1,9X,1H2,9X,1H3,9X,1H4,9X,1H5,9X,1H6,/)
      K=1
      OPRINT 20,K,PDROPC(K,2),PDROPC(K,3),PDROPC(K,4),
     1       PDROPC(K,5),PDROPC(K,6),PDROPC(K,7)
   20 FORMAT(5X,I5,6E10.4)
      ITCRMM1=ITCREM-1
      DO 30 K=J,ITCRMM1,J
   30 OPRINT 20,K,PDROPC(K,2),PDROPC(K,3),PDROPC(K,4),
     1       PDROPC(K,5),PDROPC(K,6),PDROPC(K,7)
      K=ITCREM
      OPRINT 20,K,PDROPC(K,2),PDROPC(K,3),PDROPC(K,4),
     1       PDROPC(K,5),PDROPC(K,6),PDROPC(K,7)
      PRINT 40
   40 FORMAT(///,19X,1H7,9X,1H8,9X,1H9,8X,2H10,8X,2H11,8X,2H12,/)
      K=1
      OPRINT 20,K,PDROPC(K,8),PDROPC(K,9),PDROPC(K,1)),
     1       PDROPC(K,11),PDROPC(K,12),PDROPC(K,13)
      DO 50 K=J,ITCRMM1,J
   50 OPRINT 20,K,PDROPC(K,8),PDROPC(K,9),PDROPC(K,10),
     1       PDROPC(K,11),PDROPC(K,12),PDROPC(K,13)
      K=ITCREM
      OPRINT 20,K,PDROPC(K,8),PDROPC(K,9),PDROPC(K,10),
     1       PDROPC(K,11),PDROPC(K,12),PDROPC(K,13)
      PRINT 60,DPBARC
   60 FORMAT(///,5X,*AVERAGE PRESSURE DROP, CHARGING=*,E10.4,//)
      RETURN
      END
```

```
SUBROUTINE PDROPDS  7600-7600 OPT=1                    FTN 4.6+452/ 34    1 DEC 78 . .44.59 BKY PAGE      1

      SUBROUTINE PDROPDS
      COMMON/PDROPD/PDROPD(360,13),GASVOLD(36 ,12)
      LEVEL 2,PDRUPD,GASVOLD
      OCOMMON/BCKGR/NTANKT,        FLOWA,        TEQD,
     1              CPBRIK,        PERIM,        IGAS,
     2              CTGINF,        DTGINF,       TDSOSC
      COMMON/SIZE/DZ,Z,MBRIK
      REAL MBRIK
      OCOMMON/HRGDIS/DTGI(351),    ESTTGD(361,12),ADTW(361),
     1              QEQVHE(360),   FHED(360),     TOUTHED(360),
     2              NTANKD(360),   DMDOT(360,12), RED(360,12),
     3              HD(360,12),    UOD(360,12),   IBEGIN(12),
     4              IEND(12),      DTG(360,2),    DTGSTR(360,12),
     5              DTWSTR(10,350),QSD(361),      ACUMDT(361),
     6              ITDREM,        ESTTGP2(362),  DTHETD1(361)
      OCOMMON/IJSET/I,IADJUST,IX12,IX12P1,IX6,J,JX10,JX10P1,JX5,
     1              RI,RIX12,RJ,RJX10
      LEVEL 2,DTGI
      PRINT 30,ITDREM
30    FORMAT(5X,*ITDREM=*,I4)
      DPBAR=0.0
      DO 10 ITD=1,ITDREM
      PDROPD(ITD,1)=0.0
      DO 20 ISEG=1,12
      NTANK=(NTANKT*(ISEG-1))/12+1
      OIF(IGAS.EQ.1) GASVOLD(ITD,ISEG)=1.42E-04*
     1               (DTGSTR(ITD,ISEG)-68.0)
      IF(IGAS.EQ.2) GASVOLD(ITD,ISEG)=DTGSTR(ITD,ISEG)/166.0
      IF(IGAS.EQ.3) GASVOLD(ITD,ISEG)=8.62E-05*DTGSTR(ITD,ISEG)
      OPDROPD(ITD,ISEG+1)=PDROPD(ITD,ISEG)+0.05*
     1                    DMDOT(ITD,NTANK)**2*(RI*DZ)*
     2                    GASVOLD(ITD,ISEG)/(TEQD*FLOWA**2)
20    CONTINUE
      DPBAR=DPBAR+PDROPD(ITD,13)/ITDREM
10    CONTINUE
      PRINT 40
400FORMAT(///,5X,*DISCHARGING PRESSURE DROP TABLE*,
     1       //,4X,*ITHETD*,,7X,*PRESSURE DROP*,/)
      K=1
      PRINT 50,K,PDROPD(K,13)
50    FORMAT(5X,I5,10X,E10.4)
      ITDRMM1=ITDREM-1
      DO 60 K=J,ITDRMM1,J
60    PRINT 50,K,PDROPD(K,13)
      K=ITDREM
      PRINT 50,K,PDROPD(K,13)
      PRINT 70,DPBAR
70    FORMAT(//,5X,*AVERAGE PRESSURE DROP, DISCHARGING=*,E10.4,//)
      RETURN
      END
```

II.4 HREGEN SAMPLE OUTPUT FOR THE REFERENCE STORAGE DESIGN

II.4a Input Data for this Case

```
NTANKT= 1 FLOWA=      12.00 CTGINF=    1089.00
DTGINF=     600.00 TDSUSC=     867.00


LENGTH INCREMENTS= 300 TIME INCREMENTS= 300


INPUT FOR CHARGE CYCLE

HTHETC=     8.0000 HOURS,      TOUTRM=    1089.00 K
ISTART=    1 ISTOP= 300 TINHEC=     867.00 K,    TOUTHEC=     600.00 K
QR=    441000000.00 W,    QHEC=    252000000.00 W,    QRMAX=    441000000.00W


INPUT FOR DISCHARGE CYCLE

HESTDT=     6.0000 HOURS,    DTHETD=    72.0000 SECONDS
ISTART=    1 ISTOP= 360 QHED=    252000000.00 W
TDSOHE=     600.00 K,  TINHED=     867.00 K

        RECEIVER GAS IS HELIUM
```

II.4b Output Generated During Program Iteration to a Satisfactory Design

```
STORAGE CHARGED AFTER 300 TIME INCREMENTS      CTWBAR=    1040.10
   1089.03    1089.02    1089.00    1088.81    1087.66    1083.25
   1071.43    1047.52    1009.14     958.32     901.21     845.54

STORAGE DISCHARGED AFTER 328 TIME INCREMENTS      DTWBAR=     666.03
    600.00     600.00     600.09     600.80     603.95     613.20
    633.20     667.29     715.37     773.59     835.83     895.79

IT=  1 P1(IT)= .900000 ENDT12C=     870.58
FRACSTR(IT)=-.092805 DEVIA(IT)= .007329 DDEVDP1=        5.00

STORAGE CHARGED AFTER 300 TIME INCREMENTS      CTWBAR=    1039.38
   1089.03    1089.02    1088.98    1088.70    1087.19    1082.03
   1069.36    1045.28    1007.88     958.48     901.28     841.79

STORAGE DISCHARGED AFTER 298 TIME INCREMENTS      DTWBAR=     669.10
    600.00     600.01     600.18     601.29     605.51     616.62
    638.77     674.39     722.70     779.75     839.86     897.46

IT=  2 P1(IT)= .898534 ENDT12C=     871.36
FRACSTR(IT)= .008213 DEVIA(IT)= .008922 DDEVDP1=        5.00

STORAGE CHARGED AFTER 300 TIME INCREMENTS      CTWBAR=    1038.51
   1089.03    1089.02    1088.98    1088.68    1087.09    1081.70
   1068.57    1043.84    1005.82     956.08     898.96     839.95

STORAGE DISCHARGED AFTER 301 TIME INCREMENTS      DTWBAR=     668.85
    600.00     600.01     600.17     601.24     605.37     616.34
    638.34     673.87     722.16     779.26     839.46     897.18
```

II.4c Output Data for the Reference Storage Design

BACKGROUND INFORMATION

THE STORAGE POTENTIAL FOR THIS DESIGN IS .0001095 MW-HRS OF HEAT PER KG OF BRICK

STORAGE IS BROKEN DOWN INTO 1 TANKS IN SERIES WITH105.58 M TOTAL LENGHT

STORAGE CONTAINS 13809537. KG OF BRICKS

GAS FLOW AREA= 12.00 M2 HEAT TRANSFER PERIMETER= 1171.20 M

THE RECEIVER GAS IS HELIUM

DURING CHARGE, THE MAXIMUM TEMPERATURE ALLOWED AT THE STORAGE OUTLET IS 967.00 DEG K

THIS PROGRAM SOLVES THE HEAT REGENERATOR EQUATIONS BY THE METHOD OF FINITE DIFFERENCE
TIME WAS DIVIDED INTO 300 INCREMENTS. 300 LENGHT INCREMENTS WERE USED.

CONDITIONS DURING CHARGE CYCLE

ENERGY STORED= 1512.00 MW-HRS

ITHETC	QEQVR	QR	QRMAX	QSC	QHEC
1	441000000.01	441000000.00	441000000.00	188999938.21	252000000.00
30	441000106.56	441000000.00	441000000.00	188999993.28	252000000.00
60	441000441.11	441000000.00	441000000.00	188999983.70	252000000.00
90	441001078.95	441000000.00	441000000.00	188999973.66	252000000.00
120	441001993.59	441000000.00	441000000.00	188999965.33	252000000.00
150	441003157.12	441000000.00	441000000.00	188999956.16	252000000.00
180	441004698.77	441000000.00	441000000.00	188999937.96	252000000.00
210	441007090.13	441000000.00	441000000.00	188999895.14	252000000.00
240	441011504.92	441000000.00	441000000.00	188999791.17	252000000.00
270	441021293.58	441000000.00	441000000.00	188999484.05	252000000.00
300	441052240.42	441000000.00	441000000.00	188997899.10	252000000.00

ITHETC	FR	FMIXS	FB1	FB2	FHEC	NTANKC
1	173.43	173.43	0.00	8.07	181.50	1
30	173.43	173.43	0.00	8.07	181.50	1
60	173.43	173.43	0.00	8.07	181.50	1
90	173.43	173.43	0.00	8.07	181.50	1
120	173.43	173.43	0.00	8.07	181.50	1
150	173.43	173.43	0.00	8.07	181.50	1
180	173.43	173.43	0.00	8.07	181.50	1
210	173.43	173.43	0.00	8.07	181.50	1
240	173.43	173.43	0.00	8.07	181.50	1
270	173.43	173.43	0.00	8.07	181.50	1
300	173.43	173.43	0.00	8.07	181.50	1

ITHETC	TINR	TOUTR	TINHEC	TOUTHEC	TMIXS	ACUMCT
1	600.00	1089.00	867.00	600.00	879.43	96.00
30	600.00	1089.00	867.00	600.00	879.43	2880.00
60	600.00	1089.00	867.00	600.00	879.43	5760.00
90	600.00	1089.00	867.00	600.00	879.43	8640.00
120	600.00	1089.00	867.00	600.00	879.43	11520.00
150	600.00	1089.00	867.00	600.00	879.43	14400.00
180	600.00	1089.01	867.00	600.00	879.43	17280.00
210	600.00	1089.01	867.00	600.00	879.43	20160.00
240	600.00	1089.01	867.00	600.00	879.43	23040.00
270	600.00	1089.02	867.00	600.00	879.43	25920.00
300	600.00	1089.06	867.00	600.00	879.43	28800.00

OUTPUT TABLE FOR TANK 1

ITHETC	CMDOT	REC	UOC	ESTTGC
1	74.33	4531.69	111.03	600.00
30	74.33	4532.04	111.03	600.04
60	74.39	4535.42	111.07	600.43
90	74.62	4549.64	111.24	602.01
120	75.27	4589.23	111.72	606.34
150	76.70	4676.19	112.74	615.52
180	79.44	4843.23	114.68	632.16
210	84.41	5146.23	118.04	659.51
240	93.55	5703.63	123.80	702.20
270	112.16	6838.22	134.13	767.59
300	161.94	9873.60	155.22	868.73

CTWSTR TABLE

ITHETC	LENGHT INCREMENT					
	25	75	125	175	225	275
31	948.25	777.65	674.08	618.37	602.15	600.10
61	1038.83	847.53	718.89	640.87	608.32	600.91
91	1075.67	929.43	774.37	673.58	621.19	603.76
121	1086.11	1001.32	841.29	716.91	642.75	610.63
151	1088.47	1048.80	913.73	771.51	674.52	623.86
181	1088.92	1073.52	980.19	836.48	717.99	645.93
211	1088.99	1084.01	1031.00	906.99	774.53	679.72
241	1089.01	1087.69	1063.28	974.52	844.02	728.97
271	1089.01	1088.74	1080.10	1030.04	923.00	798.72
301	1089.03	1088.98	1086.97	1067.65	1003.26	895.20

ITC	IZC	CTW	CTG
1	13	870.43	927.57
30	13	1013.37	1051.72
60	13	1073.07	1082.88
90	13	1086.36	1088.15
120	13	1088.63	1088.90
150	13	1088.95	1088.99
180	13	1089.00	1089.00

7C-2300 8-78

210	13	1089.01	1089.01
240	13	1089.01	1089.01
270	13	1089.02	1089.02
300	13	1089.04	1089.05
1	38	810.99	832.84
30	38	890.11	928.06
60	38	988.37	1019.61
90	38	1050.98	1066.23
120	38	1077.51	1082.90
150	38	1086.10	1087.62
180	38	1088.38	1088.73
210	38	1088.89	1088.96
240	38	1088.99	1089.00
270	38	1089.01	1089.01
300	38	1089.02	1089.03
1	63	751.62	771.51
30	63	808.94	834.75
60	63	888.72	921.23
90	63	972.67	1000.65
120	63	1034.13	1051.20
150	63	1067.57	1075.55
180	63	1081.98	1084.97
210	63	1087.07	1087.99
240	63	1088.57	1088.80
270	63	1088.93	1088.98
300	63	1089.01	1089.02
1	88	698.12	715.61
30	88	746.75	767.14
60	88	808.27	834.20
90	88	883.88	913.41
120	88	960.50	986.57
150	88	1020.82	1038.63
180	88	1058.43	1068.11
210	88	1077.51	1081.77
240	88	1085.47	1086.97
270	88	1088.17	1088.58
300	88	1088.89	1088.96
1	113	655.58	669.13
30	113	694.97	711.82
60	113	744.82	765.46
90	113	806.35	831.64
120	113	878.46	906.07
150	113	950.83	975.66
180	113	1010.60	1028.71
210	113	1051.19	1061.93
240	113	1073.94	1079.08
270	113	1084.36	1086.25
300	113	1088.07	1088.55
1	138	626.54	635.51
30	138	654.71	667.52
60	138	693.88	710.37
90	138	743.28	763.81
120	138	804.02	828.57
150	138	873.69	900.00
180	138	943.82	967.83
210	138	1003.87	1022.07
240	138	1047.03	1058.31
270	138	1072.69	1078.16
300	138	1084.76	1086.61
1	163	610.15	615.02
30	163	627.26	635.75
60	163	655.07	667.42

90	163	693.20	709.39
120	163	742.07	762.34
150	163	802.09	826.04
180	163	870.60	896.10
210	163	940.34	963.82
240	163	1001.83	1019.97
270	163	1047.70	1058.96
300	163	1075.48	1080.52
1	188	602.89	604.95
30	188	611.41	616.16
60	188	628.58	636.81
90	188	655.54	667.53
120	188	692.93	708.87
150	188	741.52	761.57
180	188	801.56	825.16
210	188	870.57	895.70
240	188	942.07	965.34
270	188	1006.83	1024.71
300	188	1056.04	1066.41
1	213	600.54	601.18
30	213	603.90	606.08
60	213	612.88	617.62
90	213	629.78	637.82
120	213	656.19	667.95
150	213	693.29	709.10
180	213	742.30	762.32
210	213	803.76	827.43
240	213	875.75	901.05
270	213	952.32	975.68
300	213	1023.57	1040.68
1	238	600.06	600.18
30	238	601.07	601.86
60	238	604.97	607.30
90	238	614.19	618.94
120	238	630.98	638.91
150	238	657.25	668.92
180	238	694.79	710.68
210	238	745.53	765.92
240	238	810.90	835.29
270	238	890.17	916.43
300	238	978.22	1001.97
1	263	600.00	600.02
30	263	600.23	600.46
60	263	601.64	602.59
90	263	605.96	608.41
120	263	615.43	620.23
150	263	632.37	640.30
180	263	659.12	672.91
210	263	698.30	714.68
240	263	753.20	774.68
270	263	827.36	853.64
300	263	923.37	952.02
1	288	600.00	600.00
30	288	600.04	600.09
60	288	600.46	600.79
90	288	602.20	603.30
120	288	606.90	609.48
150	288	616.74	621.64
180	288	634.25	642.36
210	288	662.48	674.78
240	288	705.53	723.12
270	288	769.56	793.57

300	288	864.31	895.15

CONDITIONS DURING DISCHARGE CYCLE

ENERGY DISCHARGED= -1513.02 MW-HRS

ITHETD	QHED	QEQVHE	QSD	FHED
1	252000000.00	252000000.00	-251996828.32	181.50
30	252000000.00	252000081.74	-251999994.41	181.50
60	252000000.00	252000375.52	-251999985.09	181.50
90	252000000.00	252000988.03	-251999973.54	181.50
120	252000000.00	252001956.90	-251999961.28	181.51
150	252000000.00	252003326.19	-251999946.02	181.51
180	252000000.00	252005265.38	-251999921.71	181.51
210	252000000.00	252008180.40	-251999877.95	181.51
240	252000000.00	252012949.81	-251999789.89	181.51
270	252000000.00	252021881.35	-251999569.10	181.52
300	252000000.00	252043736.02	-251998734.36	181.54
301	252000000.00	252045001.66	-252606947.95	181.54

ITHETD	TINHED	TOUTHED	TDSOHE	NTANKD	ACUMDT(ITD+1)
1	867.00	600.00	600.00	1	72.00
30	867.00	600.00	600.00	1	2160.00
60	867.00	600.00	600.00	1	4320.00
90	867.00	600.00	600.00	1	6480.00
120	867.00	600.00	600.00	1	8640.00
150	867.00	600.00	600.00	1	10800.00
180	867.00	600.00	600.00	1	12960.00
210	867.00	600.00	600.00	1	15120.00
240	867.00	600.00	600.00	1	17280.00
270	867.00	600.00	600.00	1	19440.00
300	867.00	600.00	600.00	1	21600.00
301	867.00	600.00	600.00	1	21614.59

OUTPUT TABLE FOR TANK 1

ITHETD	DMDOT	RED	UOD	ESTTGD(ITD+1)
1	99.09	6041.68	126.97	1089.03
30	99.10	6042.15	126.97	1089.01
60	99.15	6044.97	127.00	1088.77
90	99.35	6057.15	127.11	1087.74
120	99.93	6092.72	127.45	1084.81
150	101.27	6174.50	128.20	1078.23
180	103.96	6338.15	129.69	1065.63
210	108.98	6644.17	132.38	1043.79
240	118.28	7211.34	137.08	1008.28
270	136.51	8322.90	145.32	952.77
300	178.75	10898.34	160.75	867.70
301	181.54	11068.12	161.63	866.88

DTWSTR TABLE

ITHETD	LENGHT INCREMENT

	25	75	125	175	225	275
31	774.42	954.41	1042.26	1079.66	1088.10	1088.98
61	669.80	880.82	1004.23	1064.28	1084.60	1088.55
91	622.12	792.33	951.37	1038.91	1076.22	1086.85
121	605.97	712.80	883.45	1001.40	1060.55	1082.39
151	601.42	657.15	807.94	950.22	1035.12	1073.09
181	600.31	625.25	736.86	886.61	997.51	1056.41
211	600.06	609.74	679.89	815.88	946.04	1029.18
241	600.01	603.24	640.62	746.14	880.92	987.59
271	600.00	600.89	617.32	685.53	805.26	927.25
301	600.00	600.19	605.66	639.82	725.33	843.39

ITD	IZD	DTW	DTG
1	13	868.17	785.02
30	13	701.26	648.31
60	13	626.10	609.87
90	13	605.59	601.79
120	13	601.06	600.30
150	13	600.18	600.05
180	13	600.03	600.01
210	13	600.00	600.00
240	13	600.00	600.00
270	13	600.00	600.00
300	13	600.00	600.00
1	38	926.96	899.83
30	38	838.18	788.69
60	38	728.27	686.85
90	38	654.51	632.26
120	38	619.38	610.22
150	38	605.98	602.85
180	38	601.63	600.71
210	38	600.39	600.16
240	38	600.08	600.03
270	38	600.01	600.00
300	38	600.00	600.00
1	63	981.19	959.99
30	63	923.84	891.71
60	63	837.31	795.98
90	63	745.14	708.75
120	63	674.81	651.02
150	63	633.16	620.71
180	63	612.82	607.36
210	63	604.34	602.29
240	63	601.27	600.61
270	63	600.31	600.13
300	63	600.06	600.02
1	88	1025.71	1008.80
30	88	982.78	960.26
60	88	920.99	889.39
90	88	840.86	804.00
120	88	758.10	724.71
150	88	690.53	666.37
180	88	645.36	630.89
210	88	619.87	612.54
240	88	607.50	604.35
270	88	602.35	601.23
300	88	600.56	600.25
1	113	1057.34	1045.56

7C-2300 8-78

30	113	1026.22	1009.75
60	113	981.51	958.55
90	113	920.29	890.05
120	113	845.34	811.42
150	113	768.46	737.08
180	113	702.75	678.58
210	113	655.22	639.50
240	113	625.72	617.06
270	113	610.00	606.04
300	113	602.96	601.55
1	138	1076.11	1069.27
30	138	1056.27	1045.06
60	138	1024.90	1008.51
90	138	980.24	957.48
120	138	920.59	891.71
150	138	849.50	817.64
180	138	776.28	746.31
210	138	711.40	687.36
240	138	661.73	645.30
270	138	628.87	619.47
300	138	610.44	606.18
1	163	1084.99	1081.82
30	163	1074.37	1067.74
60	163	1054.38	1043.36
90	163	1023.34	1007.06
120	163	979.11	956.79
150	163	921.01	893.26
180	163	852.43	821.99
210	163	780.97	751.91
240	163	715.59	691.65
270	163	663.29	646.55
300	163	627.28	617.85
1	188	1088.13	1087.03
30	188	1083.52	1080.22
60	188	1072.40	1065.75
90	188	1052.51	1041.59
120	188	1021.67	1005.54
150	188	977.86	955.96
180	188	920.68	893.71
210	188	853.01	823.38
240	188	781.17	752.52
270	188	713.28	689.36
300	188	657.02	640.51
1	213	1088.89	1088.62
30	213	1087.30	1085.95
60	213	1082.01	1078.51
90	213	1070.59	1063.89
120	213	1050.64	1039.74
150	213	1019.79	1003.74
180	213	975.96	954.28
210	213	918.52	891.84
240	213	849.53	820.01
270	213	774.22	745.36
300	213	700.38	676.40
1	238	1089.01	1088.96
30	238	1088.57	1088.12
60	238	1086.43	1084.83
90	238	1080.63	1076.94
120	238	1068.86	1062.37
150	238	1048.65	1037.68
180	238	1017.36	1001.23
210	238	972.55	950.79

240	238	912.82	885.69
270	238	838.91	808.46
300	238	754.60	724.61
1	263	1089.02	1089.02
30	263	1088.92	1088.79
60	263	1088.17	1087.54
90	263	1085.57	1083.77
120	263	1079.31	1075.44
150	263	1067.10	1060.14
180	263	1046.28	1035.08
210	263	1013.74	997.17
240	263	966.15	943.41
270	263	900.41	871.56
300	263	814.43	781.26
1	288	1089.04	1089.03
30	288	1089.01	1088.97
60	288	1088.78	1088.56
90	288	1087.74	1086.96
120	288	1084.73	1082.74
150	288	1077.97	1073.90
180	288	1065.10	1057.85
210	288	1043.04	1031.31
240	288	1007.73	990.07
270	288	953.82	928.81
300	288	873.98	840.82

ITCREM= 300

CHARGING PRESSURE DROP TABLE

ITHETC	END OF ISEG					
	1	2	3	4	5	6
1	.2710E+03	.5143E+03	.7397E+03	.9488E+03	.1144E+04	.1330E+04
30	.3073E+03	.5785E+03	.8224E+03	.1047E+04	.1255E+04	.1450E+04
60	.3169E+03	.6153E+03	.8849E+03	.1129E+04	.1353E+04	.1561E+04
90	.3204E+03	.6344E+03	.9291E+03	.1198E+04	.1443E+04	.1668E+04
120	.3263E+03	.6507E+03	.9657E+03	.1261E+04	.1533E+04	.1781E+04
150	.3388E+03	.6771E+03	.1012E+04	.1335E+04	.1638E+04	.1918E+04
180	.3634E+03	.7267E+03	.1089E+04	.1445E+04	.1789E+04	.2112E+04
210	.4103E+03	.8206E+03	.1231E+04	.1638E+04	.2038E+04	.2423E+04
240	.5040E+03	.1008E+04	.1512E+04	.2015E+04	.2514E+04	.3004E+04
270	.7245E+03	.1449E+04	.2173E+04	.2898E+04	.3620E+04	.4338E+04
300	.1510E+04	.3021E+04	.4531E+04	.6042E+04	.7551E+04	.9058E+04

	7	8	9	10	11	12
1	.1510E+04	.1686E+04	.1862E+04	.2037E+04	.2213E+04	.2388E+04
30	.1635E+04	.1815E+04	.1993E+04	.2168E+04	.2344E+04	.2519E+04
60	.1756E+04	.1943E+04	.2123E+04	.2301E+04	.2477E+04	.2653E+04
90	.1877E+04	.2073E+04	.2261E+04	.2443E+04	.2623E+04	.2800E+04
120	.2009E+04	.2222E+04	.2422E+04	.2613E+04	.2799E+04	.2982E+04
150	.2175E+04	.2412E+04	.2633E+04	.2841E+04	.3040E+04	.3233E+04
180	.2411E+04	.2686E+04	.2940E+04	.3178E+04	.3401E+04	.3616E+04
210	.2786E+04	.3124E+04	.3436E+04	.3724E+04	.3994E+04	.4248E+04
240	.3476E+04	.3923E+04	.4340E+04	.4727E+04	.5085E+04	.5420E+04
270	.5042E+04	.5724E+04	.6373E+04	.6982E+04	.7550E+04	.8078E+04
300	.1056E+05	.1204E+05	.1348E+05	.1487E+05	.1619E+05	.1743E+05

AVERAGE PRESSURE DROP, CHARGING= .4420E+04

ITOREM= 301

DISCHARGING PRESSURE DROP TABLE

ITHETD	PRESSURE DROP
1	.6384E+04
30	.6151E+04
60	.5925E+04
90	.5718E+04
120	.5551E+04
150	.5461E+04
180	.5503E+04
210	.5771E+04
240	.6474E+04
270	.8196E+04
300	.1333E+05
301	.1372E+05

AVERAGE PRESSURE DROP, DISCHARGING= .6420E+04

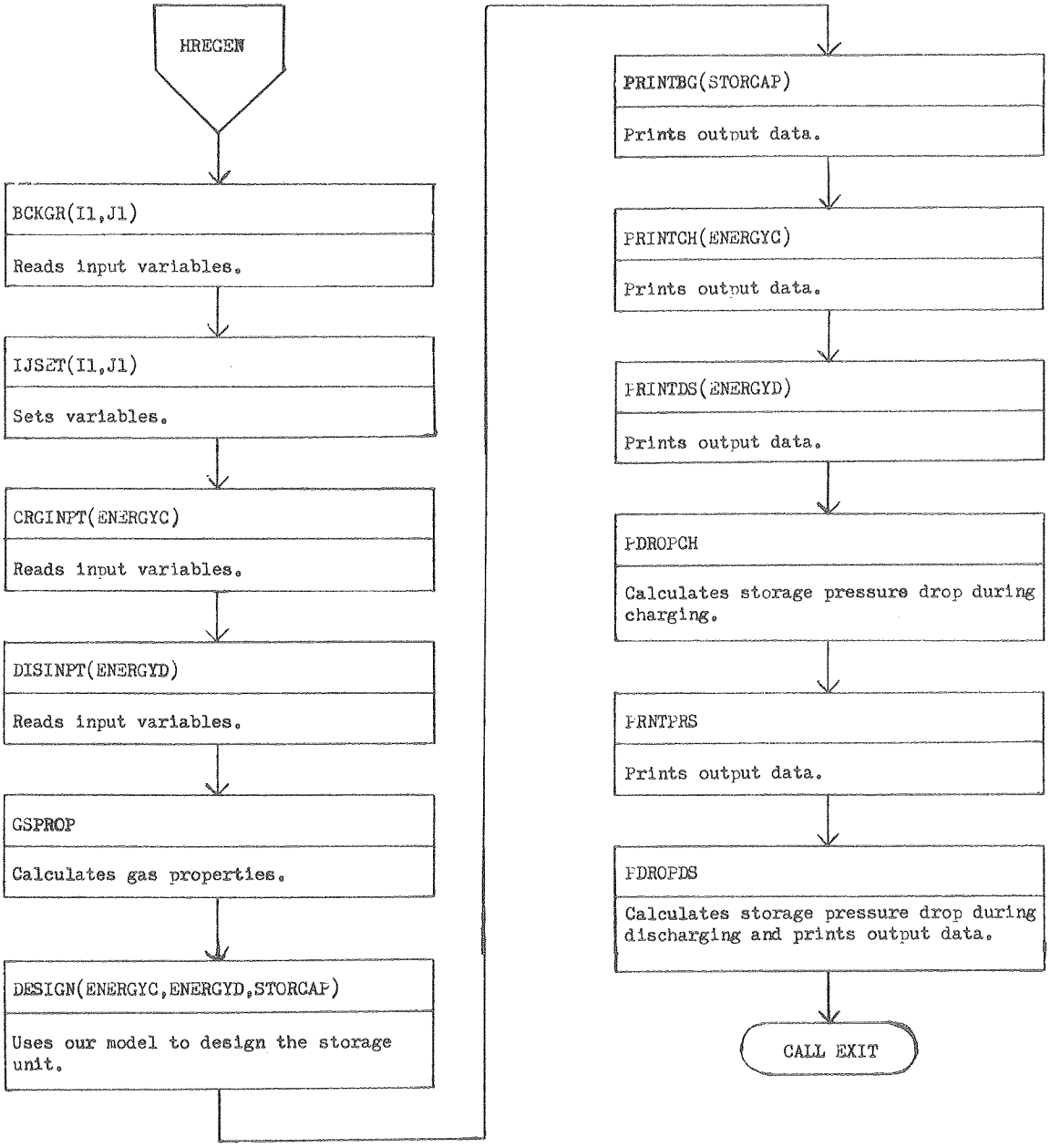

Fig. II-1. The flowchart for PROGRAM HREGEN.

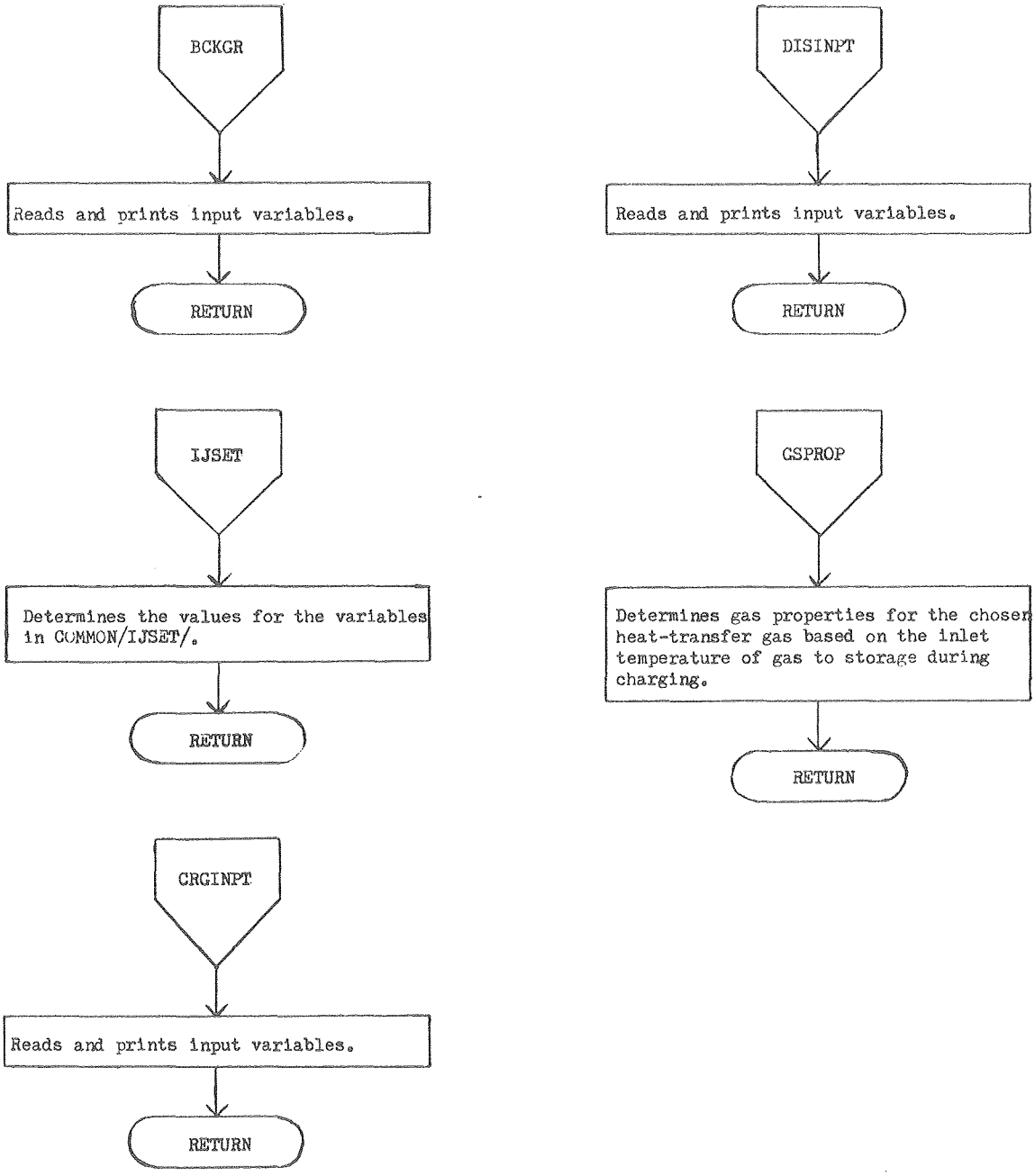

Fig. II-2. The flowcharts for SUBROUTINES BCKGR, IISET, CRGINPT, DISINPT and GSPROP.

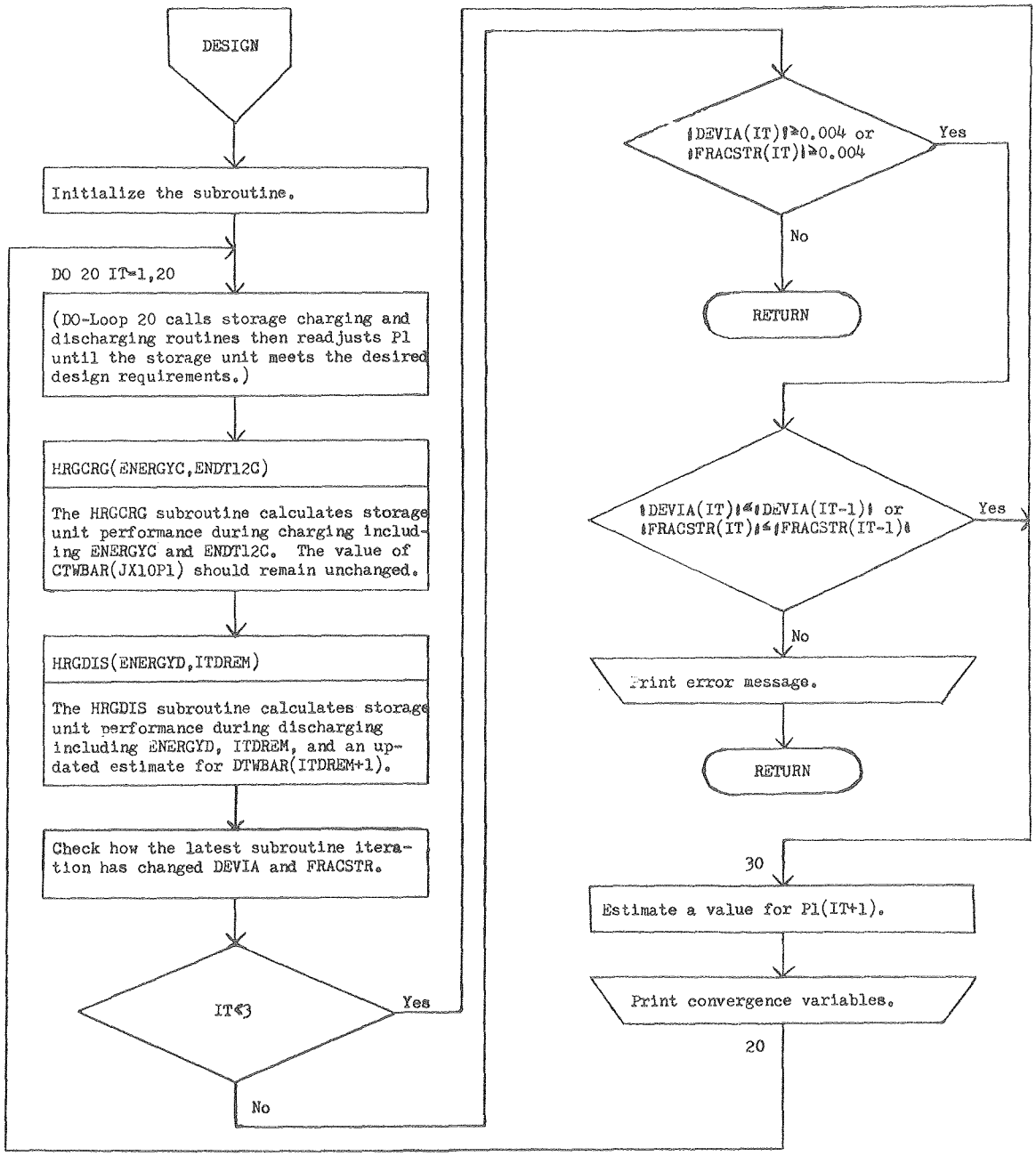

Fig. II-3. The flowchart for SUBROUTINE DESIGN.

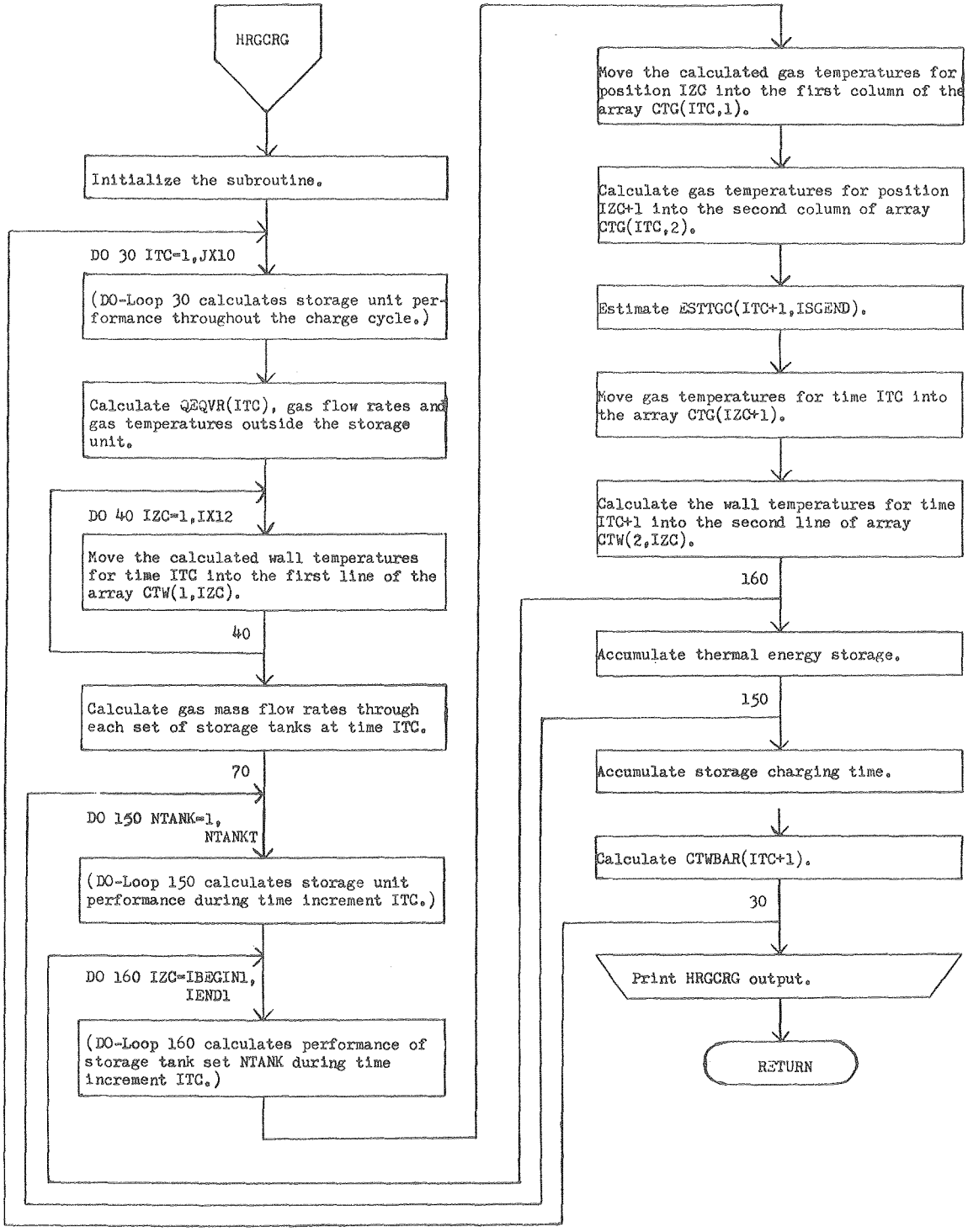

Fig. II-4. The flowchart for SUBROUTINE HRGCRG.

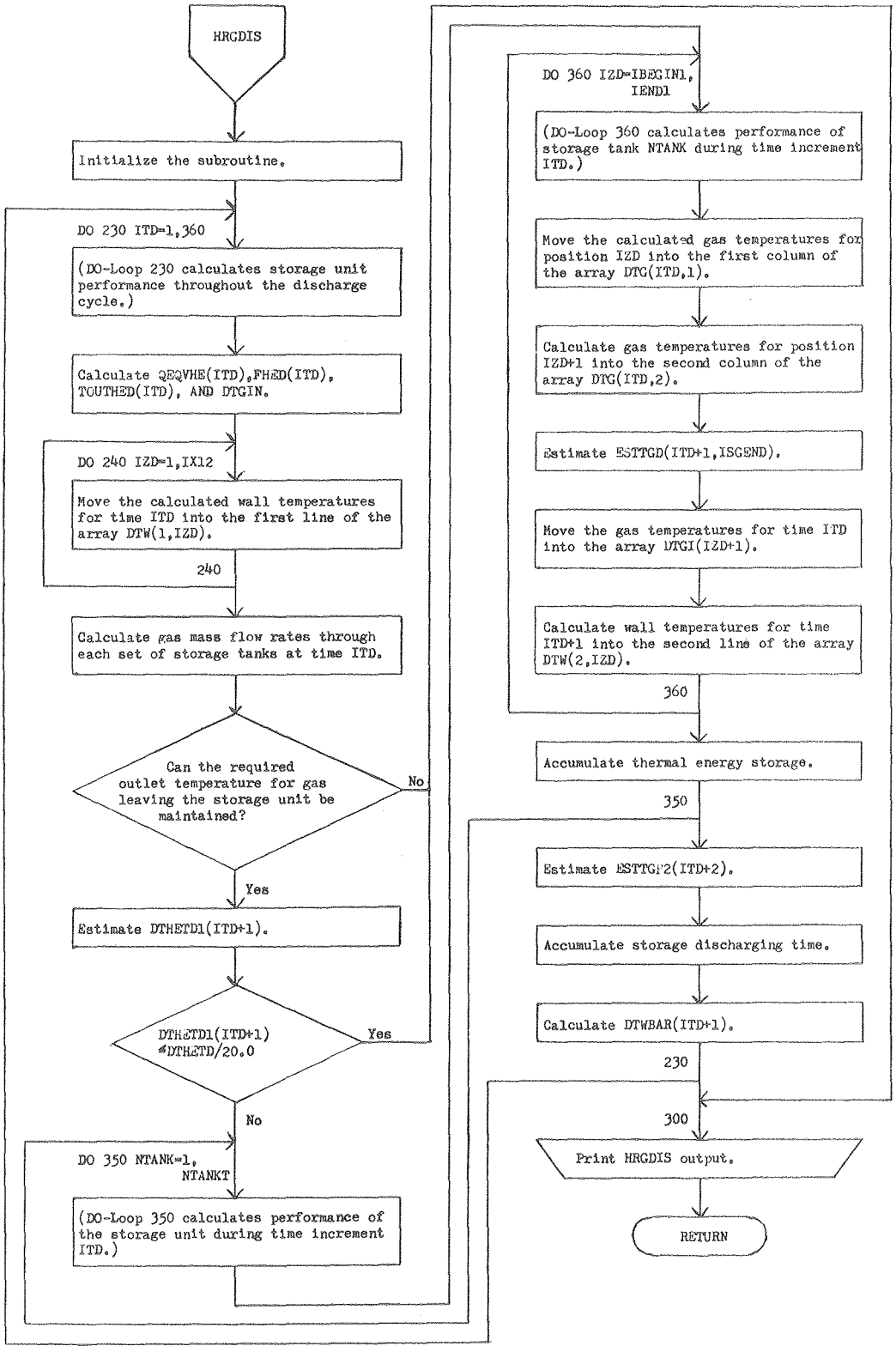

Fig. II-5. The flowchart for SUBROUTINE HRGDIS.

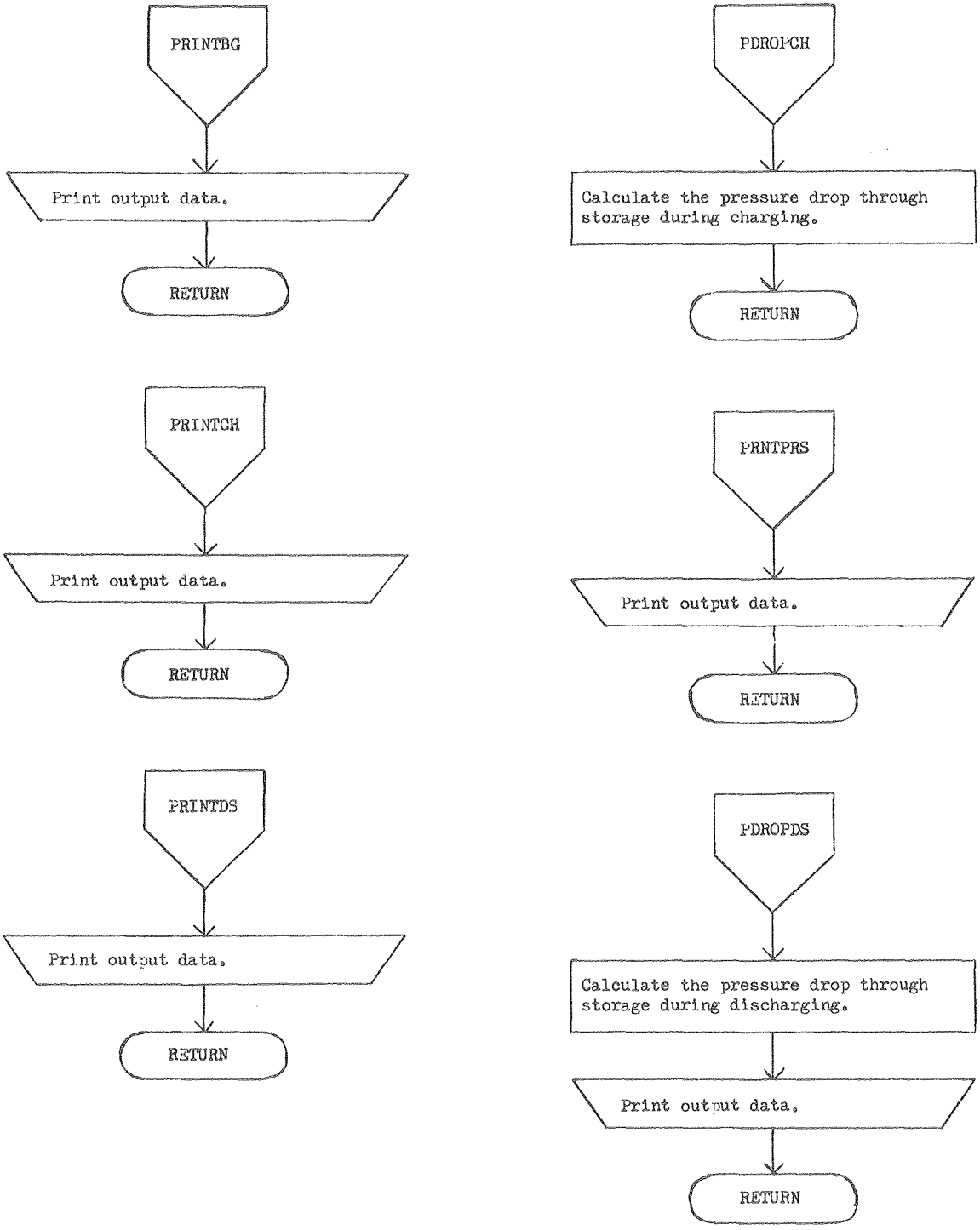

Fig. II-6. The flowcharts for SUBROUTINES PRINTBG, PRINTCH, PRINTDS, PDROPCH, PRNTPRS and PDROPDS.

APPENDIX III

Receiver Modeling Program-TUBE2

The computer program used for modeling the central receiver is reviewed in this appendix. Development of the central receiver model is discussed in Chapter 4.1. This appendix contains a program flowchart, a listing of definitions for the physical variables used, a program listing and a sample program output. The numerical values of parameters set by the data card have been included in the listing of definitions for physical variables.

III.1 DEFINITIONS OF THE PHYSICAL VARIABLES USED IN PROGRAM TUBE2

CPGAS - Gas heat capacity; J/(kg·°K)

DTODQAC - Change in the outer tube wall temperature per change in tube wall heat accumulation per area; °K/(W/m^2)

DTSRC - Correction to the effective cavity temperature estimate; °K

DZ - Incremental tube length; m

ETUBE - Tube emmisivity or tube absorbtivity, 0.88

GASVOL(100) - Gas volume for a particular length increment; m^3/kg

H - Gas film heat transfer coefficient; W/(m^2 °K)

IGAS - Symbolic representation of the heat transfer gas, (1 = water vapor, 2 = helium, 3 = nitrogen)

KG - Thermal conductivity of the gas; W/(m·°K)

KTUBE - Thermal conductivity of the tube wall; 15.0 W/(m·°K)

MU - Gas viscosity; Pa·s

NINCS - Number of length increments the tube is divided into, 95

PDDVFFF(100) - Pressure drop divided by the Fanning friction factor to the start of a particular length increment; Pa

PIE - π, 3.1415

PR - Prandlt number.

QABSGAS - Heat absorbed by the gas per tube; W

QACUM - Heat accumulated in the tube wall per area; W/m^2

QACUM2 - Heat accumulated in the tube wall per area; W/m^2

QEXCESS(11) - Excess heat which could have been absorbed by the gas for a particular effective cavity temperature estimate; W

QFROMS(100) - Heat flux per area from the cavity to the outer tube wall for a particular length increment; W/m^2

QFROMS2 - Heat flux per area from the cavity to the outer tube wall; W/m^2

QTOGAS(100) - Heat flux per area from the outer tube wall to the bulk gas for a particular length increment; W/m^2

QTOGAS2 - Heat flux per area from the outer tube wall to the bulk gas; W/m^2

RE - Reynolds number

SIGMA - Stefan-Boltzmann constant; 5.67×10^{-8} $W/(m^2 \cdot °K^4)$

TAREA - Tube cross-sectional flow area; m^2

TBULKG(100) - Bulk gas temperature at the start of a particular length increment.

TBULKO - Outlet bulk gas temperature.

TQA - Total heat available to be absorbed by the gas per tube; W

TSOURCE - Effective cavity temperature; °K

TTUBEO(100) - Outer tube wall temperature at a particular length increment; °K

TUBEFLO - Gas mass flow rate per tube; kg/s

TUBEID - Tube inside diameter; 0.0220 m

TUBEOD - Tube outside diameter; 0.0284 m

UO - Overall heat transfer coefficient from the outer tube wall to the bulk gas; $W/(m^2 \cdot °K)$

WALLTHK - Tube wall thickness; m

Z - Tube length; 9.5 m

III.2. TUBE2 PROGRAM LISTING

```
PROGRAM TUBE2     7600-7600 OPT=1                    FTN 4.6+452/034
```

```
      PROGRAM TUBE2(INPUT,OUTPUT)
      DIMENSION TTUBEO(100),TBULKG(100),QFROMS(100),
     1          QTOGAS(100),QEXCESS(18),GASVOL(100),PDUVFFF(100)
      REAL KTUBE,KG,MU
      DATA Z,NINCS,TUBEID,TUBEOD,KTUBE,SIGMA,ETUBE,PIE/
     1     9.5,95,0.0220,0.0284,15.0,5.67E-08,0.88,3.1415/
*KTUBE ESTIMATED EQUAL TO THE THERMAL CONDUCTIVITY FOR STEEL.
*****IT IS BELIEVED THAT THE THERMAL CONDUCTIVITY FOR HAYNES H-188
*****ALLOY IS LARGER THAN THIS ESTIMATE.
      DZ=Z/NINCS
      WALLTHK=(TUBEOD-TUBEID)/2.0
*READ THE CHOICE OF RECEIVER GAS (IGAS), THE HEAT ABSORBER PER TUBE
*****(TQA), AND THE INLET GAS TEMPERATURE (TBULKG(1)).
      DO 300 M=1,4
      IF(M.LE.3) IGAS=M
      IF(M.EQ.4) IGAS=1
      IF(M.LE.3) TBULKG(1)=600.0
      IF(M.EQ.4) TBULKG(1)=700.0
      DO 310 MA=1,3
      IF(MA.EQ.1) TQA=31000.0
      IF(MA.EQ.2) TQA=42000.0
      IF(MA.EQ.3) TQA=63000.0
*SET INITIAL ESTIMATES FOR THE SOURCE TEMPERATURE (TSOURCE), THE INLET
*****WALL TEMPERATURE (TTUBEO(1)), AND THE OUTLET GAS
*****TEMPERATURE (TBULKO).
      TSOURCE=1250.0
      TTUBEO(1)=TBULKG(1)+50.0
      TBULKO=1089.0
      TTUBEO(2)=TTUBEO(1)
*GAS PROPERTIES AT 1000 DEG K, FOR SPECIFIED
*****IGAS (WATER=1, ME=2, N2=3)
      IF(IGAS.EQ.1) GO TO 20
      IF(IGAS.EQ.2) GO TO 30
      IF(IGAS.EQ.3) GO TO 40
      PRINT 50
   50 FORMAT(5X,*IGAS MISREAD. PROGRAM STOPS*)
      GO TO 500
   20 KG=0.097
      MU=3.8E-05
      PR=0.92
      CPGAS=2300.0
      GO TO 60
   30 KG=0.354
      MU=4.44E-05
      PR=0.66
      CPGAS=5200.0
      GO TO 60
   40 KG=0.066
      MU=4.3E-05
      PR=0.72
      CPGAS=1100.0
   60 CONTINUE
*THE IA LOOP ADJUSTS THE OUTLET GAS TEMPERATURE SO THAT
*****THE OUTSIDE TUBE WALL TEMPERATURE AT THE GAS OUTLET IS 1089 DEG K.
*CALCULATE THE GAS FLOW PER TUBE (TUBEFLO), THE REYNOLDS NUMBER (RE),
*****THE GAS FILM HEAT TRANSFER COEFFICIENT (H), AND THE OVERALL HEAT
*****TRANSFER COEFFICIENT FROM THE OUTSIDE TUBE WALL TO THE GAS (UO).
```

```
PROGRAM TUBE2     7600-7600 OPT=1                    FTN 4.6+452/034     2
```

```
      TUBEFLO=TQA/(CPGAS*(TBULKO-TBULKG(1)))
      RE=4.0*TUBEFLO/(PIE*TUBEID*MU)
      H=0.023*KG*RE**0.8*PR**0.333/TUBEID
      UO=1.0/(1.0/H+WALLTHK/KTUBE)
*THE IB LOOP ADJUSTS TSOURCE SO THAT THE GAS ABSORBS
*****ALL OF THE AVAILABLE HEAT (TQA).
      DO 80 IB=1,10
      QABSGAS=0.0
*THE I LOOP CALCULATES HOW MUCH HEAT WILL BE TRANSFERED
*****TO THE GAS BASED ON AN ESTIMATE OF TSOURCE.
      DO 90 I=1,NINCS
      IF(I.GE.3) TTUBEO(I)=2*TTUBEO(I-1)-TTUBEO(I-2)
*THE IC LOOP DETERMINES A VALUE FOR THE OUTER TUBE WALL TEMPERATURE
*****WHICH REDUCES HEAT ACCUMULATION TO A NEGLIGIBLE VALUE.
*****THE IC LOOP IS GIVEN ESTIMATES FOR TSOURCE AND TBULKG(I).
      DO 100 IC=1,100
*CALCULATE RADIATIVE HEAT TRANSFER FROM THE SOURCE TO THE OUTER
*****TUBE WALL (QFROMS(I)) AND CONVECTIVE HEAT TRANSFER FROM
*****THE OUTER TUBE WALL TO THE GAS (QTOGAS(I)) FOR SEGMENT I,
*****BASED ON THE PRESENT ESTIMATES OF THE OUTER TUBE WALL TEMPERATURE
*****(TTUBEO(I))  AND SOURCE TEMPERATURE (TSOURCE).
      QFROMS(I)=SIGMA*ETUBE*(TSOURCE**4-TTUBEO(I)**4)*TUBEOD/TUBEID
      QTOGAS(I)=(TTUBEO(I)-TBULKG(I))*UO
      QACUM=QFROMS(I)-QTOGAS(I)
*CALCULATE WHAT THE HEAT TRANSFERS WOULD BE IF THE OUTSIDE
*****OF THE TUBE WAS ONE DEGREE HOTTER.  USE NEWTON-
*****RAPHSTON TECHNIQUES TO REESTIMATE THE OUTER WALL TEMPERATURE.
      DQFROMS2=SIGMA*ETUBE*(TSOURCE**4-(TTUBEO(I)+1.0)**4)*
     1          TUBEOD/TUBEID
      QTOGAS2=((TTUBEO(I)+1.0)-TBULKG(I))*UO
      QACUM2=QFROMS2-QTOGAS2
      DTODQAC=((TTUBEO(I)+1.0)-TTUBEO(I))/(QACUM2-QACUM)
      TTUBEO(I)=TTUBEO(I)-QACUM*DTODQAC
      IF(ABS(DTODQAC*QACUM).LE.0.01) GO TO 110
*END OF THE IC LOOP.
  100 CONTINUE
*COMPLETION OF THE IC LOOP INDICATES THAT THE PROGRAM WAS
*****UNABLE TO REACH A SATISFACTORY VALUE FOR TTUBEO(I).
      PRINT 120,I
  120 FORMAT(/,5X,*PROGRAM FAILED TO CONVERGE TTUBEO.  I=*,I4,/)
      GO TO 500
*EARLY EXIT FROM IC LOOP.
*ACCUMULATE THE HEAT ABSORBED BY THE GAS (QABSGAS) AND DETERMINE
*****THE GAS TEMPERATURE AT THE START OF THE I+1ST INCREMENT.
  110 QABSGAS=QTOGAS(I)*PIE*TUBEID*DZ+QABSGAS
      TBULKG(I+1)=TBULKG(1)+QABSGAS/(TUBEFLO*CPGAS)
*END OF THE I LOOP.
   90 CONTINUE
*ADJUST THE SOURCE TEMPERATURE SO QEXCESS GOES TO ZERO.
      QEXCESS(IB)=TQA-QABSGAS
      IF(ABS(QEXCESS(IB)).LE.TQA/1000.0) GO TO 130
      IF(IB.EQ.1) DTSRC=1
     OIF(IB.GE.2) DTSRC=QEXCESS(IB)*DTSRC/
     1                  (QEXCESS(IB-1)-QEXCESS(IB))
      TSOURCE=TSOURCE+DTSRC
*END OF THE IB LOOP.
   80 CONTINUE
```

```
      *EARLY EXIT FROM THE IB LOOP.
        130 CONTINUE
      *ADJUST TBULKO SO THAT THE OUTSIDE OF THE TUBE WALL
      *****AT THE GAS OUTLET IS 1089 DEG K.
      *END OF THE IA LOOP.
        70 CONTINUE
      *EARLY EXIT FROM THE IA LOOP.
        140 CONTINUE
      *CALCULATE THE PRESSURE DROP DIVIDED BY THE FANNING FRICTION
      *****FACTOR AS DEFINED IN PETERS AND TIMMERHAUS, PAGE 421.
            DO 150 I=1,NINCS
            PDOVFFF(1)=0.0
            IF(IGAS.EQ.1) GASVOL(I)=1.42E-04*(TBULKG(I)-68.0)
            IF(IGAS.EQ.2) GASVOL(I)=TBULKG(I)/1660.0
            IF(IGAS.EQ.3) GASVOL(I)=8.62E-05*TBULKG(I)
            TAREA=PIE*0.25*TUBEID**2
            PDOVFFF(I+1)=PDOVFFF(I)+2.0*(TUBEFLO/TAREA)**2*
           1             DZ*GASVOL(I)/TUBEID
        150 CONTINUE
      *PRINT SECTION
            IF(IGAS.EQ.1) PRINT 160
        160 FORMAT(1H1,/,5X,*THE RECEIVER GAS IS WATER*,/)
            IF(IGAS.EQ.2) PRINT 170
        170 FORMAT(1H1,/,5X,*THE RECEIVER GAS IS HELIUM*,/)
            IF(IGAS.EQ.3) PRINT 180
        180 FORMAT(1H1,/,5X,*THE RECEIVER GAS IS NITROGEN*,/)
            PRINT 190, TUBEFLO,RE,TQA,TBULKG(1),TSOURCE
        190 FORMAT(5X,*GAS FLOW=*,F10.6,* KG/SEC/TUBE*,5X,
           1       *RE=*,F10.2,5X,*TQA=*,F10.2,* WATTS/TUBE*,//,
           2       5X,*INLET GAS TEMPERATURE=*,F10.2,* DEG K*,
           3       5X,*TSOURCE=*,F10.2,* DEG K*,/)
            PRINT 230,QABSGAS,TBULKO,UO
        230 FORMAT(5X,*QABSGAS=*,F10.2,* WATTS/TUBE*,5X,*TBULKO=*,
           1       F10.2,* DEG K*,5X,*UO=*,F10.2,* WATTS/M2/DEG K*,/)
            PRINT 240,(J,QEXCESS(J),J=1,11)
        240 FORMAT(5X,*QEXCESS,*,3(I3,*=*,F10.2),/,
           1       5X,4(I3,*=*,F10.2),/,5X,4(I3,*=*,F10.2),///)
            PRINT 200
        200 FORMAT(9X,*I*,6X,*TTUBEO(I)*,4X,*TBULKG(I+1)*,
           1       6X,*QTOGAS(I)*,3X,*PDOVFFF(I+1)*,6X,*GASVOL(I)*,/)
            DO 210 I=5,NINCS,5
        210 PRINT 220,I,TTUBEO(I),TBULKG(I+1),QTOGAS(I),PDOVFFF(I+1),GASVOL(I)
        220 FORMAT(5X,I5,4F15.2,F15.6)
        310 CONTINUE
        300 CONTINUE
        500 CALL EXIT
            END
```

III.3 TUBE2 SAMPLE OUTPUT FOR THE REFERENCE CENTRAL RECEIVER DESIGN

THE RECEIVER GAS IS HELIUM

GAS FLOW= .024776 KG/SEC/TUBE RE= 32295.77 TQA= 63000.00 WATTS/TUBE

INLET GAS TEMPERATURE= 600.00 DEG K TSOURCE= 1254.16 DEG K

QABSGAS= 63000.47 WATTS/TUBE TBULKO= 1089.00 DEG K UO= 1012.51 WATTS/M2/DEG K

QEXCESS, 1= 641.91 2= 487.60 3= -.47
4= -.55 5= -I 6= -I 7= -I
8= -I 9= -I 10= -I 11= -I

I	TTUBEO(I)	TBULKG(I+1)	QTOGAS(I)	PDDVFFF(I+1)	GASVOL(I)
5	765.41	637.21	137250.69	71537.07	.379428
10	797.85	673.39	133256.78	147355.76	.401351
15	828.89	708.45	128952.38	227331.52	.422609
20	858.47	742.30	124374.16	311330.13	.443152
25	886.57	774.90	119564.25	399208.86	.462941
30	913.17	806.16	114568.56	490817.74	.481939
35	938.28	836.07	109434.93	586001.02	.500121
40	961.92	864.59	104211.48	684598.63	.517467
45	984.11	891.69	98945.09	786447.72	.533965
50	1004.88	917.38	93680.11	891384.08	.549612
55	1024.29	941.67	88457.44	999243.52	.564411
60	1042.38	964.56	83313.79	1109863.19	.578370
65	1059.21	986.10	78281.26	1223082.68	.591505
70	1074.85	1006.30	73387.17	1338745.03	.603836
75	1089.35	1025.22	68654.03	1456697.58	.615386
80	1102.77	1042.90	64099.74	1576792.71	.626182
85	1115.18	1059.39	59737.85	1698888.35	.636255
90	1126.65	1074.74	55577.95	1822848.42	.645636
95	1137.22	1089.00	51626.04	1948543.13	.654358

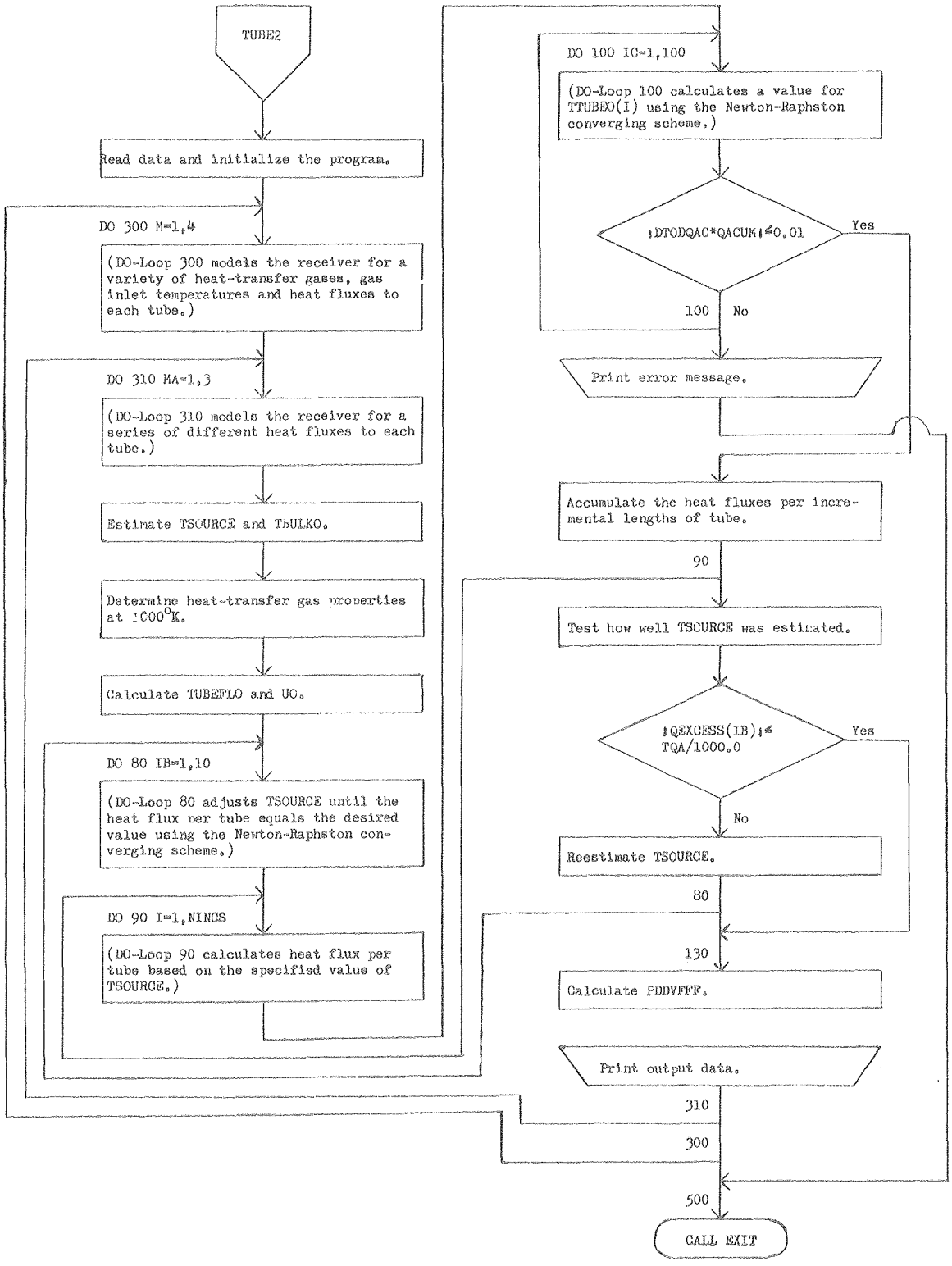

Fig. III-1. The flowchart for PROGRAM TUBE2.

TECHNICAL INFORMATION DEPARTMENT
LAWRENCE BERKELEY LABORATORY
UNIVERSITY OF CALIFORNIA
BERKELEY, CALIFORNIA 94720